Cooperative-Diversity Selection in RF Energy Harvesting Networks

By **Molefi Alfred Makuebu** - Student No. 1768540

Submitted in the fulfilment of the academic requirements for the degree of Master of Science in Engineering (MSc. Eng.) in the School of Electrical and Information Engineering in the Faculty of Engineering and the Built Environment of the University of the Witwatersrand.

Research Supervisors:
Prof. Fambirai Takawira
Dr. Jules Mouatcho Moualeu

January, 2019

Declaration

I, Molefi Alfred Makuebu declare that this dissertation has been composed solely by myself and that it has not been submitted, in whole or in part, to any previous application for a degree. Except where stated otherwise by reference or acknowledgment, the work presented here is entirely my own.

Name: Molefi Alfred Makuebu

Signed:

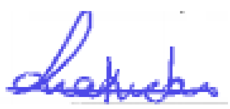

Date: ________ 14-01-2019 ________

Acknowledgements

Above all I would like to give my utmost thanks to the almighty God for giving me courage, strength and intellect up to the eleventh hour working over this research to make it a success.

I would like to express my sincere gratitude to my supervisor Prof. Fambirai Takawira for the continuous support in my MSc study, for his patience, financial assistance and immense knowledge. His guidance steered me in the right direction of research and writing of this dissertation. I could not have imagined having a better advisor, mentor and a father for my MSc study.

My sincere thanks also goes to Dr. Jules Moualeu who worked with me tirelessly to ensure I secure an opportunity at our research group. His door was always open whenever I ran into a trouble spot or had questions about my research to provide and share insightful comments, proofreading and encouragement which incentivized me to widen my research from various perspectives.

Besides my advisors, I would also like to thank the experts in the Centre for Telecommunications Access and Services (CeTAS) research group committee and my peer researchers for their validation of this research project. They also granted me an opportunity to join their group and moreover gave me access to the Convergence laboratory and other research facilities. Without their passionate participation, valuable input and precious support, this research could have not been successfully conducted.

I thank my fellow lab mates especially Mr. Mobunga Mofu for stimulating discussions, for helping out with proofreading, for sleepless but enjoyable nights while working together to meet timelines and for all the fun we had in the last eighteen months. I will also like to thank my friends, academic staff, administrative staff and support staff at Wits university for their contributions and creating the most conducive environment for me to accomplish this study. In particular, I am grateful to the following: Dr. Chabalala Chabalala and Ms. Reitumetse Khalanyane for enlightening me in the first glance of research.

Last but not least, I am gratefully indebted to my family: my parents, my brothers, sisters and friends for supporting me spiritually not only throughout the writing of this dissertation but in my life in general.

Abstract

Reliable and affordable wireless communication is very essential for sustaining economic development. High demands for data services are throttling the existing wireless spectrum. This channel throttling can be tackled by spectrum diversity tendered by cooperative communications. Through cooperative diversity, relay channels provide independently fading links which are transmission links for data generated at the source to the destination. Unlike in multiple-input multiple-output (MIMO) techniques where transmission channels are created by multiple antennas at the source device, with cooperative techniques these channels are provided by other relaying devices. Equipping small user terminals with many antennas is not always practical because of their size. The main contribution of this dissertation is to take advantage of the relay selection diversity from cooperative communication protocols and radio frequency (RF) energy from energy harvesting techniques which are the baseline for cooperation at the physical layer level to improve performance of wireless communications in terms of outage probability and extended coverage. A robust relay selection procedure is proposed on conventional relays and buffer-aided relays where relays harvest RF energy and cooperate by exploiting the broadcast nature of wireless channels.

In wireless transmissions, the signal quality is randomly degradative in nature due to bad channel quality resulting from fading effects of multi-path propagation. Cooperative diversity networks become a useful solution to provide reliable data-rate coverage through high diversity gain and an improved spectral efficiency in bps/Hz through multiplexing gains. Cooperative communications technology also becomes a favourite because of its lower RF transmit power requirements. Energy Harvesting techniques which have proven to be very potential can be deployed to convert transmit RF power into useful energy which can be stored in accumulation to supply and sustain the very same cooperative network with energy. The performance analysis of this energy harvesting relay-aided cooperative network under Rayleigh fading will be modelled in terms of the outage behaviour. If the relaying nodes in this cooperative network are equipped with buffers of finite size the performance is improved much further because of ease in the exploitation of best source-relay and relay-destination channel pairs for the relaying devices can decide when to receive and/or transmit. Conventional cooperative networks, reactive/partial opportunistic relay selection and in buffer-aided cooperative networks, Max-Max Relay Selection (MMRS) can be recognized as diversity-optimal strategies for relay selection and user scheduling in energy harvesting networks. This work aims at proving that with the same number of relays a balance can be attained between achieving a high diversity and improving cooperative network lifetime.

List of Publications

- Molefi A. Makuebu, Fambirai Takawira and Jules M. Moualeu, "Reactive Optimal Cooperative-Diversity Selection in Smart RF Energy Harvesting Network", *Accepted in proceedings of Southern Africa Telecommunication Networks & Applications Conference (SATNAC'2018) September 2018*

Contents

List of Figures

List of Tables

Abbreviations

S	Source
R	Relay
D	Destination
SNR	Signal-to-Noise Ratio
EH	Energy Harvesting
WPT	Wireless Power Transfer
SWIPT	Simultaneous Wireless Information and Power Transfer
DF	Decode and Forward
AF	Amplify and Forward
RF	Radio Frequency
FEC	Forward Error Correction
TDR	Time Division Relay
FDR	Frequency Division Relay
DFR	Division Free Relaying
CSI	Channel State Information
RTT	Ready To Transmit
CTT	Clear To Transmit
ORS	Opportunistic Relay Selection
BRS	Best Relay Selection
MMRS	Max-Max Relay Selection
S-R	Source to Relay
S-D	Source to Destination
R-D	Relay to Destination

i.i.d	independent identically distributed
MRC	Maximum Ratio Combining
ERC	Equal Ratio Combining
FRC	Fixed Ratio Combining
SNRC	Signal to Noise Ratio Combining
ESNRC	Enhanced Signal to Noise Ratio Combining
CDMA	Code Division Multiple Access
MIMO	Multiple Input Multiple Output
LOS	Line Of Sight
D2D	Device-to-Device
SIMO	Single Input Single Output
MIMO	Multiple Input Multiple Output
STBC	Space Time Block Codes
QoS	Quality-of-Service
PDF	Probability Density Function
CDF	Cumulative Distribution Function
MGF	Moment Generation Function
DTN	Delay Tolerant Network
BER	Bit Error Rate
SER	Symbol Error Rate
PER	Packet Error Rate
IoT	Internet of Things
AI	Artificial Intelligence
UHF	Ultra High Frequency
VLF	Very Low Frequency
SHF	Super High Frequency
ID	Information Decode
AC	Alternating Current
DC	Direct Current
BA	Buffer-Aided
AP	Access Point

1D	One Dimension
2D	Two Dimension
AWGN	Additive White Gaussian Noise
FEC	Forward Error Correction
PLC	Power Line Communications
4G	Fourth Generation
5G	Fifth Generation
Wi-Fi	Wireless Fidelity
AF	Amplify and Forward
LF	Linear-Process and Forward
nLF	non Linear-Process and Forward
EF	Estimate and Forward
CF	Compress and Forward
DF	Decode and Forward
PF	Purge and Forward
GF	Gather and Forward

List of Symbols

γ	Instantaneous signal-to-noise ratio per symbol
β	Gain amplification factor
μ	Statistical mean
σ^2	Variance
$\mathbb{E}(.)$	Statistical average operator
E_S	Source signal transmitted energy per symbol
E_{R_k}	k^{th} relay signal transmitted energy per symbol
h	General fading amplitude
$\overline{\gamma}$	Average signal-to-noise ratio per symbol
$f_X(x)$	Probability density function of the random variable X
$max(x, y)$	The maximum of x and y
S	Source node
D	Destination node
B	Buffer size
Q_{max}	Buffer size
R_k	k^{th} Relay node
h_{SD}	Fading amplitude between the source and the destination
h_{SR_k}	Fading amplitude between the source and the k^{th} relay
h_{R_kD}	Fading amplitude between the k^{th} relay and the Destination
$x_{R_k}(t)$	The regenerated signal from the k^{th} relay
N_0	Power spectral density of the AWGN channel
γ_{SD}	The instantaneous SNR between the source and the destination
γ_{SR_k}	The instantaneous SNR between the source and the k^{th} relay
γ_{R_kD}	The instantaneous SNR between the k^{th} relay and the destination

r	Spectral efficiency in Bits/Sec/Hz
P_{out}	Outage probability
P_{out_1}	Outage probability due to Relay 1
P_{out_2}	Outage probability due to Relay 2
$min(x,y)$	The minimum Of x and y
b^*	Best relay
$S_{(i,j)}$	State representing i energy units of R_1 and j energy units of R_2
$P_{(i_1,j_1,i_2,j_2)}$	Transition probability from state $S_{(i_1,j_1)}$ to state $S_{(i_2,j_2)}$
$P_{transition}$	Transition probability matrix
$f_X(x)$	The probability density function (PDF)
$F_X(x)$	The cumulative distributive function (CDF)
T	Frame time
τT	Harvesting Time
P_{R_k}	Transmit power of the k^{th} relay
P_S	Transmit source power
η	RF-to-DC energy efficiency
$\|h_{SR_k}\|^2$	Source to k^{th} relay channel gain
$\|h_{R_kD}\|^2$	k^{th} relay to Destination channel gain
$P^{2D}_{transition}$	Two dimensional transition matrix
$P^{1D}_{transition}$	One dimensional transition matrix
$\pi^{2D}_{i,j}$	Two dimensional steady-state vector
$\pi^{1D}_{i,j}$	One dimensional steady-state vector
n	Total number of energy states

Chapter 1

Introduction

One of the major problems in wireless sensor network deployment is the limited power supply because of the sensors' finite storage batteries. Thus, energy harvesting which caught both the industry and academia's attention recently is a promising solution to extend the wireless network lifetime. While improving network energy, an efficient cooperative communication algorithm to close coverage gaps and ensure optimal performance from the source node to the destination node is also crucial and hence maintain network integrity. This work mainly targets the exploration of cooperative communication protocols over energy harvesting networks.

Energy harvesting is a process in which energy is derived from external environmental sources such as solar, thermal, wind and wave to be stored for later use. Wireless energy harvesting will help supplement wireless sensors and user mobile stations which have varying energy consumptions depending on the network activity while primarily relying on this ambient energy from the radio-frequency (RF) signals. Two protocols used by energy harvesting modules at the receiver are time switching and power splitting. As it stands, this dissertation seeks a solution to the problem of limited energy in wireless networks which ultimately also substantially impacts performance in cooperative networks. As a measure of success in terms of performance, a decreased system outage for this cooperative setup is hoped to be accomplished in the event of relays harvesting energy to improve their lifetime.

Cooperative communication is a set of protocols enabling single-antenna devices [4] in a multi-user environment to share their antennas and generate a virtual multiple-antenna transmitter allowing them to achieve a transmit diversity. Cooperative communications can introduce significant throughput and diversity gains through relay channels. The relay channel concept was initiated by van der Meulen[5]. In practise, half-duplex relays are preferred over full-duplex as they are easier to implement than the latter. However, half-duplexing [6] comes at the cost of multiplexing gain loss as compared to full-duplexing. Practically, wireless relays work in half-duplex mode meaning they cannot receive and transmit at the same time and frequency. This challenge is due to difficulties in separating transmit and receive signals in the range of $110 - 120$dB apart. This resulting practical limitation implies that any source transmission has to be split into two parts; where in the first part the relay listens to the source, and in the second part, the source is silent to avoid interfering with the relay, thus reducing the overall spectral efficiency of the system. Although it is often the case for relaying to improve the system reliability, however it also encouters a loss in terms of transmission rate mainly known as the half-duplex multiplexing loss.

This challenge is highly rated and solutions have been attempted to address it. Among many solutions, the work done in [7] employed non-orthogonal amplify and forward relaying strategy, and the work in [8] employed the decode and forward relays. In both [7] and [8], the source transmits continually to avoid the half-duplex loss. To compensate for the multiplexing loss, the wireless network is at liberty to exploit the direct source-destination link to achieve a throughput gain or diversity through combining schemes at the receiver over other non-relaying networks [9][10]. On the other hand, due to practically large distances, shadowing or fading between the source and the destination, the source-destination link might be very weak and its availability could only be limited to higher signal-to-noise ratios (SNRs).

The relays are equipped with buffer elements and radio frequency (RF) energy harvesting modules to store packets received from source and harvest energy from the very same source signal in order to use the same energy for transmitting the signal to the destination. The buffer memory adds the flexibility of not transmitting the packet instantly if channel conditions are poor and temporarily storing it in the buffer for the next time period with the hope that channel conditions would have improved. This ensures a minimized packet error transmission although it adds a delay on the packet retransmission.

Cooperative communication is classified into the protocol nature such as fixed protocol, adaptive protocol and feedback protocol [11]. In the fixed protocol, the relay node always forwards the received signal after processing it. In the adaptive protocol, the relay node automatically decides whether to forward the received signal or not. As for the feedback protocol, the relay node assists with the transmission only if it receives an explicit request from the destination . The fixed protocol consists of fixed relaying classes called conventional relaying, while the adaptive relaying protocol is built by buffer-aided and max-link relaying protocols. In this work, the main focus is on the combination of conventional relaying protocol and adaptive relaying for relays with buffers to establish a hybrid selection scheme close to [12]. Therefore, the channel state information (CSI) based protocols from the feedback schemes are not considered. In conventional relaying, a relay is assumed to receive a packet from the source in the first time slot and forward it to the destination in the next time slot [4][13]. One of the relaying protocols in the adaptive relaying class for example would be the one followed in [14] where relays have freedom to decide on the time slot to receive and the one to transmit, called adaptive link selection.

1.1 Need for Cooperative Relaying Networks

Cooperative communications is an example protocol designed specifically in order to cope with the exponential increase of mobile devices and higher multimedia traffic demands as discussed in the introduction. This is because the more the number of mobile devices introduced the higher the number of independent paths added onto the network and thus ensuring reliability. Cooperative relay selection coupled with energy harvesting can be a lucrative solution contributing to large information exchange and shape up the future of wireless networks. With the current innovative entrepreneurial solutions involving technology, it is easy to conduct business transactions and trades virtually or primarily known as online under platforms supported by wired and wireless networks.

From an end-user's perspective, hand-held devices and wireless sensors are becoming intelligent and easily controllable to convert our world into smart world with smart homes, smart learning (e-Learning) and smart governance (e-Gov) of connected devices. These wireless protocols can support applications like video conferences, medical operations using augmented reality applications, webinars, sports and education training facility video livestreams and wireless sensor fire detection applications in forests and many commercial and military applications.

Wireless communication has now emerged as an essential need for users in their day-to-day operations. Because of its omnipresence it is now a fundamental mode of communication not hindering users' mobility. Either in mobile like 5G which is already being rolled-out in some countries, wireless fidelity (Wi-Fi) or wireless Device-to-Device (D2D) communications as in Global Positioning Systems (GPSs) in cars, asset management systems or medical application devices, the researchers and engineers are constantly seeking a solution for the efficient usage of a saturating wireless spectrum. They are also working hard to combat fading effects resulting from channel impairments such as path loss, scattering, shadowing and interference resulting in wireless users' poor experiences. Therefore, cooperative relaying in wireless networks takes advantage of the broadcast nature of wireless channels to overcome the above mentioned fading effects to improve reliability of wireless networks.

1.2 Related Works

Cooperative diversity networks are classified into two major categories, namely information-theoretic which mainly focuses on the capacity of cooperative diversity networks and communication-theoretic mainly concerned with reliability of cooperative networks with certain modulation schemes. The concept of relaying was also extensively studied by Sato[15]. An information-theoretic analysis of relaying channels was extended by Cover and Gamal[16]. In all of these contributions, the source node communicates with a target node via the relay node and the resulting capacity of this configuration was found to exceed that of a direct traditional link even though the analysis was done on Gaussian channels only and not on wireless fading channels(Rayleigh, Rician, Nakagami-m etc).

Later on in the 90's, Concept Group Epsilon (CGE) was digging more into the relaying concept to analyse power gains due to shorter relaying links as a basis of improving base station coverage to reach for mobile stations out of reach or at cell edges. Sendonaris, Erkip and Aazhang [17] suggested a useful cooperation protocol to boost capacity and lower outage probability at a given rate. Their work showed that retransmission of source packets by the relay node to the destination yields very high degrees of diversity because both channels Source-Destination and Relay-Destination are uncorrelated.

Our motivation for attaining a cooperative transmission strategy is gathered from the known concept of activating as few relay links as possible to save time slots and reduce overhead information [18] for feasibility. The work in [10] already proved that selection strategy with stable power supply can achieve the maximal diversity gain, which is equal to the number of available relay nodes under independent and identically distributed Rayleigh fading channels when there is no direct link.

There is significant amount of research that focuses on the design of simultaneous wireless information and power transfer (SWIPT) coupled with cooperative communication networks [19][20]. Most of these works further explore the characterization of wireless energy harvesting and information transmission and also focus on the fundamental trade-offs between the two. In [19] and [21], the receiver is able to decode information and energy signals that have to be separated either by time switching or power splitting architectures at the receiver. Energy Harvesting (EH) is very beneficial in relay networks as shown in [22], [23] and [24]. The energy harvesting gives wireless nodes the ability to operate incessantly using ambient energy to significantly extend network lifetime and decrease maintenance costs [25]. Design and analysis of energy harvesting and relay selection has been achieved in a number of references including but not limited to [23][24][26][27], the references therein and in [28]. Recent developments in energy harvesting communications include the possibility of energy sharing and transfer between nodes as discussed in [29], [30].

In the observation of the work done in energy harvesting and relay selection in [23][24][26][27], and [31], of particular interest are references [27] and [26]. In [27], a harvest-then-cooperate protocol is proposed in a time-switching cooperative communication network with downlink wireless energy transfer and uplink wireless information transmission. The authors in [27] considered a network with a hybrid Access Point (AP), source (S) and a relay (R) that has no traffic. The hybrid AP has a constant power supply while both S and R are equipped with rechargeable batteries to harvest from the AP and store. No model was introduced in this work to show how the accumulating energy at the selected relay can improve its signal-to-noise ratio (SNR) but instead the assumption is that there is no accumulation which is not practical.

There is also some work that has been done in incorporating cooperative relaying with energy harvesting in [32][33]. In [32] performance analysis of cognitive radios was analysed where the secondary system was a cooperative network built with a source, a cluster of K relays and the destination. Data transmission between the source and the destination was assumed to be entirely over relays, and relay nodes were also assumed to harvest energy by time switching protocol from the same source signal and forwarded to the destination. The secondary network was using opportunistic relay selection where the relay selected to receive was required to transmit. An exact outage probability expression in [32] was derived considering maximum values of the source transmit power, relay powers, energy harvesting efficiency at relays and the interference constraint at the primary receiver. However, the authors in [32] assumed no batteries and therefore did not cater for the energy accumulation but rather assumed all the energy is used up as the relay transmits.

The work related to the proposed study focuses on the performance analysis of energy harvested in relay-aided cooperative network with multiple relay nodes in terms of outage behaviour [26]. Based on the Markov property of energy buffer status in [26], an on-off model is proposed to characterize the stochastic property of harvested energy flow. This on-off energy model has some shortcomings as these two states do not quantify the exact or an estimate of the accumulating energy in the battery but rather assume it as available (on) if above some threshold or not (off) if below the threshold.

On the other hand, some work in [34][35][36][37] and references therein, have been done in relaying networks using data buffers of finite and infinite sizes to model the optimal performance of cooperative communications. This dissertation considers a modelling approach such as the one done in [12] to implement a hybrid relay selection protocol. Besides the novelty of the hybrid scheme, it was also found to outperform the pre-existing schemes.

1.3 Motivation

Based on the need for cooperative relaying networks, this research is motivated by the following factors:

- The current advancement in technology has led to an increase in elegant devices and number of mobile devices. Over half a billion mobile devices and connections were added in 2015 as illustrated in Figure 1.1. It is also surmised that by 2020, mobile connections will increase by 12 billion globally which is a compound growth rate of more than 8% while mobile devices in use will be between $8-9$ billion. While taking these numbers into account, real significant capacitive outcomes can be achieved when implementing cooperative relaying protocols that can ensue an improved balanced Quality-of-Services (QoS).

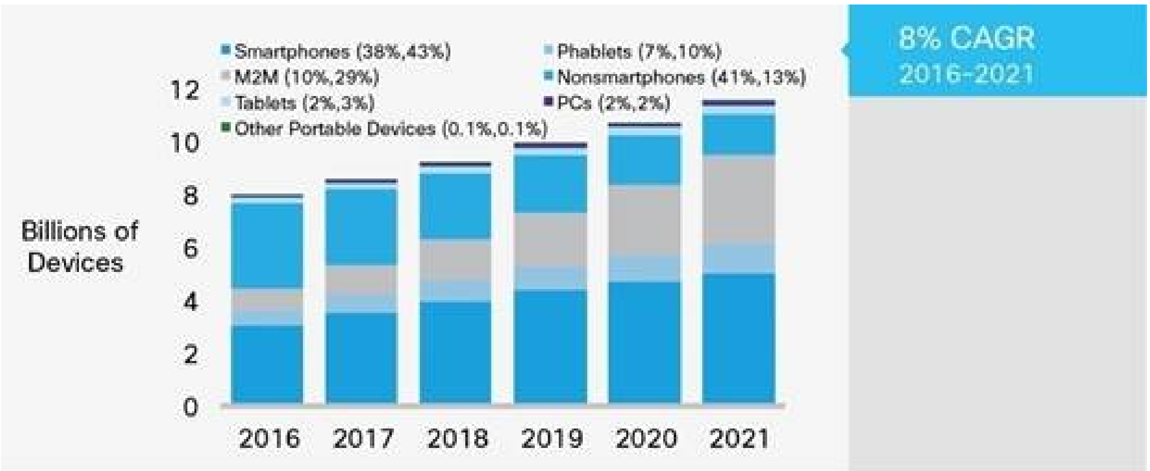

FIGURE 1.1: Exponential global growth of mobile devices by Cisco VNI Mobile, copied from [1]

The global rise of mobile users will lead to many relaying devices during communication as presently it is still not practical to have multiple antennas on mobile devices and sensors. Through the use of the cooperative relay diversity and energy harvesting, this is research targeted on the analysis and on improvement of performance in the event of optimal relay selection to forward the source's data.

- It is normal for performance to degrade as number of wireless users is increasing in many communication protocols. Unlike in other communication protocols, an increase in wireless users leads to a better diversity in cooperative communications. This is because performance evaluation of relay selection with energy harvesting can improve the complex nature of time varying transmission channels.

1.4 Research Problem

This work deals with the main challenges facing cooperative diversity networks which are how to increase performance and diversity gains without sacrificing the spectral efficiency and also extend lifetime of cooperative communication networks by support of operational sustainable energy. To resolve these mentioned challenges the following measures would have to be undertaken:

- The first part of this dissertation mainly focuses on performance analysis of partial relaying in opportunistic RF harvesting using decode and forward regenerative relaying without buffer-aided relaying. The performance is evaluated under flat rayleigh fading and energy harvesting time dependent on channel power gain where the CSI at the relays and destination is assumed to be perfect.
- In the second part, a robust hybrid and adaptive rate algorithm achieving high performance with better diversity gains while also addressing an efficient usage of the spectrum by combining both ORS and MMRS selection schemes and by adopting harvesting scheme is devised. Lastly, a comparison and contrast of the performance analysis with the results of other schemes is provided to conclude which is the best.

From [38], it has been proven that smart relay selection can outperform a certain class of distributed space-time codes and beamforming protocols. Also given its simplicity that only one node transmits and thus a simple transceiver design in principle can be implemented.

Having cooperation in wireless communication may influence a few design challenges not only limited to security and billing but also including relay selection, channel estimation and how to harvest RF energy optimally to transmit the source's data. This main design challenge of selecting to transmit has been investigated without inclusion of RF energy harvesting and with inclusion of RF energy harvesting to analyse how it influences performance. However, there remain some unanswered primary questions that still need to be addressed for the development of cooperative networks such as,

How to achieve relay selection in varying ambient RF energy harvesting networks?

The preceding unanswered question is the main research question this dissertation has resolved.

In order to address the above main question, the following sub-questions also have to be covered:

- *How to analyse a discretized RF energy model to quantify energy of relays?*
- *How harvested RF energy influences relay selection in cooperative networks?*

The hypothesis of this research is that, an efficient relay selection with a perfect CSI using RF energy harvesting can be an important factor in optimizing performance of cooperative communications.

To answer these questions, the following has been done:

- Adequate understanding of the operation of cooperative communications and energy harvesting networks.
- Developing a realistic model for energy evolutions in RF harvesting networks under a simplistic assumption that energy is only expended during transmission.
- Formulating and implementing a relay selection network that adopts the energy harvesting and storage techniques.
- Formulating and developing a cooperative RF-powered relay network equipped with buffers to add a flexibility of receiving and/or transmitting.
- Determining system analysis and synthesis by deriving outage probability as a performance analysis of the schemes developed in the second and the fourth bullets above.

1.5 Contributions

The main contributions achieved:

- A robust approach is proposed to mathematically model and quantify exact unit step energy evolutions from harvested RF signal as compared to the work done in [26]. This novel approach has not been reported in the existing literature according to the authors' knowledge.

- Formulate the exact closed-form expression of outage probability for partial relaying in opportunistic RF harvesting as a function of system energy states.
- Lastly, then derive closed-form expression of outage probability for the hybrid relay scheme as a function of relay buffer states and system energy states.

1.6 Organization of the Dissertation

The rest of this dissertation is therefore structured as follows:

- **Chapter 2** - A broad survey on cooperative communication in wireless networks is carried out. It covers an exhaustive literature review on cooperative communications, its advantages and disadvantages, relaying protocols and relaying strategies (for e.g. Decode-and-Forward, Amplify-and-Forward), cooperative network design, performance analysis of cooperative systems and the core concepts of relay selection and relaying schemes were discussed.
- **Chapter 3** - This chapter discusses the concepts of radio frequency energy, different methods of how it can be harvested and its importance in the future wireless communications. It also provides relevant work conducted on the utilization of cooperative communication with network nodes harnessing RF energy and how it can improve diversity of the cooperative architecture.

- **Chapter 4** - This chapter introduces the first contribution of this research. The goal is to develop a novel and effective relay selection scheme harnessing RF energy. A system model is proposed with the selection algorithm. Performance evaluation is accomplished by reckoning outage probability of the best relay that decoded the message of the source and forwarded it successfully to the destination node. Monte-carlo simulations are performed to confirm the analytical model.

- **Chapter 5** - The use of buffers on the relays to store and forward the message from the source as packets is an enabling technique to enhance the performance of the cooperative model proposed in Chapter 4 is studied here. A cooperative network is considered and the relay selection algorithm is extended such that the source can transmit sequentially. The best relay to receive will store the packets if there is enough space to accommodate them. The best relay to transmit will forward the packets to the destination node if there are packets in the buffer and it has enough energy to transmit them. A Markov model is derived to decide when a selected relay can receive and/or transmit and when it has enough energy to transmit the packets to the end node. Extensive simulations are used to verify the mathematical analysis in terms of outage probability of the system.

- **Chapter 6** - This chapter presents a summary of the contributions conducted in the research, future research work, and conclusions drawn. The contributions made throughout the dissertation are foregrounded and recommendations for the future research in relay selection and energy harvesting were made.

1.7 Summary

This chapter laid the basic foundation of the dissertation, the research problem, motivation and the fundamental contributions. The significance of the research was clearly stated and its relevance towards contributing to the advancement in wireless communications by incorporating improved relay selection schemes and RF energy in cooperation.

Chapter 2

Background on Cooperative Communication

2.1 Introduction

Cooperative relaying communications is a novel concept for wireless communications providing higher throughput gains and energy efficiency whilst there is also a higher degree of freedom for signal path to reach the destination [39]. This communication system is quite different from the normal traditional mobile station-to-base station because there are supportive relays or users along the channel towards the destination.

Basically, when a source device transmits a signal to a destination another nearby device overhears the transmission and relays the signal to the destination and therefore the final decoding is based on one or both of the two signals depending on the channel conditions they both traversed. The use of intermediate relay nodes to help with transmission from a source S to destination D is to enhance the coverage area and relax the link budget at the same time. Splitting the transmission distance from S to D is efficient for lowering propagation path loss which as a matter of fact reduces the end-to-end signal attenuation and thus relaxing the link budget.

2.2 Cooperative Communications

Signal fading in wireless networks resulting in severe distortions due to multi-path propagation can be mitigated by use of diversity. The Rayleigh channel is known to provide poor performance because there is no line of sight (LOS) path, and hence a high transmission power is necessary to compensate the outage rate. Typically three common ways mainly used to compensate for the outages introduced by multi-path fading are: forward error correction (FEC), adaptive equalization, and diversity techniques (time, frequency, space, polarization, multiuser, cooperative) [40]. In practice, a combination of all of these techniques may be used to combat the outage rate.

The most popular diversity methods are:

- Frequency Diversity: It is transmission of information on more than one carrier frequency. Since the signal over multiple paths is separated by more than the coherence bandwidth and not correlated then it will not experience the same fades.
- Time Diversity: It is repeated information transmissions at times that exceed the coherence time of the channel. These repeated transmissions of the signal at the receiver with different and independent fading conditions provide diversity.
- Space Diversity: The signals received from the spatially separated antennas would have uncorrelated envelopes for antennas separated by more than one half wavelength.
- Cooperative Diversity: Usage of intermediary nodes to assist with information transmission from a source node to a destination node, this in turn extends the coverage area and adds new degrees of freedom.

However, cooperative communications is a very useful technique providing profound improvements for the wireless link with minimal costs. It takes the advantage of the two most fundamental features of wireless medium being broadcast in nature and having the ability to achieve diversity through independent channels. The main advantage of cooperation is that if one propagation path is in deep fade then another independent path may have a signal of higher quality which is correctly decoded at the receiver [40].

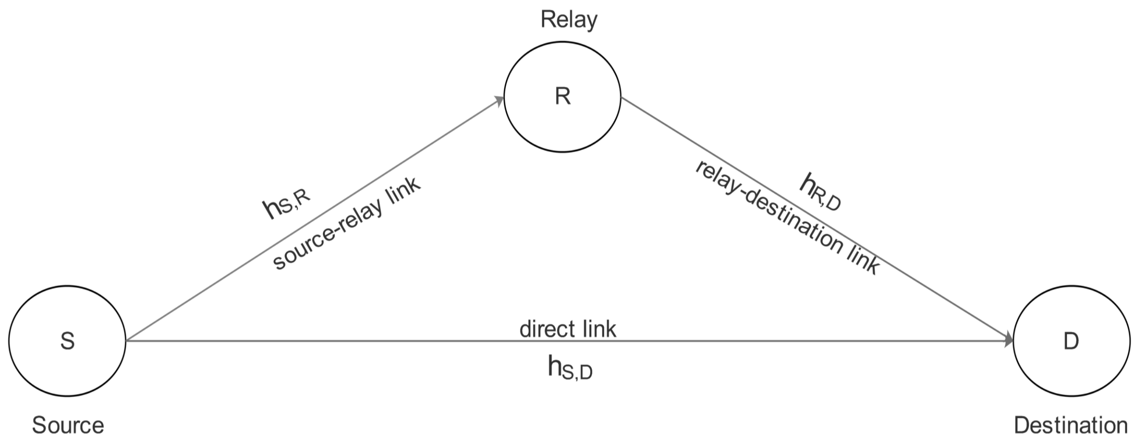

FIGURE 2.1: Cooperative Relay Network with the direct link

Wireless channels are broadcast in nature, that is, a signal transmitted in a wireless medium is omni-directional. Therefore, to facilitate a proper cooperative communication with a minimal interference, suitable access methods must be ensured to take care of the duplexing method as well as access coordination and resource allocation.

In a cooperative communications design, there is a source node which is originating transmit data, relay node for relaying source data and the sink/destination node where data is directed to. Different duplexing procedures in cooperative relays are applied which make use of the following duplex principles:

- Time Division Relaying (TDR): Incoming and outgoing information streams at the relay are separated in time and allocated to different slots. Both streams are not necessarily in the same frequency band[39]. It realizes a half-duplex relay by nature.

- Frequency Division Relaying (FDR): Reception and transmission at the relay happen at different frequency bands and incoming and outgoing information streams are not scheduled on time[39]. It is realizing a half-duplex relay.

- Division Free Relaying (DFR): Reception and transmission of the relay information stream happen at the same time over the same frequency band then realizing a full-duplex relay[39].

Cooperative diversity can go much further as mentioned above to combine all signal transmissions from different relay nodes by different combining schemes. The most common being the Maximum Ratio Combining (MRC), Equal Ratio Combining (ERC), Fixed Ratio Combining (FRC), Signal to Noise Ratio Combining (SNRC), Enhanced Signal to Noise Combining (ESNRC). These techniques were studied with the idea of boosting strong signal components and attenuating the weak (relatively noisy) components but in some cases it is assumed the direct link is in deep fade and communication is only possible through relays. An interesting application of this technique is the rake receiver for detecting direct-sequence Code-Division Multiple Access (CDMA) signals over a dispersive channel. Again, cooperative diversity brings together the two key spectral-efficiency areas, that is conventional relaying and MIMO systems in a case where an intermediate cluster of nodes is seen as multiple antennas and therefore many advantages will therefore follow including spatial diversity, spatial multiplexing and power saving.

Figure 2.2 shows cooperative communication model where the source S and destination D communicate over a channel with a fading coefficient $h_{S,D}$ and with the help of the relay terminal cluster of size K to forward the original signal via fading coefficients h_{S,R_k} and $h_{R_k,D}$ where R_k is the k^{th} relay node. Communication via the relay takes place in two stages as dictated by the inability of the relay to receive and transmit over the same frequency. The relay receives the noisy version of the signal because of channel fading, the signal is able to be processed and transmitted at an increased capacity in order to improve reliability of end-to-end transmissions between S and D terminals.

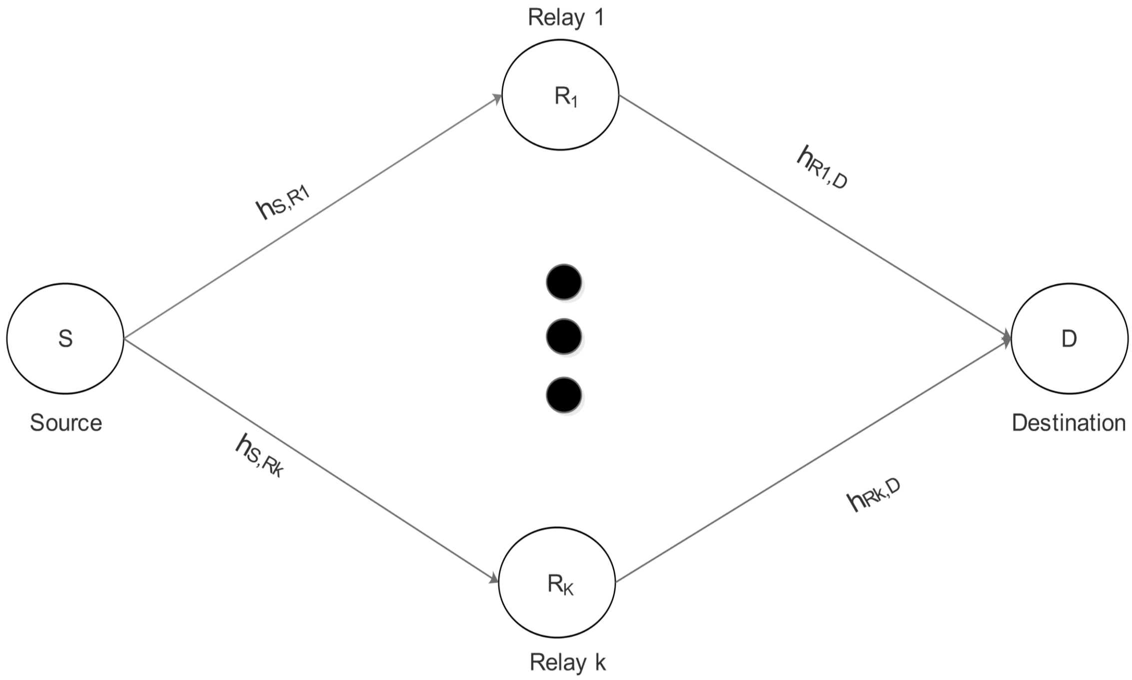

FIGURE 2.2: Cooperative Diversity Network for K Relays

2.2.1 Advantages and Disadvantages of Cooperation

The advatages of cooperation:

- Prominent performance gains are achievable due to pathloss gains as well as diversity and multiplexing gains which result into decreased transmission powers, higher capacity or better coverage because of optimal planning and resource management.
- In traditional systems users at the cell edge suffer from capacity and coverage but cooperative relaying allows a balance by granting all users an opportunity of equal quality of service regardless of the position within the cell.
- Using relays allows the system to have a minimal infrastructure which lowers the deployment and maintenance costs [41].
- Cooperative relaying is not only a more cost effective solution but it also lowers capital and operational expenditures. This is because it can be used with

existing wireless technologies without any additional infrastructure cost by just taking advantage of the broadcast nature inherent to the wireless channel.

The disadvantages of cooperation:

- Having many users and relays at operational level makes relaying a complex task and requires sophisticated schedulers to manage various user traffic and applications of relayed data.
- There will be an increased overhead when incorporating handover, synchronization, security and billing into a full operational system.
- An added complexity for determining the optimum relaying and the best partner.
- Challenges in handling increased intra and inter-cell interference if power savings gained more especially from relay selection are not used to decrease transmission power of relaying nodes but to boost capacity.
- There will be increased end-to-end latency of delay-sensitive services like voice and multimedia web applications induced by decoding packets at the relay.

2.2.2 Relaying Protocols

The role played by relay nodes in cooperative networks, makes us aware of two different behaviours being cooperative behaviour and egocentric behaviour, the latter currently dominating today's wireless networks. With the current self-centred behaviour, nodes separately communicate with the base station without the help of other nodes(no mutual help relationship). Because nodes are competing with each other for resources, it is in this behaviour where nodes experience the impact of the channel segregatedly to those with good channel conditions enjoy large data rates whereas those with poor channels suffer low data rates.

It is due to the cooperative and egocentric behaviours that the two classes of relaying protocols were developed, namely transparent and regenerative (digital) relaying. In transparent (analog) relaying, the relay does not modify the information on the source signal but may rather amplify or phase-rotate the analog signal as received from a certain frequency to another frequency band.

A practical design challenge related to the choice of transparent relaying protocols is the choice of amplification factor of the relay based on the constant output power, fixed gain amplification and variable gain amplification. Examples of transparent relaying include:

- Amplify and Forward (AF): The signal received by the relay is amplified, frequency translated and retransmitted and different amplification factors can be used [10].
- Linear-Process and Forward (LF): This relaying involves use of linear operations such as phase shifting performed on the signal in the analog domain which helps distributed beam-forming [42].
- Nonlinear-Process and Forward (nLF): This method performs non-linear operations such as non-linear amplification of the received signal before retransmission to minimize end-to-end error rate [43][44].

Another class is regenerative (digital) relaying called digital because processing is in the digital domain and requires baseband processing. This class of relaying protocols unlike the transparent which mainly relies on the amplification gain is dependent on a large number of parameters that can be optimized which include the choice of channel code, choice of interleaver, choice of waveform and modulation, power control and choice of receiver. Examples of the common digital relaying protocols include:

- Estimate and Forward (EF): The analog signal is down-converted to baseband signal and a detection algorithm applied on it to estimate the original signal and then retransmitted using the same or different modulation scheme [45].

- Compress and Forward (CF): It operates in a similar manner to the EF protocol but compresses the decoded information at the relay before forwarding it to the destination node [46].

- Decode and Forward (DF): It detects the signal, decodes it and re-encodes it before retransmission. It is also used in vast applications because of its performance with respect to error rate [16].

- Purge and Forward (PF): Since cooperative systems are interference limited, PF allows interference between different relaying streams and eliminates much of it [39].

- Gather and Forward (GF): It is an extension of CF but source coding is performed in both sampled information and the original information aggregated over a few communication sub-carriers [39].

In what follows, the most common relaying strategies from both analog and digital relaying classes are presented. These two protocols which form a basis for cooperation are AF and DF. The analysis of both protocols is done as a measure of examining resemblances and distinguishing the characteristic nature of analog and digital relaying classes.

2.2.2.1 Decode-and-Forward

Often times, the regenerative relaying Decode and Forward is seen to outperform transparent methods in some cases and is then preferred. In this DF strategy, the relay decodes the received signal and forwards it as is, thus minimizing complexity at the destination. The signal is prone to corruption by noise which may introduce error propagation in case a relay incorrectly detects a message and forwards as thus.

The decoding and re-encoding process of the signal at the relay is known as making a hard decision, as the information sent by the relay does not include any additional information about the reliability of the source-relay link. When uncoded modulation is used this protocol is also known as Detect-and-Forward as the processing of the relay is detection of the signal. For the relay function, the general case is given by: $f_{DF}(\gamma_{SR_k}) = \hat{X}$, where $\hat{X}$ denotes the decoded/detected signal at the relay and γ_{SR_k} is the SNR between the source and the k^{th} relay.

Due to the simplicity of the relay function, the decode-and-forward protocol has attracted a lot of attention and interest in the wireless communications community. Although the relay function is straightforward, the decoder at the destination is not as simple. When using optimal detector such as Maximum Likelihood detector for higher order modulation it becomes complex. Therefore intensive analysis has to be done in finding a detector that would achieve full diversity order.

2.2.2.2 Amplify-and-Forward

In amplify-and-forward (AF) relay protocol the relay amplifies its received signal to maintain a fixed transmit power. The AF relay function is an amplification of the received signal: $f_{AF}(\gamma_{SR_k}) = \beta\gamma_{SR_k}$, with the amplification factor β, the relay transmit average power constraint coefficient and γ_{SR_k} is the SNR between the source and the k^{th} relay. This amplification factor β ensures that the average transmit power at the relay is constant. This β is the same as derived by laneman and wornell in [47]. The form of AF relay function is independent of the modulation scheme of the source symbol because the transmitted signal at the relay is linear at a specific instantaneous signal-to-noise ratio.

2.3 Cooperative Network Design

The source, relay nodes and the destination node can be arrayed in many arrangements with the inclusion of the direct link. One common array is serial relaying where the source and the destination are connected by a chain of relays assumed to use orthogonal channels to relay the information. The other grouping is parallel relaying where the source and the destination are connected by a set of parallel relays also using orthogonal channels. Space-time relaying connects the source and the sink by a parallel set with space-time encoded channels.

Based on the different node behaviours as discussed in relay protocols section, it is worth discussing and illustrating how the system information is dealt with at system and network level. Therefore section 2.3 will show how basic information flows from cooperative relaying systems in subsection 2.3.1 and also discusses the fundamental design parameters affecting the performance of such systems in subsection 2.3.1.1.

2.3.1 Basic Information flow Aspects

- Direct link: In a non-cooperative network with a single source, information can reach the destination node by means of a single direct link.

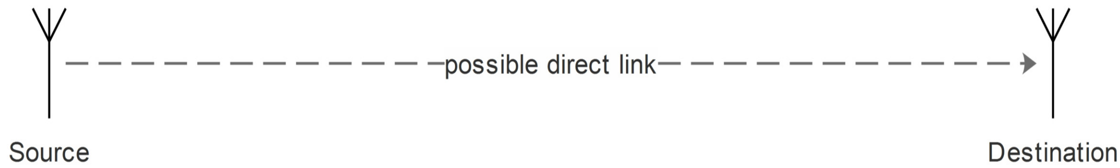

FIGURE 2.3: Direct link information flow

- Serial Relaying: In a serial relay setup, a series of relays connect the source and the destination in a multi-hop or chain configuration assuming orthogonal channels to relay the source information.

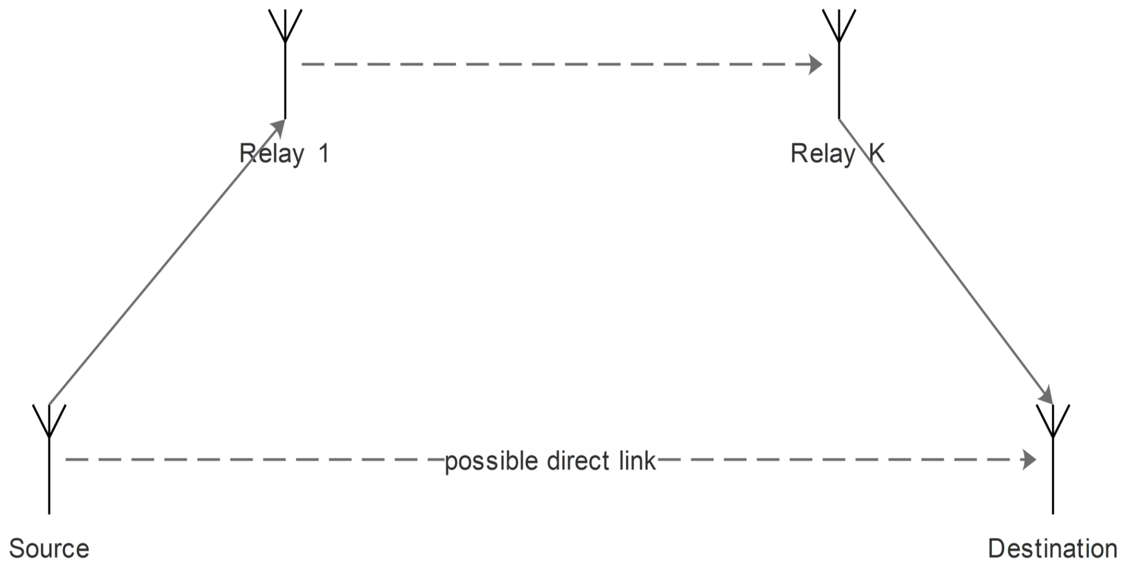

FIGURE 2.4: Serial relaying information flow

- Parallel Relaying: A parallel cluster of relays connect the source and the destination assuming orthogonal channels to relay the source information all at the same time.

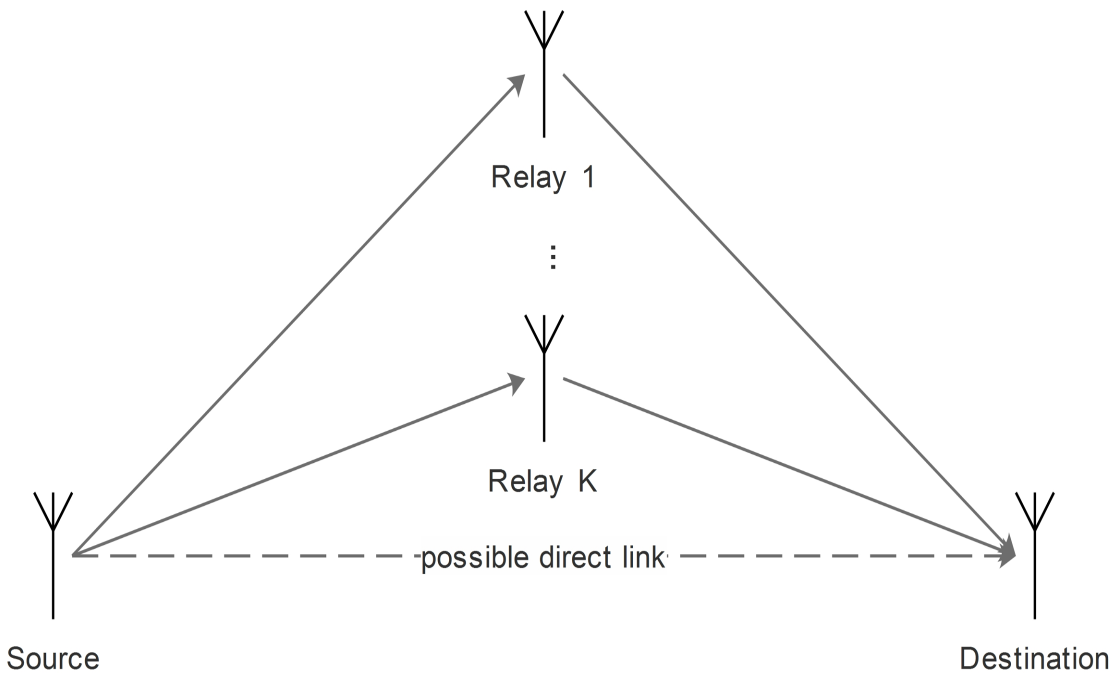

FIGURE 2.5: Parallel relaying information flow

- Space-Time: Space-time relaying makes use of a parallel set of relays to connect the source node to the destination with the use of space-time encoded channels instead of orthogonal channels in parallel relaying to relay the source's information.

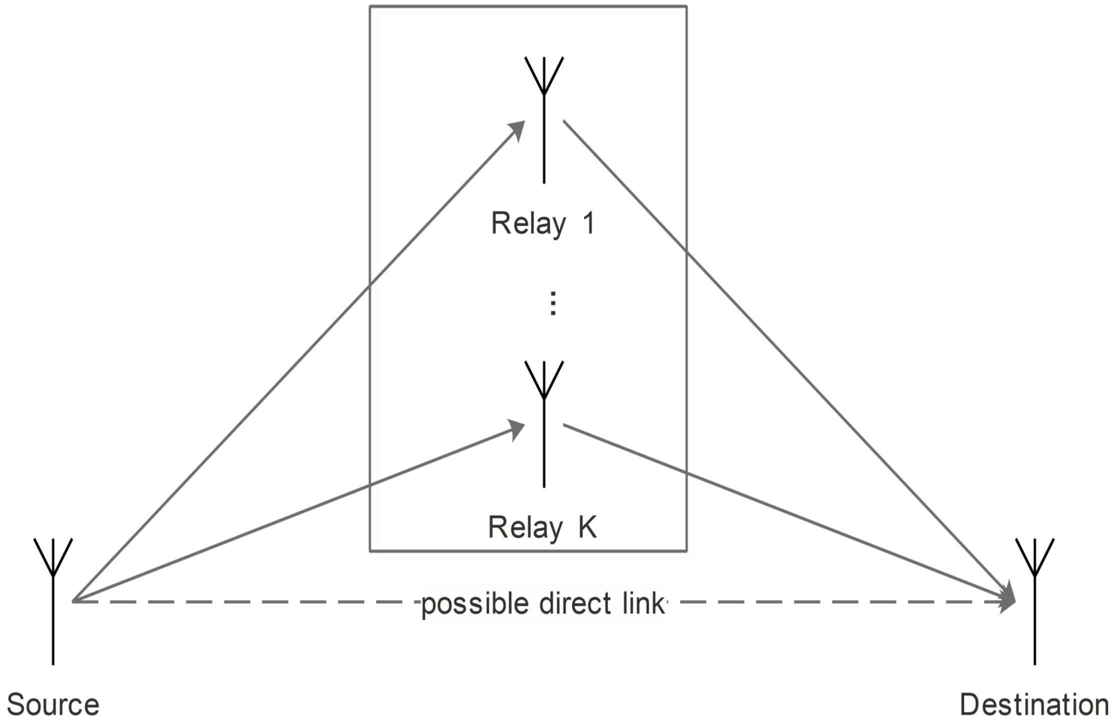

FIGURE 2.6: Space-Time relaying information flow

2.3.1.1 Design Parameters

Important design parameters that impact the optimization and performance of cooperative relaying include but not limited to power constraints, resource optimization, feedback and interference. In cooperative networks it is very important to understand whether power constraints apply per relay node or on an information basis and how additional relays can affect the shared power. Resource optimization can also be performed depending on the comparison of network parameters such as path loss exponent between the source and the relay, and the relay and the destination. The CSI feedback channels from the sink to the source node can strongly impact the performance of the system as well.

2.4 Performance Metrics of Cooperative Systems

There are important performance metrics used to analyse the performance of cooperative systems. Many a times, these metrics are used to assess the system performance and determining optimum system configurations of relaying placement and selection protocols.

- Average Error Rates: The instantaneous bit (BER), symbol (SER) or packet error rate (PER) is mainly calculated while given average noise power and channel realization. For a channel that varies fast with all channel realizations covered then average BER, SER and PER are calculated and used to characterize the system performance. Moment generating function (MGF) is used for calculating SER in closed form expression as shown in [48], [49] while approximations and asymptotic expressions are typically used for BER [50][51] and PER [52][53] which is the most recognizable in real-world systems.

- Outage Probability: For channels that do not vary sufficiently fast with all channel realizations not covered during transmission then assuming averages is unrealizable because a new value will be generated in each transmission. Therefore, the concept of outage is used to measure the probability for certain performances that cannot be met. The most common approach was covered in references [54][55] to measure outage of cooperative relaying networks.

- Throughput: This quantity provides a clear indication of how much capacity can be offered per user through the usage of a particular communication protocol. End-to-end system throughput can be calculated as a function of average rates and/or outages as in [56][57].

- Latency: This important quantity measures the delay in delivering a packet to the intended destination from its inception at the source. It typically comprises of the time the packet spends in the buffer queue, the time it requires to successfully deliver it via the wireless media and the time to process it [58][59].

2.5 Relay Selection

Extensive work has been done [39] to show that multi-relay transmissions with orthogonal channels improve multiplexing and diversity gains. The only hiccup is that they are computationally intensive as more channel resources are required, and again an adoption or development of better combining schemes is compulsory which adds complexity and some overhead at the receiver. Hence, a better spectral efficient concept of relay selection came about to use minimal power constraints. Despite getting rid of cooperative repetitions, relay selection is found to achieve the same diversity as multi-relay transmissions while using just one relay to forward the data at low computational complexities.

2.5.1 Relay Selection Procedure

Relay selection is the process of determining the best (based on channel conditions) relay R to forward information from the source. Assuming a practical cooperative relaying topology, a source S wants to send data to the destination D in the midst of several relay nodes in between S and D. Then S will distribute its data among all the relay nodes and the destination node will select which relay node to forward to it the message from S.

The relay selection process is achieved in a sequence of transmission steps just as in Transmission Control Protocol three-way handshake. Initially the source S sends a Ready-to-Transmit (RTT) pilot signal to adjacent relays and the destination D, and in response of the RTT then D sends back the Clear-to-Transmit (CTT) signal to the source and relays. Both these signalling messages are sent with the same carrier frequency (f_c) and same power to be used for the payload. Based on the RTT signal, a possible relay R_k will estimate the instantaneous channel quality (CSI) h_{SR_k} between itself and the source, while using the CTT from D to estimate channel state information h_{R_kD} between itself and the destination D. This protocol is proposed in [60].

Relay selection schemes that are buffer state based assume finite buffer-aided cooperative relaying systems. Considering the instantaneous channel conditions on both Source-Relay (S-R) signal path and Relay-Destination (R-D) path, and the amount of available buffer memory on the possible relay, the average channel conditions can be calculated as the function of both S-R (h_{SR_k}) and R-D (h_{R_kD}). Henceforth, any selection process either being Best Relay Selection or Max-Max Relay Selection can be utilized depending on both the channel quality and the buffer state of the relay nodes.

2.5.2 Conventional Relay Selection

Why relaying? It has been proved by authors in [61] that more relays in a cooperative diversity network achieve a higher system diversity but performing relay selection process can also achieve the same diversity with a better and higher spectral efficiency with only one relay link[62].

Using all relays to participate in the relayed information can lead to a further capacity but if some of them are transmitting in orthogonal channels to avoid interference, then this will limit system throughput. This setup will perform poorly as compared to relay selection because of considerable amount of information to be sent from the destination to all relays such as CSI of forwarding channels from relays to the destination. From the works in [61][62], it has been observed that the best-relay selection also achieves full spatial diversity of order $N+1$ for sufficiently large SNR and outperforms the N-relay cyclic protocol. Therefore it is apparent that relay selection can facilitate system design for non-orthogonal multi-hop relay networks that can improve system performance and capacity with only one relay. In the below sub-sections the relaying protocols are listed and narrated.

2.5.2.1 Opportunistic Relay Selection

In this selection protocol as clearly detailed in [60] packet delivery is merely based on the relay with the best average end-to-end channel. Out of a K relay cluster where $k \subseteq \{1, ..., K\}$, the relay R_k with high end-to-end channel quality will receive the packet into its data buffer in the first time slot from the Source S and forwards it to the Destination D after decoding it in the next time slot using energy in the energy buffer or battery. With the assumption that S-R and R-D channels remain constant during both time slots, ORS scheme can achieve a diversity gain of K. However, the ORS scheme does not allow the freedom to exploit the best S-R and R-D channels by different relays but instead allows both channels of the same relay in the very same consecutive time slots and thus affecting the overall system transmission rate and throughput.

The main advantage of the ORS algorithm is that with minimal channel resources used in a controlled manner then spectral efficiency of cooperative networks can always be enhanced. This is only possible in a manner that, if there are K relays in a cooperative network transmitting at a time then a maximum diversity order of K can be achieved with all resources required for all K relays to transmit to the destination. On the other hand, with the best-relay selection algorithm only one relay has to be used to forward data to the destination node with the same diversity order of K exactly equal for the case of K relay simultaneous transmissions but with relatively minimal resources due to the usage of only one relay instead of the set K.

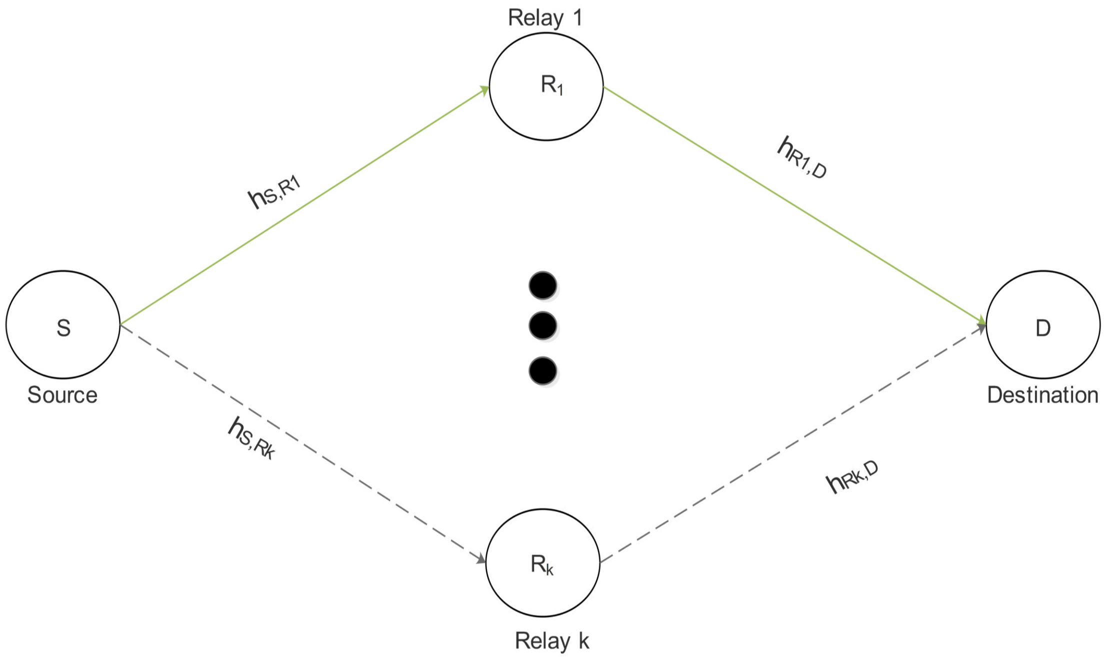

FIGURE 2.7: System Model for ORS Scheme, First Solid line:link for relay Reception Time slot 1, Second Solid line:link for relay Transmission Time slot 2

The solid lines on the Fig. 2.7 demonstrate the route with the best end-to-end SNR that will be chosen to transmit the source's data.

Relay selection is possible without a global CSI for each relay or a central network controller, one way this can be achieved is if there are distributed timers at each relay and hence each relay can estimate its own instantaneous channel power towards the source and the destination[63].

The selected relay provides the best end-to-end link between the source and the destination. This relay selection policy can be written as

$$b^* = \arg\max \min_{k\in \{1,..,K\}} (\gamma_{SR_k}, \gamma_{R_kD}) \tag{2.1}$$

Where b^* denotes the selected relay. Even though this scheme achieves a maximum diversity equal to number of relays K, it does not take into account the effect of equipping relays with buffers to explore their potential benefits.

2.5.2.2 Reactive Relay Selection

This is opportunistic relay selection performed after the source transmission and also commonly known as partial relaying. In a reactive mode, for relays that use DF coordination strategy and had successfully decoded the message will participate in cooperation[60].

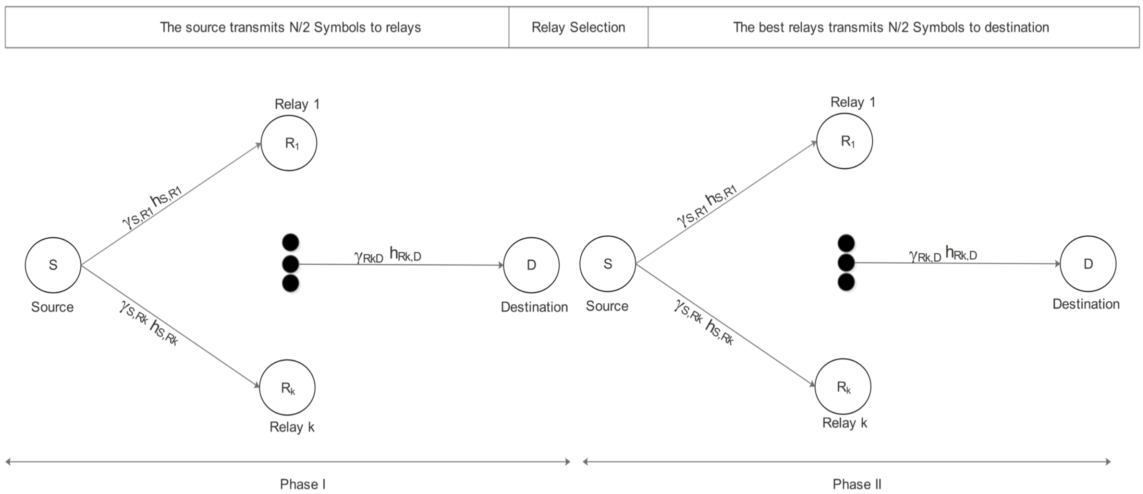

FIGURE 2.8: Reactive Selection Scheme

From Fig. 2.8 the source transmits $N/2$ symbols in the first phase and relay selection performed immediately after the source's transmission. In the last phase, the relay forwards to the destination.

2.5.2.3 Proactive Relay Selection

This is opportunistic relay selection performed before the source transmission. In a proactive mode, only a specific set of relays that were selected prior to the source transmission will participate in relaying the source data[60].

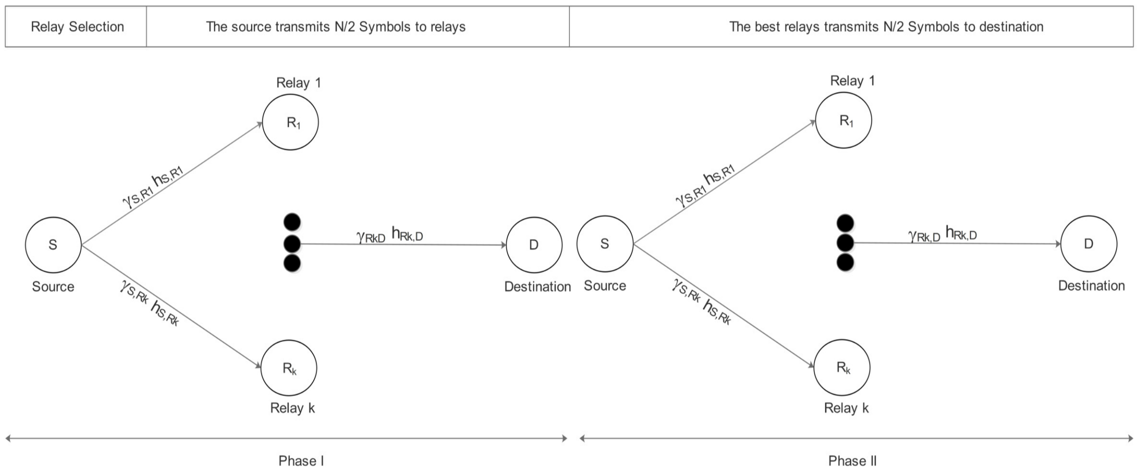

FIGURE 2.9: Proactive Selection Scheme

From Fig. 2.9 the relay selection is performed prior to the source's transmission in the first time slot, and in the second time slot, the selected relay just forwards to the destination.

2.5.2.4 Max-min Relay Selection in Successive Relaying

In [64], [65] and [66] it has been shown that a max-min selection policy implemented in a successive relaying network has a special form if inter-relay interference is cancelled at the relays. Instead of considering SR_k and R_kD channel gains only, the quality of handling interference cancellation is also handled. With a simple interference cancellation, the following two cases for relay selection follow.

- If relay R_k performs interference cancellation, then it might be selected to receive based on

$$b^* = \arg\max \min_{k\in \{1,..,K\}} (\gamma_{SR_k}, \gamma_{R_kD}) \tag{2.2}$$

  Where b^* denotes the selected relay.

- If R_k cannot perform interference cancellation, then it is selected among the relays by

$$b^* = \arg\max \min_{k\in \{1,...,K\}} (\frac{\gamma_{SR_k}}{R_tR_k}, \gamma_{R_kD}) \tag{2.3}$$

Where b^* denotes the selected relay.

2.5.3 Buffer-Aided Relay Selection

Usage of multiple buffer-aided relays to establish communication between the source and the destination node adds an improvement of performance in terms of throughput and reliability as compared to using a single relay and non-buffered multiple relays. Relay selection attracts interest due to its superior performance and easy implementation. For a well-known opportunistic relay selection (ORS) [67] , transmission is conducted on a relay link with the best end-to-end channel quality out of the available relay links. In the first time slot the packet is sent from the source to the selected relay which decodes and forwards it to the destination in the second time slot. ORS achieves a diversity gain of N, where N is the number of links with the assumptions that both S-R and R-D channels are constant during transmission. The main disadvantage of the ORS is not being able to utilize best S-R and R-D channels for more than one relay within the transmission block.

Depending on the channel conditions between the relay and destination (R-D channel), relays are not forced to retransmit the packets in the same time slot through the use of buffers and hence the relay with the best S-R channel can be selected for reception and relay with the best R-D channel be selected for transmission. This protocol is referred to as the adaptive relay Max-Max relay selection (MMRS).

Adoption of buffer-aided relays allows further improvements in cooperative relaying's performance. Storing packets and transmitting them in favourable conditions increases network's throughput, resilience and diversity [67]-[68]. The analysis in [67]-[68] established that buffering provides better throughput, increased stability region and desirable traffic load for each relay. Ample work in the line of research for detailed descriptions of ORS algorithms with buffer-aided relays has been conducted in [69]-[70]. [12] extends the ORS scheme of [60] by employing buffer-aided relays, allowing more degrees of freedom in the selection process because relays participate without necessarily decoding preceding packets successfully.

It is has been discovered that when the delay in buffer-aided protocols is tolerated then Hybrid Relay Selection (HRS) and MMRS schemes provide the same diversity gain as ORS but with significantly reduced SNR requirements. Krikidis et al [71] took advantage of the buffer-aided (BA) relaying epitome drifting away from the common dual-hop conventional policy to propose the max-link relay selection that adapts to activate each slot with the best fading conditions. From this max-link protocol, the first time slot is either used to select a non-full relay to receive the source's packet or a non-empty relay to transmit to the destination, and therefore a diversity order of $2K$ can be achieved with a larger number of relaying nodes. A max-link concept has also been extended in [72] to answer for the inclusion of a direct link source-destination. It has been found in the application of extended max-link scheme that it is resilient to low transmit SNRs.

With a single relay network, Zlatanov et al. [73] demonstrated adaptive link selection for both delay-unconstrained and delay-constrained cases. In the first case, they formulated an optimal link selection policy as a function of the exact CSI. For the latter case of delay-constrained link selection, they compared various link thresholds to the optimal policy for starving the relay's buffer and reducing number of stored packets. This framework is broadened further in [74], where authors presented different cases of CSI at the Transmitter (CSIT) availability determining adoption of fixed or adaptive transmission rates.

Performance of buffer-aided relaying and better spectral efficiency can be achieved by bringing up algorithms with full-duplex characteristics when half-duplex relays are available by advanced successive relaying developed in [75] and [76]. For a relay operating in full-duplex, only one channel is used for end-to-end transmissions because there is concurrent reception and transmission at a relay. Albeit full-duplex characteristics being useful by reducing CSI overhead and improving spectral efficiency they increase hardware complexity, loop interference from relay's output to input [77][78] and inter-relay interference because simultaneous transmissions. To mitigate all of these challenges, efficient interference cancellation techniques must be employed.

Delay and diversity issues in buffer-aided relay selection policies have been investigated in [34] where novel relay selection policies aiming at reducing average delay by involving the buffer size of the relay nodes into the selection process were proposed [36]. Relay selection policies for full-duplex buffer-aided relays have also been developed. Half-duplex and full-duplex relaying are compared in a single network relay in [35]. Full-duplex relays are equipped with multiple antennas where a certain number is used as receivers and the rest as transmitters, in most cases the number is split into half unlike half-duplex relays where all antennas are either used for reception or transmission. With respect to the analysis in [35] it has been deduced and the conclusion drawn that the half-duplex buffer-aided relaying can exceed the throughput performance of full-duplex buffer-aided relaying only if extra delay can be controlled and again the number of antennas at the source and the destination are greater than or equal to that at the relay [79][80].

It has been found according to [67] that in conventional cooperative networks, half-duplex relays transmit and receive in a prefixed schedule, inhibiting them of the flexibility to exploit best source-relay and relay-destination channels, hence limiting performance. Buffer-aided protocols are found in [67] and [37] to perform much better in comparison to conventional protocols by providing significant gains in terms of throughput, diversity, and signal-to-noise ratio.

In as much as buffer-aided protocols sound interesting and a way to go for an improved system performance and by the introduction of new degrees of freedom, it has some practical challenges. The exploitation of the channel with the best SNR may not always be possible for the relay as it has to accumulate information in its buffer before transmitting. The other challenge is that, storing packets in the buffer introduces some additional delay[37], which has to be managed for delay-sensitive applications like teleconferencing. This management requires up to date CSI which increases the complexity of implementing these protocols and this requires an outlook of DTN (Delay Torrent Networks) concepts[81][82].

2.5.3.1 Buffer-Aided Opportunistic Relay Selection

Relay selection as shown in the preceding sections has attracted much attention due to its superior performance and simplicity of implementation. One of the most well-known relay selection protocols is opportunistic relay selection also known as best relay selection [36], [69]-[70]. With this protocol, the relay with the best end-to-end channel is chosen for transmission for each an every packet transmission. The packet is sent to the relay in the first time slot, and the relay forwards it to the destination in the second time slot. It has also been proven in [60] that the best relay protocol achieves a diversity gain of K in slow fading conditions where source-relay and relay-destination channels remain constant during both time slots, where K is the number of relays.

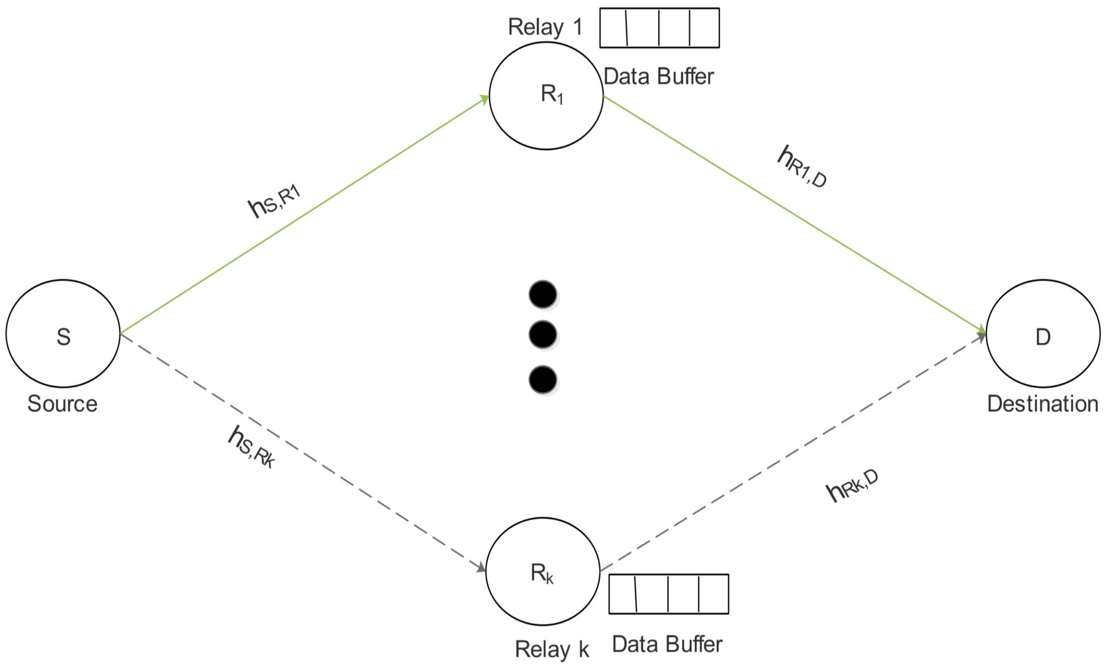

FIGURE 2.10: System Model for ORS Scheme with Buffers, First Solid line:link for relay Reception Time slot 1, Second Solid line:link for relay Transmission Time slot 2

The selected relay provides the strongest end-to-end link between the source and the destination. This relay selection policy can be written as

$$b^* = \arg \max_{k \in \ \{1,2\}} (\gamma_{SR_k}, \gamma_{R_k D}) \tag{2.4}$$

Where b^* denotes the selected relay.

2.5.3.2 Max-Max Relay Selection

In this selection protocol there is an increased freedom to the relay elected for reception and transmission because the selection process is a function of channel conditions and the buffer space only irrespective of which relay is chosen for reception and its end-to-end channel qualities [12]. Its operation is also considered in an adaptive rate transmission and perfect channel state information of the S-R and R-D channels for instance in order for the relay to decode, it requires full CSI of h_{SR_k} channel. This can easily be achieved since the relays are equipped with finite buffers of maximum size B or Q_{max}. The only disadvantage of this protocol is to easily lead to buffer overflow in the possibility of one relay R_k selected multiple times for reception and leads to buffer starvation in the possibility of the same relay R_k selected for transmission multiple times.

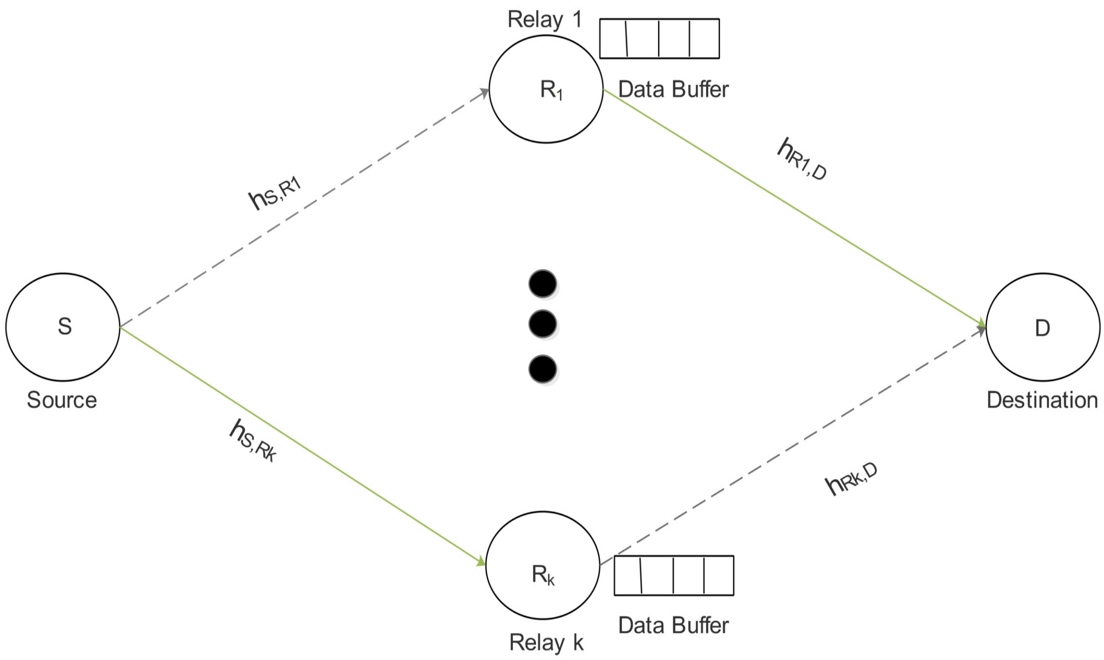

FIGURE 2.11: System Model for MMRS Scheme, First Solid line:link for relay Reception Time slot 1, Second Solid line:link for relay Transmission Time slot 2

2.5.3.3 Hybrid Relay Selection

According to section 2.5.2.1 and 2.5.3.2, it can be gathered from the former section that ORS reduces the amount of required resources. Although ORS achieves the full diversity order with minimal resources, contrarily it does not allow exploitation of the best S-R and R-D for different relay channels, thus compromising the maximum achievable performance rate. From the latter section, it was also discovered in [12] that MMRS can easily achieve the possible maximum transmission rate in the system while using the CSI of both S-R and R-D channels in the presence of buffer storage. The only challenge with MMRS is trading-off finite buffer memory for high performance rate in the sense that it will easily result in buffer overflow if relay R_k is selected multiple times for reception, and also in buffer starvation whenever R_k is favoured for transmission multiple times.

A hybrid scheme of the two schemes ORS and MMRS has been studied in order to balance the trade-off between the required performance rate and usage of available limited buffer memory. This form of hybrid scheme was proposed before in [12] but the energy harvesting concept which will address network lifetime as a major challenge and how it can optimize performance was not considered at all. Since the relays will be harvesting energy prior to decoding and retransmission, the choice of relaying protocol for retransmission of the source signal will depend on the channel conditions and buffer states, therefore this will facilitate power control as well managing interference. There is also no doubt that reduction in transmit powers and energy harvesting will constitute great power savings.

2.6 Conclusion

This chapter introduces the advantages and disadvantages of cooperative communications, relaying protocols, network design, performance analysis, selection procedure, selection diversity, conventional and buffer-aided relay selection schemes in cooperative communications from the literature's perspective. A study of the current literature in this relay selection chapter asserts the essentials by in-depth of the existing cooperative relay protocols and proposes a design in establishing a full operational cooperative communication model. It has also been vividly discussed that substantial diversity outcomes can be achieved when efficiently selecting relays with a higher SNR. A distinct focus on how harvested RF energy plays a major role in improving relays' SNRs has been discussed thoroughly in Energy Harvesting chapter 3. How this RF energy influences relay selection, when to select relays and how relay selection is holistically performed either in conventional relaying or buffer-aided approach have also been rigorously covered in chapter 3, 4 and 5 in order.

Chapter 3

Background on Energy Harvesting

3.1 Introduction

This chapter presents energy harvesting (EH), its advantages and disadvantages to the world of communications, its different protocols and what it bears for the future. Energy harvesters provide small amounts of power for low-energy electronics. The energy source for energy harvesters is ambient, for example, it can be scavenged from temperature gradients resulting from combustion engines and large scale of electromagnetic energy from radio and television broadcasting. Crystal radio is one of the ancient applications of ambient power from electromagnetic radiation.

EH is a process of capturing and converting energy such as heat, sound and Radio Frequency (RF) signals into electricity. The environment contains natural and ready to use energy sources as opposed to batteries and super-capacitors. Various studies have researched the possibility of using these natural energy sources in wireless network communications [31][83]. Energy harvesting using natural resources has not been exploited effectively because of the irregular nature of the ambient sources. Many EH techniques are environment-specific and feasibility of implementation does not make easy it for their utilization [84].

The whole world is getting ready for industry 4.0 which is Artificial Intelligence (AI) automation and data exchange in manufacturing technologies using cyber-physical systems, Internet of things (IoT) and cloud computing. Current developments are focusing on integrating sensors, microprocessors and wireless communication to revolutionize monitoring and maintenance of systems. In future, machines, structures and even the environment will be embedded with wireless sensors to collect health reports status or any other information status, compress for storage purposes and then forward to the intended processing node [85].

The prime question is who will change the millions of depleted batteries in those wireless sensors? A possible solution is to seek a reliable and renewable power source in the same environment as the sensors such as strain, vibration, light, motion and radio frequency to generate an indefinite amount of energy. Additionally, incorporating efficient and robust relay routing protocols that will further help with strict power management at higher data rates. Since the environment is a free good source of available energy compared to expensive preloaded energy in batteries or supercapacitors, therefore the best alternative is to look into energy harvesting which can be comprehended as power harvesting and energy scavenging from ambient RF signals. This wireless energy can be harvested using two protocols, namely power-splitting and time switching. With time switching, within an allocated time slot an optimal fraction of the time τT is taken to be in the energy harvesting mode and the remaining $(1-\tau)T$ taken for the information decoding and transmitting mode while in power splitting energy harvesting process and information decoding are concurrent.

There are three main methods of EH. With the first method, the source and relay nodes harvest energy from external sources such as solar, wind, or electromechanical energy [22][86]-[87]. With the second method, the source node has its own fixed power supply, and relays are equipped with batteries which harvest energy from RF signals of the source [28], [22]. In the third method, the source and relay nodes have their own fixed power supplies with a separate EH receiver to allow low-powered wireless devices to utilize harvested energies more especially in sensor networks [88], [89].

According to [90], RF energy can be classified into two categories:

- Ambient RF energy: This is ambient and unfixed energy which is freely available. Its transmission has a frequency range of 0.2 − 2.4GHz (Ultra High Frequency (UHF) band) with radiations from domestic appliances such as television, Bluetooth, Wi-Fi and many more.
- Dedicated RF energy: It is an on-demand energy supply resulting from higher power densities due to directed transmissions and mainly used to recharge nodes with predictably high requirement amounts of energy. This energy transfer is still possible under the Industrial, Scientific and Medical (ISM) bands ($2.4 - 2.5GHz$) and is better suited for supporting applications with QoS constraints.

3.2 Advantages and Disadvantages of Wireless Energy Harvesting

The advantages of wireless energy harvesting are:

- It works anytime because RF signals are readily available.
- Conventional power sources can be replaced.
- Supply power on demand and in mobility conditions.
- Unlimited spectrum of sources.
- It can also help with tracking capabilities.
- Efficient source of energy.
- It lowers electric tariffs.
- No wastage or toxic emissions, green energy
- It provides back up energy while travelling.

- No need for a periodic replacement of a battery.
- Extended life for devices due to recharging of storage battery in sleep mode.

The disadvantages of wireless energy harvesting are:

- In as much as EH sounds interesting, there are some associated design challenges it brings forth. Unlike with regular power supply solutions with a constant available power throughout the operation, EH solutions are dependent on time with random energy arrivals. For example, RF signals might be available throughout all day but with variations in channel fading conditions and environmental aspects. This limited power output mainly depends on the RF-to-DC conversion efficiency.
- Sensitive to external environment and not available commercially. The sun light is mostly available throughout the day but not at night and the harvesting period is roughly constant over a specified time, while with wind and other sources, a pattern of harvesting periods vary stochastically with bursts of harvested energy. This makes it difficult for adapting communication techniques where uninterrupted network operations are achievable.
- Wireless energy sources like solar are also not an exception and have a number of limitations due to their dependency on external sources prone to atmospheric changes, physical obstacles and radio wave source uptime.
- The received power from the sources is too low and its level often varies with time.
- The system performance is also affected over time because of the performance of electronic components like capacitors, diodes, storage battery and others.
- Design of receivers in wide frequency ranges is practically challenging for the fact that devices designed specifically to operate in one frequency band are limited only on that spectrum.

- Materials used in some devices may reach limit lifespan and degrade over time. For example in piezoelectric materials.

3.3 How RF Wireless Energy Harvesting Works

RF energy harvesting uses power conditioning and storage capacitors to conserve harvested energy from the environment. It mainly utilizes radiations from RF sources such as television and radio broadcasting transmitter stations, cellular base stations, communication satellites and any other radio transmitting devices can also be considered as a source for wireless energy harvesting. RF waves used in the harvesting system are part of electromagnetic spectrum. The maximum power available in RF energy harvesting is about 0.7 μWatt for 2.4 GHz and 1 μWatt for 900 MHz frequency theoretically which can all be achieved within a range of 40 meters through free space. The frequency range and operating power depends on the specific application of the transmitter.

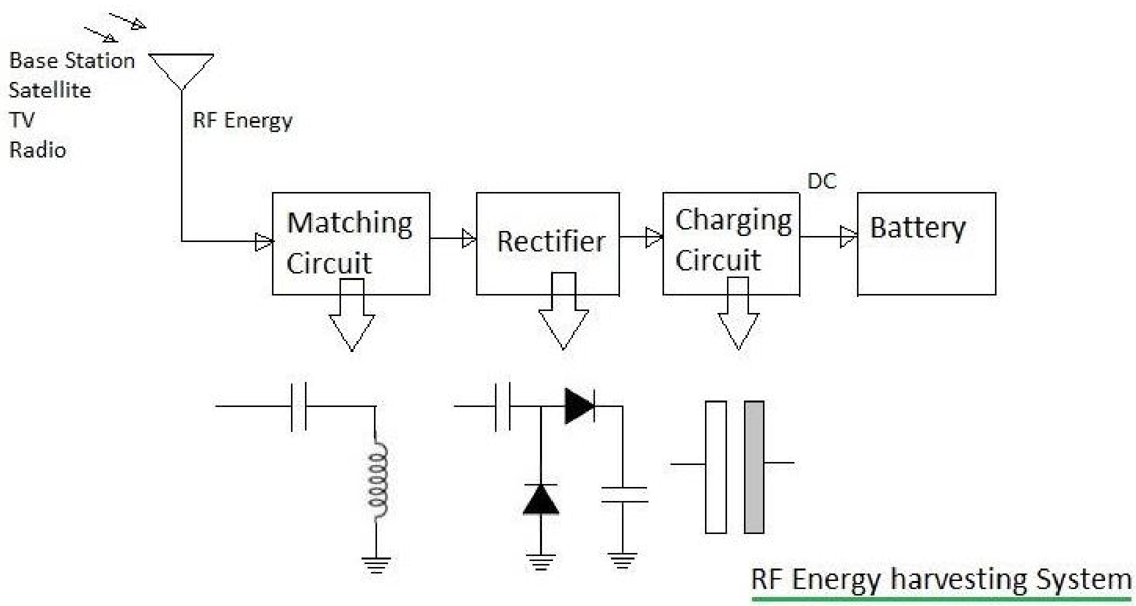

FIGURE 3.1: RF energy harvesting system Block Diagram with Components

Fig. 3.1 depicts the diagram of components in the RF energy harvesting system. It converts RF energy to DC energy, hence it is also referred to as an RF to DC converter. The system consists of an antenna module, matching network module, voltage multiplier circuit (rectifier circuit) and energy storage circuits. The figure also clearly mentions distinct circuit components within each of the modules. The antenna is perfectly tuned to a specific frequency to catch RF radiations from different sources available in free space. The antenna converts the electromagnetic energy into electrical signals to be fed to an AC to DC converter. The RF energy then goes to the matching network module via the transmission channel. The matching network is used for coupling maximum RF energy into the circuit. The circuit is made of capacitor and inductor components. The voltage multiplier is made of diodes and capacitors to increase the charging delay before storing it in the energy storage. The DC power attained from the rectifier circuitry is stored either in the capacitor or the battery for later use.

3.4 Energy Harvesting Protocols

3.4.1 Time Switching Protocol

To perform EH and information decoding, a receiver has to have two sets of independent antennas or may share the same antenna(s). The latter (sharing) is not demanding and requires less hardware complexity because it can be implemented with single antenna(s) [91]. With the same antenna(s) being shared, the time-switching architecture can be applied where a simpler switch selects either EH or information decoding at a time [91]. The relays are assumed to have no fixed power supplies and thus replenish energy from ambient radio signals opportunistically. Time switching EH in a receiver mechanism is simply a timing microcontroller controlling the switching operation between the energy harvesting process and information decoding in a relay node. The microcontroller operates exactly like a mechanical timer in an electric switch built-in television sets to put them to sleep or television receiver after a set period of time. The time switching scheme is practically favourable for the development of high level wireless power transfer (WPT) networks which are mainly designed to operate separately at various power sensitivities for e.g. 50 dBm for information transmission and 10 dBm for energy receivers [92].

Two relay nodes take turns to receive energy or information from the source over different time blocks. Therefore, as a result when one relay node receives information from the source, the other can opportunistically harvest energy from the same signal broadcast by the source, and vice versa. Hence, one relay operates as an information decoding (ID) receiver while the other as an EH receiver [92]. The same set of receiving antennas are shared by both EH and ID receivers in the relay, which is referred to as co-located EH and ID receivers. This colocation concept poses a challenge in determining an optimal information-energy trade-off because of the amount of time taken to either harvest or decode as both have an impact on the system performance.

It is also further assumed the relays use a time switching protocol where each relay can either harvest energy or only decode source information due to practical receiver circuit limitations. Therefore the energy harvesting time constraint is determined by the k^{th} relay power (P_{R_k}) from harvested energy as compared to the minimum threshold power ($N_0(2^{2R_{threshold}} - 1)$) required to decode the source information [93], where $R_{threshold}$ is the minimum rate required for transmission. The power spectral noise density ($N_0 = 2\sigma^2$) is the noise experienced by all receivers, mainly the relays in the first time slot and the destination in the second time slot. According to the threshold constraint if the relay power P_{R_k} due to wireless energy harvesting is less than the decoding threshold power, then energy harvesting time τT that is less than the overall time slot T ($\tau T < T$) will be extended to allow more time to harvest energy but at the same time not compromising the decoding of information which must take the remaining $(1 - \tau)T$ fractional time of the whole time slot.

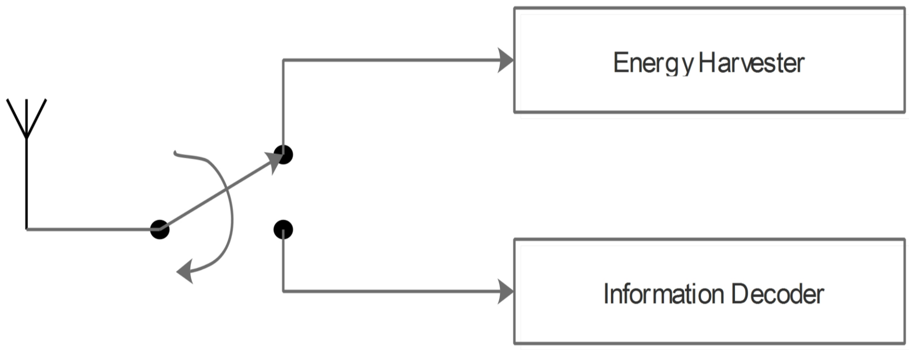

FIGURE 3.2: Time Switching Model

The time switching receiver mechanism is as shown in Fig. 3.3 where the source broadcasts its signal in the first phase. The relays will overhear the sources signal to harvest energy before decoding it. In the second phase the relays will decode the sources signal and then forward it to the destination in the third phase. The harvested energy of relays during the harvesting period τT will be a function of the sources power, RF-to-DC energy efficiency η and the source-to-relay channel gain $|h_{SR}|^2$. The relay transmit power will simply be the harvested relay energy per time taken to decode the source's information at the relay.

As shown in Figure 3.3, the time τT is the fraction of the transmission time that is taken by the relay to harvest RF energy from the source signal. The remaining $(1-\tau)T$ fraction will be divided equally among the information relaying to the source and the destination due to the half-duplex model of the relays with single-antennae.

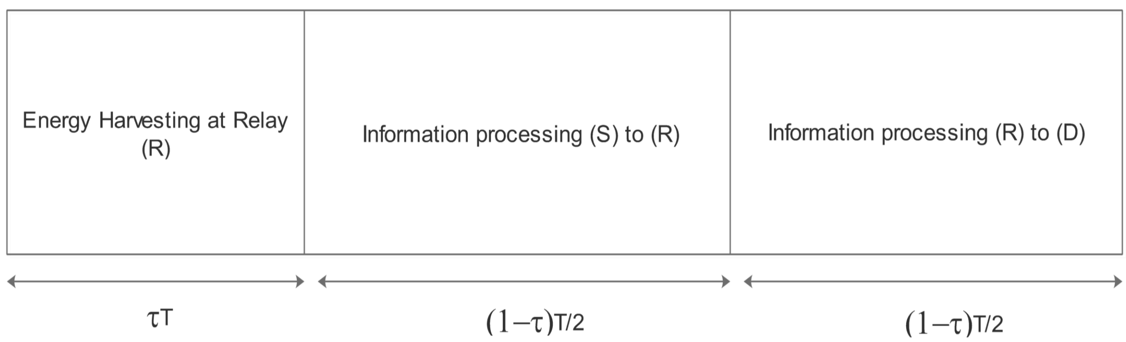

FIGURE 3.3: Time Switching Protocol frame transmission

3.4.2 Power Splitting Protocol

One of the most important energy harvesting protocols is called power splitting (PS). With PS, the power and information transfer to the energy harvesters and information decoders are simultaneously achieved through a set of power splitting devices on the same receiver. There is at least one splitting device for each receiving antenna. Unlike in time switching, with PS, RF signals also present another opportunity for wireless energy harvesting and wireless information transmission proceeding concurrently without switching receivers. Studies in [94], [95] provide performance limitations of systems with simultaneous wireless information and power transfer (SWIPT), where the receivers are able to decode information and harvest energy independently from the same RF signal. In power splitting, the receiver splits the signal into two streams of different power for decoding information and for harvesting energy separately to enable energy harvesting with simultaneous information transmission. The receiver can also dynamically adjust the splitting power ratio for information decoding and energy harvesting for CSI based systems [96].

The received signal from the antenna is initially corrupted by average white gaussian noise (AWGN) in the RF band, which is assumed to have zero mean and some equivalent baseband power. The RF-band signal is then fed into a power splitter, which is also assumed to be perfect without any noise induced [92]. Suppose after the power splitter shown in Fig. 3.4, the portion of the signal to the energy harvester block is ρ while that to the information decoder is 1-ρ. Then, the signal on the information decoder will go through the sequence of standard operations for it to be converted from RF band to baseband. In this process, the signal will be corrupted by an additional noise which is independent of the initial noise but still AWGN. The baseband power of the received RF-band signal before and after power splitting must sum to one if the antenna noise and processing noise have the same distribution [92].

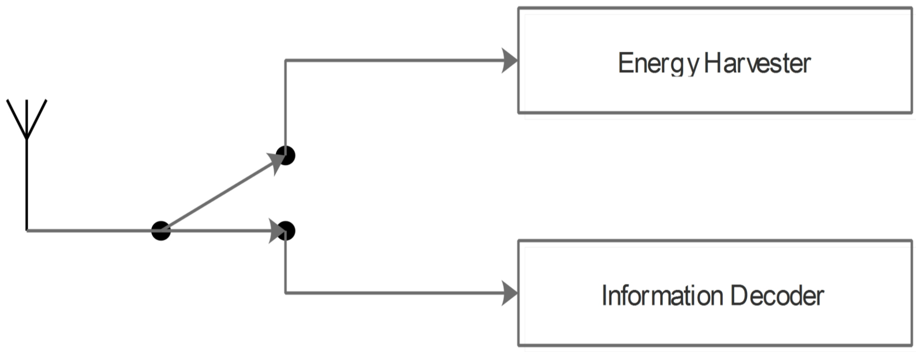

Figure 3.4: Power Splitting Model

3.5 Wireless Power Transfer in Communication

Radio Frequency (RF) energy harvesting is the best potential method for replenishing the future wireless networks. The RF radiation pattern is wide-angled; radio waves can carry both information and energy simultaneously [90]. This important phenomenon from RF harvesting can be found in applications such as cognitive radio networks, wireless body area networks and other wireless systems. RF wave radiation frequencies range from $3kHz$ (Very Low Frequency (VLF)) to $300GHz$ (Super High Frequency (SHF)) and are used as energy carriers by converting energy within them into DC (RF to DC). The amount of energy that can be harvested is reliant on the transmission power emitted from the RF source, the antenna gains of the RF source and the intermediate receiving relays, the distance of the receiving relay cluster antennae from the source antenna and the path loss exponent.

Wireless power transfer (WPT) is an EH technology that overcomes the mentioned challenges of many EH techniques in [94] such that network nodes can charge their batteries from the electromagnetic radiation. This green energy can be harvested using the most two known methods in WPT, ambient signals and/or dedicated power sources like a base station. Many contributions on WPT have focused on short distance (near-field) than long-distance (far-field) energy transmissions. Near-field distance considers the exchange of electromagnetic power over several meters while far-field distance values the exchange of wireless electromagnetic power over several kilometres [84]. Near-field WPT has many setbacks such as distance constraints, maintaining field strengths in within safety levels, high capital expenditure, difficulties in resonant inductive tuning, use of high frequencies and infeasibility of air ionization techniques [97]. Therefore, far-field techniques need to be improved further.

The integration of WPT with communication networks creates a need for technology carry-over of both the information and power simultaneously to end users. The concept of SWIPT was then derived from this requirement and was first introduced in [94] on a theoretical standpoint. Recently, the application of SWIPT has caught attention in wireless communication networks [98][99]. In this era of rolling-out 5G communication, IoT and Big Data, SWIPT technology can be of fundamental importance for energy and information transmission within types of current and future communication networks. With rapid advancement of technology, wireless transceivers are becoming power efficient and smaller in size.

RF signals are not only a power source for functional devices in the network but have distinct features for both power and information transmission combined. A simple example will be exactly like in the case of a power-line communication (PLC) which is a kind of communication technology that carries both information and power simultaneously through wired connections. The only difference is that PLC is more appropriate for in-home applications as compared to outdoor communication methods [100]. Energy efficiency and radio interference are technical problems affecting the deployment of wireless PLC devices. SWIPT as one of the promising technologies for future wireless networks can be a solution towards pushing this idea of PLC in practice becoming true. SWIPT can also ensue in desirable gains in terms of power consumption, spectral efficiency, interference management and transmission delay by enabling simultaneous transmission of both power and information [84], [94], [101].

A comprehensive survey on 5G wireless networks was done in [102] with a brief explanation about 5G energy requirements provided with the basic foundation to EH. [84] provided a regular overview of SWIPT with the latest research advances and future challenges. An essential rectifier circuit for implementation of SWIPT technology is explicated in [84] as well. A broad survey on the current research of RF EH networks was done in [99]. It covers the operation of communication protocols and circuit designs for various types of RF EH networks. In [101], exquisite smart antenna applications in SWIPT with MIMO and relaying were discussed in line with SWIPT and receiver architectures. Additional foundational aspects of EH and SWIPT technologies with respect to their recommendations were laid out in [84], [99], [101]. In [103], Ulukus summed up advances and results in EH and WPT in the perspective of signal processing, communication theory and wireless networking.

Besides EH sustaining the network lifetime it also improves fairness on selecting relays. As shown in Fig. 3.5, the schematic diagram of the WPT harvesting module to convert DC into energy and its microcontroller functional switch to a wireless transceiver for information reception and transmission.

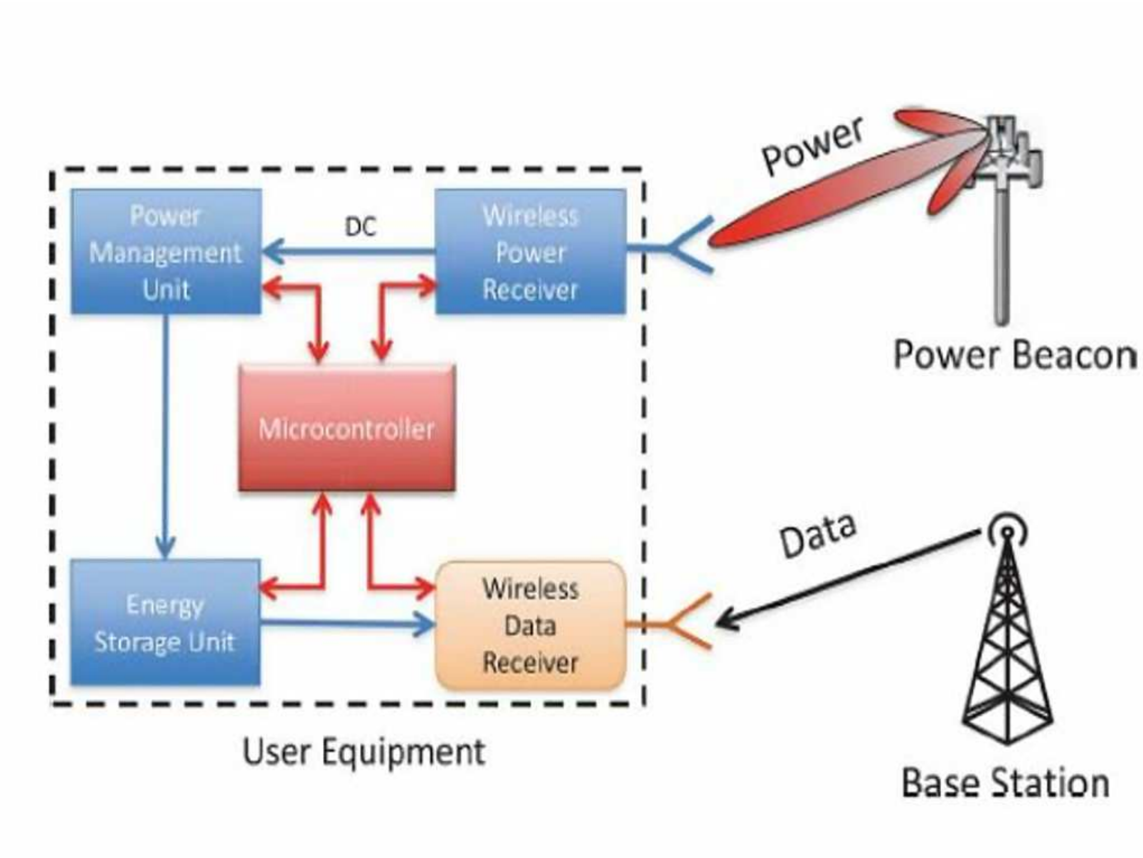

FIGURE 3.5: WPT relay architecture design modelling, copied from [2]

Albeit the assumption that the receiver has the ability to harvest and decode information simultaneously from the same RF signal, this is slightly infeasible over practical communication distances. The experimental insight on the practical implementations of wireless energy and data transfer paradigm in two-hop decode-and-forward relay has been done in [90], and it was revealed that the reliable energy transfers can only be realizable provided the inter-node distances are up to the order of 1 meter. For any inter-node distances greater than that the setup is unlikely to work.

3.6 The Future of Wireless Energy Harvesting

A lot of literature in EH focuses on discussing trade-offs and challenges between energy efficiency and network performance measures like throughput, bandwidth and delay, a few among many are [104][105]. EH promises to solve energy inefficiency in a way that avoids toxic CO_2. Based on the different geographic locations, energy can be generated from different sources like the sun light using solar cells or wind using wind turbines. For example, solar harvesting solution is mostly suited for most of African and Asian countries because of the availability of sun light for most of the day time on the other hand wind turbines harvesting are more suitable to European regions with a cloudy and windy climate.

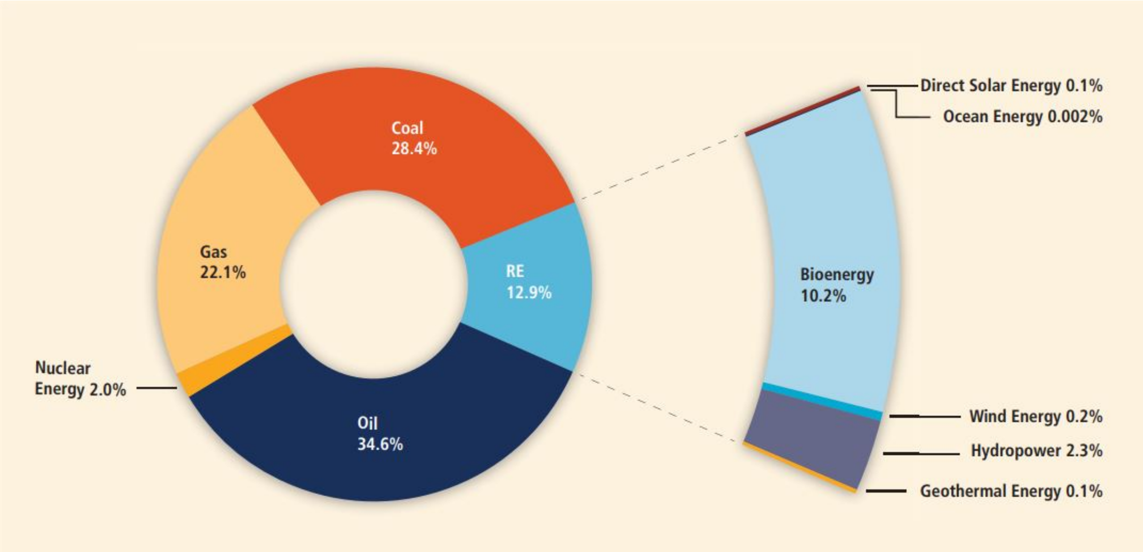

FIGURE 3.6: Shares of energy sources in global total energy supply in 2008, copied from [3]

In Fig. 3.6, a decomposed study of energy sources in global primary energy supply is shown [3]. According to [3], only 13% of the total energy supply is harvested from renewable energy sources, while toxic traditional methods still dominate on the total contributions. Although capital expenditure of setting up fully operational EH solutions making use of renewable sources might be higher than that of traditional means but the operational costs in the long run will be worth the incurred capital risk. EH solutions are a great opportunity for both enterprises and beneficiaries by mantaining a balance between infeasible costs of building a constant power supply or generator costs and service delivery.

Wireless EH has a lot of potential in applications of IoT and smart home automation projects. Smart sensor technology has capabilities of producing low power devices with advanced embedded technology typically operating at micro watt input power. Wireless sensors for temperature, humidity and proximity sensors are used in industrial, smart home and automobile industry. Wireless charging of electronic devices will be possible with an advancement in wireless energy harvesting technology. Future mobile devices will also be capable of using wire-free charging technology as an alternate power source. Wearable devices and medical sensors will use wireless energy as a power source. Advanced security devices with smart sensor technology will also make use of power from wireless energy harvesting. Its an added advantage that it operates in wireless media though there are many challenges in wireless security currently, on the other hand its also a call for a more secured wireless media. Due to the compact size of the EH modules and an increasing number of RF transmitting devices, wireless EH can easily be implemented.

3.7 Conclusion

RF energy harvesting is the potential method of energy replenishment for the next generation of wireless networks. Unlike other unpredictable energy harvesting methods that depend on environmental conditions for instance solar energy utilizing the energies of the sun, and wind energy facility using wind turbines to generate electricity at the power plant, on the contrary RF energy harvesting constraints can be predictable and on demand as well. Even though RF energy is better suited for QoS based applications, its efficiency is deemed to be small due to the low RF-to-DC conversion efficiency and it is also limited to the receiver sensitivity. This chapter discussed a detailed analysis of RF energy harvesting and its protocols. It implicates how RF charging is different from the conventional constant charging though it is a special case of a constant power charging, because the RF power received is fixed from a source transmitting constantly at a fixed distance. It can also be gathered from this chapter that RF energy plays a significant role in bridging the gap between data and energy sensitivity of the receiver. RF harvesting efficiency can also be improved by simultaneous charging of multiple nodes to meet QoS requirements of relaying nodes which in turn boosts diversity gains.

Emerging technologies like IoT will require an efficient and sustainable energy source to connect an exponentially increasing number of wireless devices and billions of smart devices and sensors for a broad spectrum of applications. Reliable and long-term sustainable energy sources are also necessary for efficient systems and networks designed to match with people's requirements. Therefore, beyond any doubt, wireless energy harvesting is an area for future developments delivering effective solutions in IoT, medical, industrial and other smart home applications.

Chapter 4

Reactive Relaying in Opportunistic RF Harvesting

4.1 Introduction

This chapter focuses on relay selection process integrated with energy harvesting at the relay nodes to mitigate wireless channel impairments. Because of increasing spectrum demands for wireless data services at low costs, cooperative relay communications can play an essential role to providing a sustainable economic development. Reactive relaying in energy harvesting networks is a promising technique to deal with channel fading. The main aim of this chapter is to actualize cooperative networking in energy harvesting networks by introducing a relay selection strategy based on the reactive relay selection approach [106], [107].

This chapter formulates and evaluates a reactive relay selection in energy harvesting networks with two relays, $K = 2$. The system model in analysis considers a source, two relays and a destination. The source frame is forwarded by the relays in two slots and only relays are capable of harvesting energy from the sources signal. The fairness in relay selection among these two relays is mainly influenced by the amount of harvested energy and relay channel gains. Outage events are evaluated over the two relays that resulted into a Markov model and a framework analysis was constructed to determine the system outage.

4.2 System Model

Figure 4.2 shows a cooperative communication model where the Source S and Destination D communicate over a channel with a fading coefficient $h_{S,D}$ and with the help of the relay terminal cluster of size K to resend original signal via fading coefficients h_{S,R_k} and $h_{R_k,D}$. All of them with single antennas and half-duplex capability in a fading wireless environment. The source-destination link is assumed not to be good enough to allow communication. Communication via the relay takes place in two stages as dictated by the inability of the relay to receive and transmit over the same frequency. The relay receives the noisy version of the signal because of channel fading, processes and retransmits it to increase capacity and improve reliability of end-to-end transmissions between S and D terminals.

In a signal block, $x_S(t)$ denotes the narrow-band transmit signal at source (S) with zero mean and $\mathbb{E}[|x_S(t)|^2] = 1$ where $\mathbb{E}(.)$ is the statistical mean operator. Since the communication is via the relay-aided link S-R_k-D, in the first half phase information transmitted from S to R_k and the received signal at the relay is,

$$y_{SR_k}(t) = \sqrt{P_S} h_{SR_k}(t) x_S(t) + n_{R_k}(t), \tag{4.1}$$

where P_S is the source transmit power, $n_{R_k}(t)$ the additive noise at R_k with zero mean and variance N_0, and $h_{SR_k}(t)$ denotes the fading coefficient between S and R_k.

In the second half phase, the received information at the relay retransmitted from R_k to D is,

$$y_{R_kD}(t) = \sqrt{P_{R_k}} h_{R_kD}(t) x_{R_k}(t) + n_D(t) \tag{4.2}$$

where $x_{R_k}(t)$ denotes the retransmitted signal at R_k and P_{R_k} is the transmit power at R_k. h_{R_kD} is the channel fading coefficient between R_k and D. $n_D(t)$ is the additive noise at the destination node with zero mean and variance N_0.

A practical model of the minimal energy required by a relay node not only to activate itself but also to transmit the source's signal and the harvested energy can be modelled as a stationary random process [108][109]. If this energy is denoted by e_a for some a^{th} signal block then its value can be assumed to be constant for the duration of the a^{th} signal block because though in reality it is time-varying but its variance is very slow as compared to variations in channel fading. If the battery capacity of the k^{th} relay node is assumed to be E_{max} then energy stored at the k^{th} relay depends on the sum of the residual energy and the difference between the harvested energy e_h and the consumed energy e_c. The energy for the next $a + 1$ transmission block can be formulated by following equation 4.3 from [26],

$$e_{a+1} = \begin{cases} e_a + e_h - e_c, & \text{if } e_a + e_h - e_c \subseteq [0, E_{max}] \\ e_a + e_h, & \text{if } e_a + e_h - e_c < 0 \\ E_{max}, & \text{if } e_a + e_h - e_c > E_{max} \end{cases} \tag{4.3}$$

The amount of energy at the a^{th} transmission block and the consumed energy during the all block are independent of each other and e_a can be regarded as a Markov stochastic process. However, for the purpose of modelling simplicity and without loss of generality, a discretized model with a large number energy states is proposed. These states are assumed to be accumulating with a fixed step energy E_0 as formulated in equation 4.4. This follows the assumption that energy accumulates in multiples of E_0 as shown in Fig. 4.2. Whenever a relay is chosen to transmit, it loses all of the accumulated E_0 energy multiples it gained from idling intervals.

$$e_{a+1}(t) = \begin{cases} e_h, & \text{if relay was chosen to transmit in block a, } e_h = E_0 \\ e_a(t) + e_h, & \text{if relay was not chosen to transmit, } e_a(t) + e_h \subseteq [nE_0, E_{max}] \end{cases} \tag{4.4}$$

The harvested energy e_h is fixed and equal to the to the step E_0. The sum of the previous block energy $e_a(t)$ and the harvested energy is the multiple of unit steps nE_0 to the maximum n^{th} step limit contraint equivalent to the battery capacity, E_{max}.

The battery size, E_{max} is the fixed multiple number of unit steps nE_0. The unit step E_0 depends on the number of states and is therefore mathematically defined as,

$$E_0 = \frac{E_{max}}{n}.$$

This unit step E_0 is directly proportional to the harvesting time τT,

$$E_0 = \frac{E_{max}}{n} \propto \frac{\tau T}{n}.$$

If it is assumed the least practical harvesting time that assures the least realizable energy is 0.2 seconds then the unit step is

$$E_0 = \frac{1}{n}.$$

If the minimum harvesting time required is doubled (2×0.2) then by proportionality the energy step is, $E_0 = \frac{2}{n}$ and if tripled (3×0.2), the step is $E_0 = \frac{3}{n}$.

All relaying nodes use time switching protocol where the receiver mechanism is divided into three phases as shown in Fig. 4.1. In the first phase the relays harvest energy from the source for a duration of τT. The decoding phase where the selected relay decodes the sources signal follows lasting for a period of $\frac{(1-\tau)T}{2}$ and in the last phase, the decoded signal at the relays is forwarded to the destination for the same period of time in decoding.

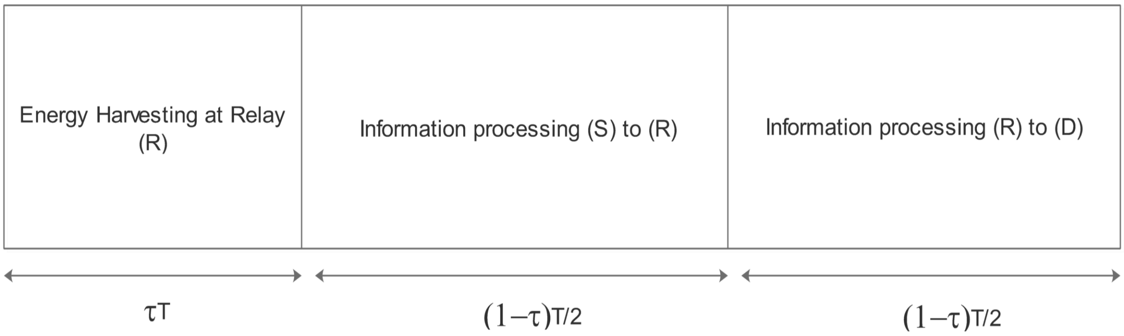

FIGURE 4.1: Time Switching Protocol frame transmission

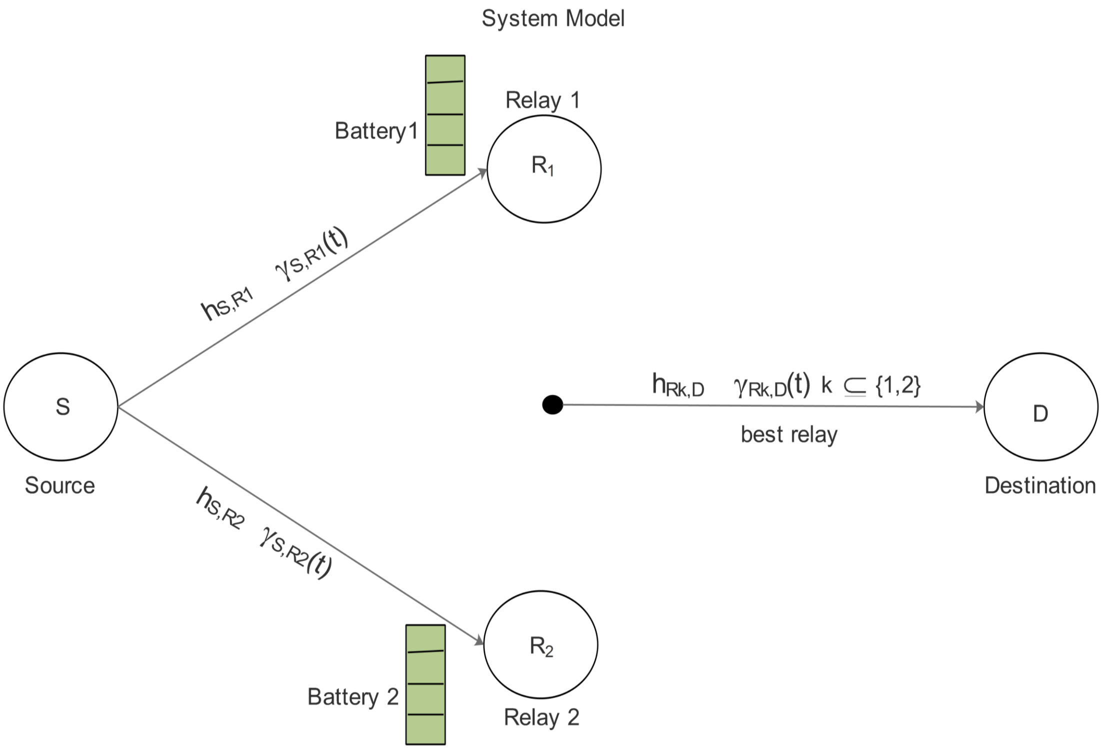

FIGURE 4.2: Reactive Relaying Network with Opportunistic RF energy harvesting model

4.2.1 Relay Selection Scheme

According to the above system model shown in Figure 4.2, a cooperative diversity network of two relays equipped with energy harvesting modules is considered. For $k \subseteq \{1, 2\}$, the k^{th} instantaneous source-relay SNR over time, $\gamma_{SR_k}(t)$ is determined. The equation 4.5 is used such that h_{SR_k} is the instantaneous channel coefficient in the current time t.

$$\gamma_{SR_k}(t) = \frac{|h_{SR_k}|^2 E_S(t)}{N_0} \tag{4.5}$$

To determine the k^{th} instantaneous relay-destination SNR, $\gamma_{R_kD}(t)$, the equation 4.6 is used.

$$\gamma_{R_kD}(t) = \frac{|h_{R_kD}|^2 E_{R_k}(t)}{N_0} \tag{4.6}$$

h_{SR_k} in 4.5 and h_{R_kD} in 4.6 are complex gaussian channel coefficients. All gain contributions are independent and identically distributed such that the envelopes of both h_{SR_k} and h_{R_kD} are Rayleigh (central chi-square) distributed. $E_S(t)$ is the transmit symbol energy of the source, $E_{R_k}(t)$ is the transmit symbol energy of the relay.

Generally, the probability density function under Rayleigh fading is given by:

$$f_\gamma(\gamma) = \frac{1}{\overline{\gamma}} \exp\left(-\frac{\gamma}{\overline{\gamma}}\right), \text{where } \overline{\gamma} \text{ is the average SNR} \tag{4.7}$$

The average SNR of the k^{th} relay node over the relay-destination link is given by equation 4.8:

$$\overline{\gamma}_{R_kD} = \frac{\mathbb{E}\{|h_{R_kD}|^2\} E_{R_k}(t)}{N_0} \tag{4.8}$$

The average SNR of the source-relay link of the k^{th} relay node is given by equation 4.9:

$$\overline{\gamma}_{SR_k} = \frac{\mathbb{E}\{|h_{SR_k}|^2\} E_S(t)}{N_0} \tag{4.9}$$

The general cumulative distribution function for the density function in equation 4.7 is given by:

$$F_\gamma(\gamma) = 1 - \exp\left(-\frac{\gamma}{\overline{\gamma}}\right) \tag{4.10}$$

This work adopted reactive opportunistic relaying where the best relay b^* is chosen after the source transmission among the cluster of $K = 2$ possible relay candidates. Each relay in the cluster is required to know its own instantaneous signal-to-noise ratio but not the phase between the link $R_k \rightarrow D$.

The best relay b^* is chosen based on the instantaneous channel strength between the $R_k \rightarrow D$ links among the two relays (R_1, R_2) and the amount of harvested energy where $k \in \{1, 2\}$:

$$b^* = \arg \max_{k \in \ \{1,2\}} (\gamma_{R_k D}) \tag{4.11}$$

4.2.2 Energy Model for a Single Relay

The energy harvesting process by relays is only performed till the end of the τT period as graphically shown in Fig. 4.1. That is, the transmit energy for a relay chosen to forward in the next frame would be the sum of harvested energy at a time and the initial energy as shown in equation 4.12.

$$E_{R_k}(t) = \alpha P_S |h_{SR_k}|^2 \tau T + E_{R_k}(t-1), \tag{4.12}$$

where α is the energy harvesting efficiency but for purposes of complexity it has been fixed.

It is assumed that a relay chosen to transmit during at a certain time frame exhausts all its energy, and hence its energy during the next frame is only from harvesting and is given by equation 4.13.

$$E_{R_k}(t) = \alpha P_S |h_{SR_k}|^2 \tau T, \tag{4.13}$$

where α is the energy harvesting efficiency due to the RF-to-DC conversion with the harvesting period τT. Hence, the energy of the k^{th} relay is given by equation 4.12 or equation 4.13 on the basis of whether it was chosen to transmit in the previous time frame.

The transmission power of the k^{th} relay is dependent on the transmit energy of the relay and both a function of source transmit power, P_S, is represented as:

$$P_{R_k}(t) = \frac{2E_{R_k}(t)}{(1-\tau)T} \tag{4.14}$$

There are only two probability events in reactive relay selection, either the relay is chosen to transmit or not, events=$\{Transmit, Transmit^{\complement}\}$ where $\complement$ is the complement, in this instance meaning relay not chosen for transmission.

According to the above set of events in reactive relaying, it can be proven that RF energy arrivals in relay harvesting modules are purely Markovian because of the time-varying relay channel gains. The main assumption is that all energy is only expended during transmission, otherwise it accumulates in the battery until the battery is full.

Since the direct link is in deep fade and communication is via relay selection of the best $b^* \rightarrow D$ link, if we also assume E_0 to be the required minimum relay energy for transmission then this phenomena translates into two interesting generic states for energies of both relays: $(1, j)$ and $(i, 1)$, where $i \neq 1$ and $j \neq 1$ are energy gaining factors of R_1 and R_2 respectively. This is due to the fact that only one relay can transmit at a time.

Fig. 4.3 is the energy quantization of the single relay with n energy states when chosen and not chosen for transmission.

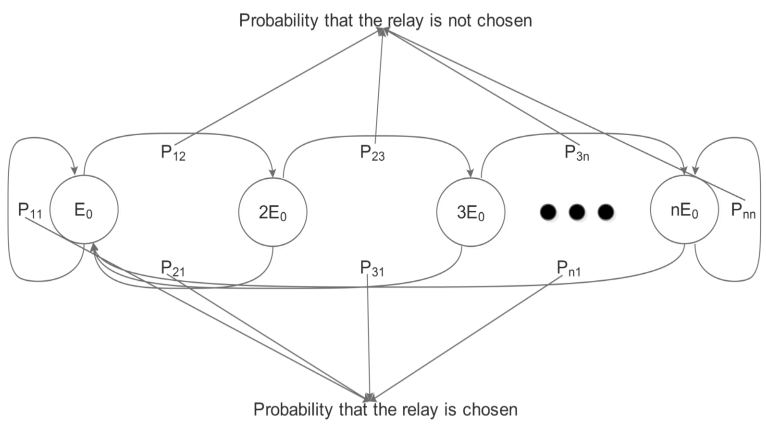

FIGURE 4.3: Single relay energy quantizations in transmission and idle mode

4.2.3 Markovian Analysis for a two-relay System

A full Markov model for a two-relay system incorporating relays, R_1, R_2 and their energy transitions was designed as derived from an energy evolution model of a one relay in 4.3 from the above subsection.

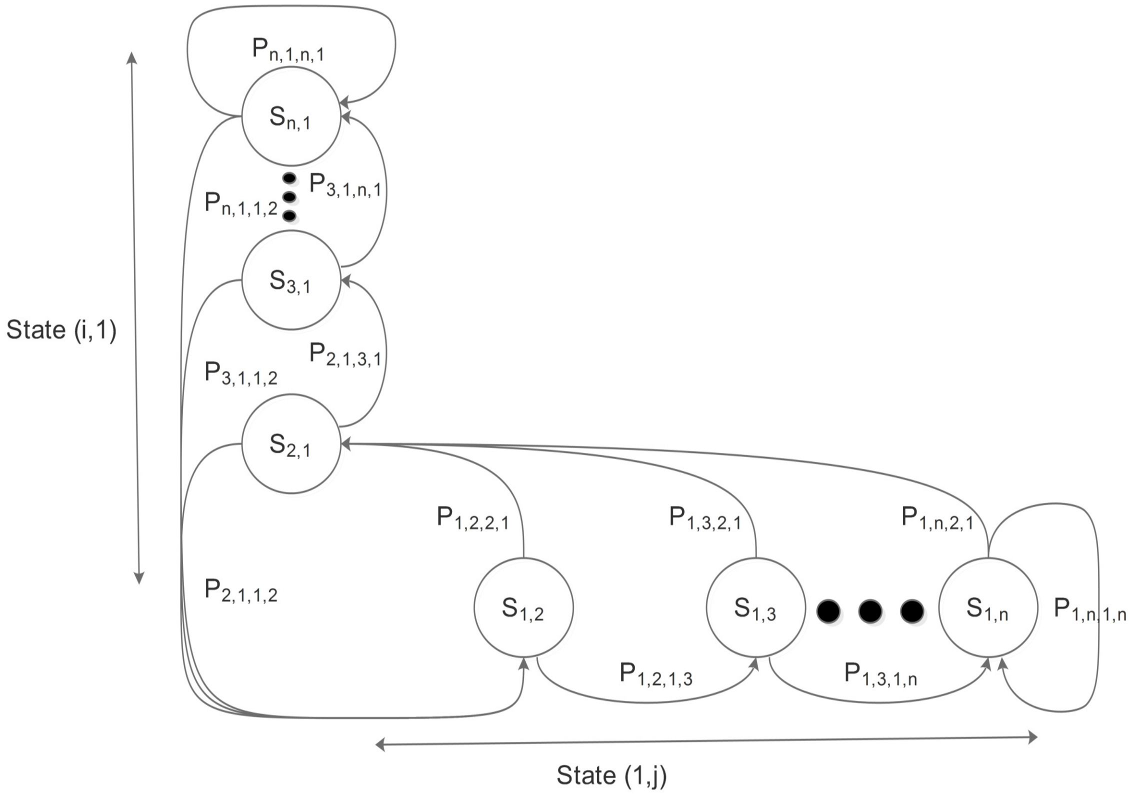

FIGURE 4.4: System states transitions for Reactive Relaying in 4.2

Definition of States: The states are represented as $S_{i,j}$ where $i \Rightarrow$ Relay 1 energy state and $j \Rightarrow$ Relay 2 energy state for e.g. $S_{1,2}$ means relay 1 has E_0 of energy while relay 2 has $2E_0$ energy units.

- $S_{1,j}$: Refers to a state where R_1 has a unit energy and R_2 has j energy units, such that $j \subseteq \{1, ..., n\}$.
- $S_{i,1}$: This state is the opposite of the state $S_{1,j}$, relay R_2 has a unit energy while R_1 has i energy units, where $i \subseteq \{1, ..., n\}$.

Assumption: The system at an instance of time can only be in the state $(1, j)$ or $(i, 1)$ with an adoption of the literature energy harvesting concept where all the energy gained is expended during transmission [26].

4.2.3.1 n-State Transition Matrix for the System

The probability of being in a particular state (i, j) is $\pi_{i,j}^{2D}$, for e.g. $\pi_{1,2}^{2D}$ is the probability that the system is in state $S_{1,2}$ and likewise the same convention was also followed for the remaining states and probabilities. That is probabilities $\pi_{2,1}^{2D}$, $\pi_{1,n}^{2D}$, $\pi_{n,1}^{2D}$ would be for the following states $S_{2,1}$, $S_{1,n}$, $S_{n,1}$ accordingly. From this probability convention then another one can be drawn from it for the transition probabilities. That is for the system to transition from state $S_{1,2}$ to $S_{2,1}$ would be denoted as $P_{1,2,2,1}$. In the similar fashion, probabilities for system state transitions from $S_{1,n}$ to $S_{1,n}$, from $S_{2,1}$ to $S_{1,2}$, from $S_{n,1}$ to $S_{n,1}$ were denoted as $P_{1,n,1,n}$, $P_{2,1,1,2}$, $P_{n,1,n,1}$ accordingly.

The state transitioning of the above explained states is as follows, $P_{(i_1,j_1,i_2,j_2)}$: $S_{(i_1,j_1)} \Rightarrow S_{(i_2,j_2)}$ where $S_{(i_1,j_1)}$ is the initial state for initial R_1,R_2 energy and $S_{(i_2,j_2)}$ is the final state for both R_1,R_2 energy.

Due to the nature of the Markovian model in Fig. 4.4 which ignored a higher proportionate number of other states despite the fact that it is two-dimensional $(2D)$ then it could be stretched and simplified into and solved as a one-dimensional $(1D)$ model. This was useful as transition matrix was also simplified from $2D$ to $1D$. After a simplified stretching the $2D$ states (i,j) were then formulated and mapped into a $1D$ variable (q).

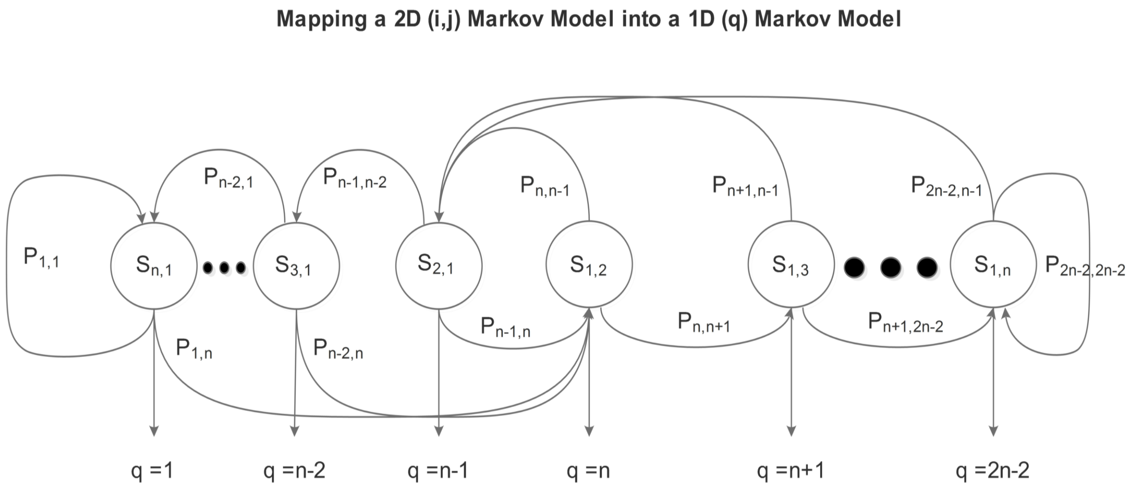

FIGURE 4.5: Mapping a $2D$ (i,j) Markov model into a linear $1D$ (q) Markov model

The case equation in 4.15 shows the mathematical relationship on the mapping of $2D$ state (i,j) into $1D$ state (q).

$$q = \begin{cases} n + (j-2), & \text{if } i = 1 \\ n + (1-i), & \text{if } j = 1 \end{cases} \tag{4.15}$$

Where n is the total number of states in an n-state Markov model.

The generalized transition matrix for n states in $1D$ form for the model in Fig. 4.4 is given by matrix 4.16.

$$P_{transition} = \begin{Bmatrix} P_{n,1,n,1} & ... & 0 & 0 & P_{n,1,1,2} & 0 & ... & 0 \\ P_{3,1,n,1} & ... & 0 & 0 & P_{3,1,1,2} & 0 & ... & 0 \\ 0 & ... & P_{2,1,3,1} & 0 & P_{2,1,1,2} & 0 & ... & 0 \\ 0 & ... & 0 & P_{1,2,2,1} & 0 & P_{1,2,1,3} & ... & 0 \\ 0 & ... & 0 & P_{1,3,2,1} & 0 & 0 & ... & P_{1,3,1,n} \\ 0 & ... & 0 & P_{1,n,2,1} & 0 & 0 & ... & P_{1,n,1,n} \end{Bmatrix} \tag{4.16}$$

The generalized transition matrix for n states after remapping the model into a special $1D$ Markov model as done in Fig. 4.5 is as shown in matrix 4.17.

$$P_{transition} = \begin{Bmatrix} Q_{1,1} & ... & 0 & 0 & Q_{1,n} & 0 & ... & 0 \\ ... & ... & ... & ... & ... & ... & ... & ... \\ Q_{n-2,1} & ... & 0 & 0 & Q_{n-2,n} & 0 & ... & 0 \\ 0 & ... & Q_{n-1,n-2} & 0 & Q_{n-1,n} & 0 & ... & 0 \\ 0 & ... & 0 & Q_{n,n-1} & 0 & Q_{n,n+1} & ... & 0 \\ 0 & ... & 0 & Q_{n+1,n-1} & 0 & 0 & ... & Q_{n+1,2n-2} \\ 0 & ... & 0 & Q_{2n-2,n-1} & 0 & 0 & ... & Q_{2n-2,2n-2} \end{Bmatrix} \tag{4.17}$$

An example transition matrix for $n = 3$ when there are only 2 states $\{S_{1,2}, S_{1,3}, S_{2,1}, S_{3,1}\}$ in $2D$ model but 4 states all in a stretched $1D$ model, looks like 4.18,

$$P_{transition} = \begin{Bmatrix} P_{3,1,3,1} & 0 & 0 & P_{3,1,1,2} \\ P_{2,1,3,1} & 0 & P_{2,1,1,2} & 0 \\ 0 & P_{1,2,2,1} & 0 & P_{1,2,1,3} \\ 0 & P_{1,3,2,1} & 0 & P_{1,3,1,3} \end{Bmatrix} = \begin{Bmatrix} Q_{1,1} & Q_{1,2} & Q_{1,3} & Q_{1,4} \\ Q_{2,1} & Q_{2,2} & Q_{2,3} & Q_{2,4} \\ Q_{3,1} & Q_{3,2} & Q_{3,3} & Q_{3,4} \\ Q_{4,1} & Q_{4,2} & Q_{4,3} & Q_{4,4} \end{Bmatrix} \tag{4.18}$$

4.3 Performance Analysis

4.3.1 Evaluation of Transitional Probabilities

Conditions to avoid outage using reactive relay selection scheme:

- The relay-destination SNR ratio γ_{RD} must be greater than the threshold SNR γ_{th}.

If the target data rate is r_{th}, then this would result into the threshold SNR γ_{th} given by $\gamma_{th} = 2^{2r_{th}} - 1$ as derived in Shannon-Hartley theorem of the amount of information a channel can carry or channel capacity.

For the time τT of the time slot taken to harvest energy from the source the remaining time $(1-\tau)T$ is equally split between decoding and transmission to the destination node into $\frac{(1-\tau)T}{2}$ seconds.

If the system is assumed to be in state $(i, 1)$ where relay 1 is chosen, then transmit powers of R_1 and R_2 can be defined as follows:

$$P_{R_1} = \frac{iE_0}{((1-\tau)T)/2}, \text{Transmit power if relay 1 is chosen} \tag{4.19}$$

$$P_{R_2} = \frac{E_0}{((1-\tau)T)/2}, \text{Transmit power if relay 2 is chosen} \tag{4.20}$$

The instantaneous Source-to-Relay Signal-to-noise ratios of both relay R_1 and R_2 are respectively expressed as:

$$\gamma_{SR_1} = \frac{P_S|h_{SR_1}|^2}{N_0}, \text{for relay 1} \tag{4.21}$$

$$\gamma_{SR_2} = \frac{P_S|h_{SR_2}|^2}{N_0}, \text{for relay 2} \tag{4.22}$$

The instantaneous Relay-to-Destination Signal-to-noise ratios of both relay R_1 and R_2 are respectively as per the equations below:

$$\gamma_{R_1D} = \frac{iE_0}{((1-\tau)T)N_0/2}|h_{R_1D}|^2, \text{for relay 1} \tag{4.23}$$

$$\gamma_{R_2D} = \frac{E_0}{((1-\tau)T)N_0/2}|h_{R_2D}|^2, \text{for relay 2} \tag{4.24}$$

The relay selection criteria is as given in equation 4.11 which is based on the maximum between either of these two $(\gamma_{R_1D}, \gamma_{R_2D})$.

Now the probability of choosing relay 1 given all the other equations and the assumption above would be:

$$Pr\{\gamma_{b^*} = \gamma_{R_1D}\} = Pr\{\gamma_{R_1D} > \gamma_{R_2D}\} = Pr\{\gamma_{R_1D} - \gamma_{R_2D} > 0\} \tag{4.25}$$

For the density function, the convention that the parameter of the exponential distribution is its mean rather than the reciprocal of its mean was used. For the independent random variables γ_{R_1D} and γ_{R_2D}, assuming $Z = \gamma_{R_1D} - \gamma_{R_2D}$, then the density of Z can be determined using 4.7.

The cumulative probability distribution of Z was obtained using equation 4.10 with works from [110]-[111] to give the following equation,

$$\begin{aligned} F_Z(z) &= Pr\{\gamma_{R_1D} - \gamma_{R_2D} \leq z\} \\ &= \int_{y=0}^{\infty} Pr\{\gamma_{R_1D} \leq z + \gamma_{R_2D} | \gamma_{R_2D} = y\} f_{\gamma_{R_2D}}(y) dy \\ &= \int_{y=0}^{\infty} F_{\gamma_{R_1D}}(z + \gamma_{R_2D}) f_{\gamma_{R_2D}}(y) dy \end{aligned} \tag{4.26}$$

To get the density function, a differentiation of the above CDF with respect to z was done and it resulted in:

$$\begin{aligned} f_Z(z) &= \int_{y=0}^{\infty} F_{\gamma_{R_1D}}(z + \gamma_{R_2D}) f_{\gamma_{R_2D}}(y) dy \\ &= \int_{y=max(0,-z)}^{\infty} f_{\gamma_{R_1D}}(z + \gamma_{R_2D}) f_{\gamma_{R_2D}}(y) dy \\ &= \int_{y=max(0,-z)}^{\infty} \frac{1}{\overline{\gamma}_{R_1D}} \exp\left(-\frac{z+y}{\overline{\gamma}_{R_1D}}\right) \frac{1}{\overline{\gamma}_{R_2D}} \exp\left(-\frac{y}{\overline{\gamma}_{R_2D}}\right) dy \\ &= \frac{\exp\left(\frac{-z}{\overline{\gamma}_{R_1D}}\right)}{\overline{\gamma}_{R_1D} + \overline{\gamma}_{R_2D}} \int_{y=max(0,-z)}^{\infty} \frac{\overline{\gamma}_{R_1D} + \overline{\gamma}_{R_2D}}{\overline{\gamma}_{R_1D} \cdot \overline{\gamma}_{R_2D}} \exp\left(-y\left(\frac{1}{\overline{\gamma}_{R_1D}} + \frac{1}{\overline{\gamma}_{R_2D}}\right)\right) dy \\ &= \frac{\exp\left(\frac{-z + min(0,z)}{\overline{\gamma}_{R_1D}} + \frac{min(0,z)}{\overline{\gamma}_{R_2D}}\right)}{\overline{\gamma}_{R_1D} + \overline{\gamma}_{R_2D}} \end{aligned} \tag{4.27}$$

Then, finally the density function can be expressed as:

$$f_Z(z) = \begin{cases} \dfrac{\exp\left(-\dfrac{z}{\overline{\gamma}_{R_2D}}\right)}{\overline{\gamma}_{R_1D} + \overline{\gamma}_{R_2D}}, & \text{if } \gamma_{R_1D} < \gamma_{R_2D} \\ \\ \dfrac{\exp\left(-\dfrac{z}{\overline{\gamma}_{R_1D}}\right)}{\overline{\gamma}_{R_1D} + \overline{\gamma}_{R_2D}}, & \text{if } \gamma_{R_1D} > \gamma_{R_2D} \end{cases} \tag{4.28}$$

Integrating the above PDFs expression to get the CDFs as:

$$F_Z(z) = \begin{cases} \dfrac{\overline{\gamma}_{R_2D}}{\overline{\gamma}_{R_1D} + \overline{\gamma}_{R_2D}} \exp\left(-\dfrac{z}{\overline{\gamma}_{R_2D}}\right), & \text{if } \gamma_{R_1D} < \gamma_{R_2D} \\ \\ \dfrac{\overline{\gamma}_{R_1D}}{\overline{\gamma}_{R_1D} + \overline{\gamma}_{R_2D}} \exp\left(-\dfrac{z}{\overline{\gamma}_{R_2D}}\right), & \text{if } \gamma_{R_1D} > \gamma_{R_2D} \end{cases} \tag{4.29}$$

At $z = 0$ then the distribution functions are:

$$F_Z(z) = \begin{cases} \dfrac{\overline{\gamma}_{R_2D}}{\overline{\gamma}_{R_1D} + \overline{\gamma}_{R_2D}}, & \text{if } \gamma_{R_1D} < \gamma_{R_2D} \\ \\ \dfrac{\overline{\gamma}_{R_1D}}{\overline{\gamma}_{R_1D} + \overline{\gamma}_{R_2D}}, & \text{if } \gamma_{R_1D} > \gamma_{R_2D} \end{cases} \tag{4.30}$$

4.3.2 Deduction of Transitional Probabilities

Based on the definition of transitional probabilities in equation 4.30 and considering the case when the system is in state $S_{i,j}$ such that $i \neq 1$, $j = 1$, then the final state $S_{i,j}$ would be given by the following probabilities:

Case 1: if relay 1 is chosen then the probability is as below:

$$\begin{aligned}
P_{i,1,1,2} &= Pr\{\gamma_{b^*} = max(\gamma_{R_1D}, \gamma_{R_2D})\} \\
&= Pr\{P_{R_1D}|h_{R_1D}|^2 > P_{R_2D}|h_{R_2D}|^2\} \\
&= Pr\left\{\frac{iE_0}{(1-\tau)/2}|h_{R_1D}|^2 > \frac{E_0}{(1-\tau)/2}|h_{R_2D}|^2\right\} \\
&= \begin{cases} \dfrac{1}{1+\dfrac{i\mathbb{E}\{|h_{R_1D}|^2\}}{\mathbb{E}\{|h_{R_2D}|^2\}}}, & \text{if } |h_{R_1D}|^2 < |h_{R_2D}|^2 \\ \dfrac{1}{1+\dfrac{\mathbb{E}\{|h_{R_2D}|^2\}}{i\mathbb{E}\{|h_{R_1D}|^2\}}}, & \text{if } |h_{R_1D}|^2 > |h_{R_2D}|^2 \end{cases}
\end{aligned} \tag{4.31}$$

Case 2: if relay 2 is chosen then the probability is as below:

$$\begin{aligned}
P_{i,1,1+i,1} &= Pr\{\gamma_{b^*} = max(\gamma_{R_2D}, \gamma_{R_1D})\} \\
&= Pr\{P_{R_2D}|h_{R_2D}|^2 > P_{R_1D}|h_{R_1D}|^2\} \\
&= Pr\left\{\frac{E_0}{(1-\tau)/2}|h_{R_2D}|^2 > \frac{iE_0}{(1-\tau)/2}|h_{R_1D}|^2\right\} \\
&= \begin{cases} \dfrac{1}{1+\dfrac{\mathbb{E}\{|h_{R_2D}|^2\}}{i\mathbb{E}\{|h_{R_1D}|^2\}}}, & \text{if } |h_{R_2D}|^2 < |h_{R_1D}|^2 \\ \dfrac{1}{1+\dfrac{i\mathbb{E}\{|h_{R_1D}|^2\}}{\mathbb{E}\{|h_{R_2D}|^2\}}}, & \text{if } |h_{R_2D}|^2 > |h_{R_1D}|^2 \end{cases}
\end{aligned} \tag{4.32}$$

Now, when the system is in state S_{i_1,j_1} such that $i = 1$,$j \neq 1$, then the final state S_{i_2,j_2} is given by the following probabilities:

Case 1: if relay 2 is chosen then the probability is as below:

$$\begin{aligned}
P_{1,j,2,1} &= Pr\{\gamma_{b^*} = max(\gamma_{R_2D}, \gamma_{R_1D})\} \\
&= Pr\{P_{R_2D}|h_{R_2D}|^2 > P_{R_1D}|h_{R_1D}|^2\} \\
&= Pr\left\{\frac{jE_0}{(1-\tau)/2}|h_{R_2D}|^2 > \frac{E_0}{(1-\tau)/2}|h_{R_1D}|^2\right\} \\
&= \begin{cases} \dfrac{1}{1+\dfrac{j\mathbb{E}\{|h_{R_2D}|^2\}}{\mathbb{E}\{|h_{R_1D}|^2\}}}, & \text{if } |h_{R_2D}|^2 < |h_{R_1D}|^2 \\ \dfrac{1}{1+\dfrac{\mathbb{E}\{|h_{R_1D}|^2\}}{j\mathbb{E}\{|h_{R_2D}|^2\}}}, & \text{if } |h_{R_2D}|^2 > |h_{R_1D}|^2 \end{cases}
\end{aligned} \tag{4.33}$$

Case 2: if relay 1 is chosen then the probability is as below:

$$\begin{aligned}
P_{1,j,1,j+1} &= Pr\{\gamma_{b^*} = max(\gamma_{R_1D}, \gamma_{R_2D})\} \\
&= Pr\{P_{R_1D}|h_{R_1D}|^2 > P_{R_2D}|h_{R_2D}|^2\} \\
&= Pr\left\{\frac{E_0}{(1-\tau)/2}|h_{R_1D}|^2 > \frac{jE_0}{(1-\tau)/2}|h_{R_2D}|^2\right\} \\
&= \begin{cases} \dfrac{1}{1+\dfrac{\mathbb{E}\{|h_{R_1D}|^2\}}{j\mathbb{E}\{|h_{R_2D}|^2\}}}, & \text{if } |h_{R_1D}|^2 < |h_{R_2D}|^2 \\ \dfrac{1}{1+\dfrac{j\mathbb{E}\{|h_{R_2D}|^2\}}{\mathbb{E}\{|h_{R_1D}|^2\}}}, & \text{if } |h_{R_1D}|^2 > |h_{R_2D}|^2 \end{cases}
\end{aligned} \tag{4.34}$$

4.3.3 Derivation of the steady-state probabilities

To determine the probability of being in a particular system state, a steady-state equation in 4.35 was used for a $2D$ state and equation in 4.37 for an equivalent $1D$ state.

$$\pi_{i,j}^{2D} = P_{transition}^{2D}\pi_{i,j}^{2D} \tag{4.35}$$

$P_{transition}^{2D}$ is called the transition probability matrix and $\pi_{i,j}^{2D}$ is the steady-state probability vector. $P_{transition}^{2D}$ is a stochastic matrix for each row i and all the columns add to 1. The steady-state is such that,

$$\sum_{i=1}^{n}\sum_{j=1}^{n}\pi_{transition}^{2D} = 1 \tag{4.36}$$

The derivations of state probabilities when the system is reduced to $1D$ were as follows:

$$\pi_q^{1D} = P_{transition}^{1D}\pi_q^{1D} \tag{4.37}$$

By the law of total probability, all the state probabilities must add to 1,

$$\sum_{q=1}^{2n-2}\pi_q^{1D} = 1 \tag{4.38}$$

Where $\pi_{i,j}^{2D}$ and π_q^{1D} are steady-state vectors (or a steady-state distributions), $P_{transition}^{2D}$ and $P_{transition}^{1D}$ are the probability transition matrices hence the determination of the system state at the steady state.

4.3.4 Derivation of probability of outage

There is outage only when the last hop, b^*(best relay) $\rightarrow D$ is in outage which basically means the SNR of the chosen relay falls below the threshold SNR, $\gamma_{R_kD} < \gamma_{th}$. For the best relay b^*, then probability of the system outage would be the probability that the best relay SNR is less than the threshold, $\gamma_{b^*} < \gamma_{th}$. With the assumption that the system is in state $(i, 1)$ then $b^* = R_2$, $\gamma_{b^*} = \gamma_{R_2D}$. An adoption of the probability density function was clearly enunciated in equation 4.7. The corresponding cumulative distributive function followed is also as formulated in equation 4.10.

As relay R_2 represents the best relay in this instance, then the outage of the system can be expressed as follows:

$$F_{\gamma_{R_2D}}(\gamma_{th})|_{(i,1)} = Pr[P_{R_2}|h_{R_2D}|^2 < \gamma_{th}] = 1 - \exp\left(\frac{-\gamma_{th}}{\frac{P_{R_2D}\mathbb{E}\{|h_{R_2D}|^2\}}{N_0}}\right) \tag{4.39}$$

Using the link outage expression in equation 4.39 what follows also is the formulation of respective outage expressions of relay R_1 and R_2 when the system is in the state $(i,1)$ and the state $(1,j)$.

The link outage of relay R_1 when the system is in state $(i,1)$ implying $i \neq 1, j = 1$ and substituting γ_{R_1D} with the expectation of equation 4.23,

$$\begin{aligned} P_{out_1}|_{(i\neq 1, j=1)} &= 1 - \exp\left(\frac{-\gamma_{th}}{\overline{\gamma}_{R_1D}}\right) \\ &= 1 - \exp\left(\frac{-\gamma_{th}}{\frac{\frac{iE_0\mathbb{E}\{|h_{R_1D}|^2\}N_0}{(1-\tau)T}}{2}}\right) \\ &= 1 - \exp\left(\frac{-2\gamma_{th}}{iE_0(1-\tau)T\mathbb{E}\{|h_{R_1D}|^2\}N_0}\right) \end{aligned} \tag{4.40}$$

The link outage of relay R_2 when the system is in state $(1,j)$ entailing $i = 1, j \neq 1$ and substituting γ_{R_2D} with the static expectation of equation 4.24,

$$\begin{aligned} P_{out_2}|_{(i=1, j\neq 1)} &= 1 - \exp\left(\frac{-\gamma_{th}}{\overline{\gamma}_{R_2D}}\right) \\ &= 1 - \exp\left(\frac{-\gamma_{th}}{\frac{\frac{jE_0\mathbb{E}\{|h_{R_2D}|^2\}N_0}{(1-\tau)T}}{2}}\right) \\ &= 1 - \exp\left(\frac{-2\gamma_{th}}{jE_0(1-\tau)T\mathbb{E}\{|h_{R_2D}|^2\}N_0}\right) \end{aligned} \tag{4.41}$$

4.3.5 Derivation of Overall System Outage

It is apparent to note that the system outage would be the sum of the outage due to relay R_1 at system state $i \neq 1, j = 1$ and relay R_2 at state $i = 1, j \neq 1$. The overall system outage probability would then be given by the following equation,

$$\begin{aligned} P_{out|(i,j)} &= \sum_{i=2}^{n} [P_{out_1|(i\neq 1,j=1)} \pi_{i,1}^{2D}] + \sum_{j=2}^{n} [P_{out_2|(i=1,j\neq 1)} \pi_{1,j}^{2D}]. \\ &= \sum_{q=1}^{n-1} [P_{out_1|(i=q+1,j=1)} \pi_{q}^{1D}] + \sum_{q=n}^{2n-2} [P_{out_2|(i=1,j=\frac{q+2}{2})} \pi_{q}^{1D}] \end{aligned} \quad (4.42)$$

4.4 Numerical Results and Simulations

This section illustrates the results developed by numerical simulations. Without loss of generality, it was assumed that the minimum acceptable rate r is 1 bps. Moreover, it was also assumed that the number of relays K is 2 and average SNRs $\overline{\gamma}_{SR_k} = \frac{\mathbb{E}\{|h_{SR_k}|^2\}E_S}{N_0}$, $\overline{\gamma}_{R_kD} = \frac{\mathbb{E}\{|h_{R_kD}|^2\}E_{R_k}}{N_0}$ for harvesting times $\tau = 0.2$, 0.4 and 0.6 seconds. The transition matrix is calculated from SNR values of the two relays depending on which was selected when the other was harvesting. Fig. 4.7 and 4.8 illustrate the outage probability of a cooperative network as a function of SNR when the relays are harvesting energy for $\tau = 0.2$ seconds with four system states while Fig. 4.12 and 4.13 illustrate results for three steady states under the same conditions. The analytical results were also aligned with the Monte Carlo simulations for both 4 and 3 system states accordingly.

4.4.1 The performance analysis of Four states

The attached Fig. 4.6 showed the analytical simulations aligned with the Monte Carlo simulations for 4 energy states.

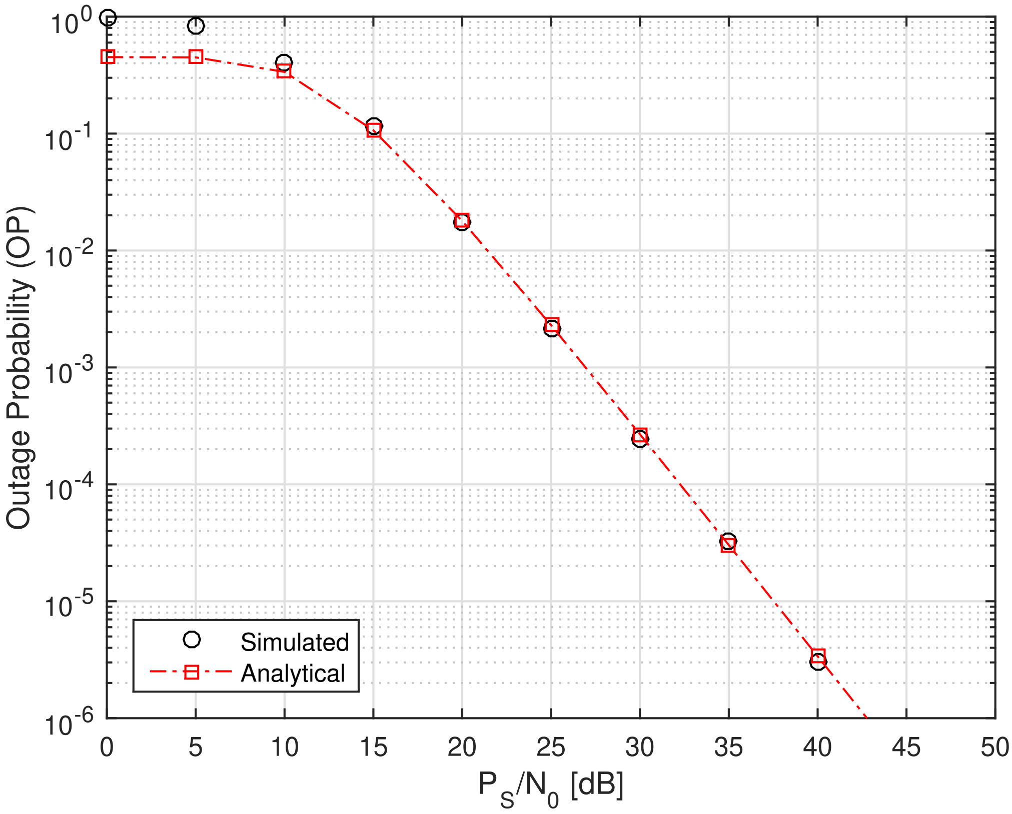

FIGURE 4.6: Monte Carlo simulations and analytical results for 4 Energy states Quantization, harvesting time $\tau = 0.2$ seconds

The results in Fig. 4.6 is a validation that the proposed analytical model is practically realizable because it matches the simulation framework. The same approach was also followed with 3 energy states per relay as a matter of showcasing that the concept holds for any number of energy states, n.

The outage behaviour of the enlisted four states $(\pi_{1,5}^{2D}, \pi_{1,4}^{2D}, \pi_{1,3}^{2D}, \pi_{1,2}^{2D}, \pi_{2,1}^{2D}, \pi_{3,1}^{2D}, \pi_{4,1}^{2D}, \pi_{5,1}^{2D})$ with bit rate, $r = 1Bit/s$ and $\tau = 0.2$ seconds, the following results were obtained,

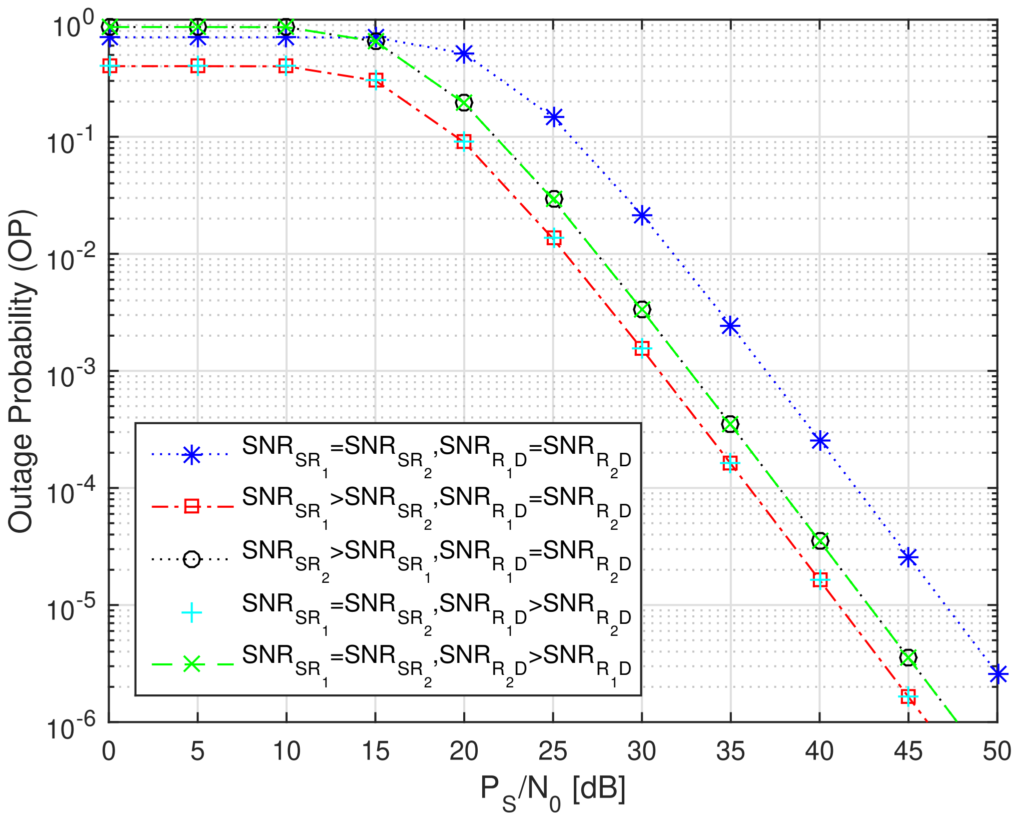

FIGURE 4.7: Results with 4 Energy states Quantization and variable average SNRs, harvesting time $\tau = 0.2$ seconds, where SNR on the legend is the average $\overline{\gamma}$ of the link.

The results in Fig. 4.7 show the performance of four harvesting states with variable average SNRs. The performance is observed when all the average S-R and R-D SNRs are equal, when S-R_1 > S-R_2 or S-R_1 < S-R_2 with fixed R-D values of both relays and lastly when R_1-D > R_2-D or R_1-D < R_2-D with fixed S-R values for both relays. All the SNR variations were done with a fixed harvesting time of 0.2 seconds. Since the relay selection scheme is mainly based on the reactive relay-destination link, therefore it can be deduced from the plot that highest R-D link performs better. From these results, it can be concluded that the higher the SNR of a transmitting link the higher the probability of selecting such a link and the lower the system outage meaning a better uptime.

All the intermediate results acquired with variable SNR conditions mainly including the transition probabilities and steady-state probabilities are presented in tables below. A simple correlation can be observed when all average SNRs are equal that the state probabilities of either relaying via R_1 or R_2 is equal. When average SNRs are such that $\gamma_{R_1D} > \gamma_{R_2D}$, the state probabilities of using R_1 to relay are higher than using R_2, likewise the state probabilities of using R_2 if $\gamma_{R_2D} > \gamma_{R_1D}$ are also higher.

The intermediate values for the outage results in Fig. 4.7 when $\overline{\gamma}_{SR_1} = \overline{\gamma}_{SR_2}$ and $\overline{\gamma}_{R_1D} = \overline{\gamma}_{R_2D}$,

TABLE 4.1: Estimated state transition matrix for Fig. 4.7

		F	i	n	a	l	(q)		
		$\pi^{2D}_{1,5}$	$\pi^{2D}_{1,4}$	$\pi^{2D}_{1,3}$	$\pi^{2D}_{1,2}$	$\pi^{2D}_{2,1}$	$\pi^{2D}_{3,1}$	$\pi^{2D}_{4,1}$	$\pi^{2D}_{5,1}$
I	$\pi^{2D}_{1,5}$	0.1667	0	0	0	0.8333	0	0	0
n	$\pi^{2D}_{1,4}$	0.2000	0	0	0	0.8000	0	0	0
i	$\pi^{2D}_{1,3}$	0	0.2500	0	0	0.7500	0	0	0
t	$\pi^{2D}_{1,2}$	0	0	0.3333	0	0.6667	0	0	0
i	$\pi^{2D}_{2,1}$	0	0	0	0.6667	0	0.3333	0	0
a	$\pi^{2D}_{3,1}$	0	0	0	0.7500	0	0	0.2500	0
l	$\pi^{2D}_{4,1}$	0	0	0	0.8000	0	0	0	0.2000
(q)	$\pi^{2D}_{5,1}$	0	0	0	0.8333	0	0	0	0.1667

TABLE 4.2: Estimated steady-state vector for Fig. 4.7

$\pi^{2D}_{1,5} = \pi^{1D}_{q=1}$	0.0070
$\pi^{2D}_{1,4} = \pi^{1D}_{q=2}$	0.0290
$\pi^{2D}_{1,3} = \pi^{1D}_{q=3}$	0.1160
$\pi^{2D}_{1,2} = \pi^{1D}_{q=4}$	0.3480
$\pi^{2D}_{2,1} = \pi^{1D}_{q=5}$	0.3480
$\pi^{2D}_{3,1} = \pi^{1D}_{q=6}$	0.1160
$\pi^{2D}_{4,1} = \pi^{1D}_{q=7}$	0.0290
$\pi^{2D}_{5,1} = \pi^{1D}_{q=8}$	0.0070

The intermediate values for the outage results in Fig. 4.7 when $\overline{\gamma}_{SR_1} > \overline{\gamma}_{SR_2}$ and $\overline{\gamma}_{R_1D} = \overline{\gamma}_{R_2D}$,

TABLE 4.3: Estimated state transition matrix for Fig. 4.7

		F	i	n	a	l	(q)		
		$\pi^{2D}_{1,5}$	$\pi^{2D}_{1,4}$	$\pi^{2D}_{1,3}$	$\pi^{2D}_{1,2}$	$\pi^{2D}_{2,1}$	$\pi^{2D}_{3,1}$	$\pi^{2D}_{4,1}$	$\pi^{2D}_{5,1}$
I	$\pi^{2D}_{1,5}$	0.3750	0	0	0	0.6250	0	0	0
n	$\pi^{2D}_{1,4}$	0.4286	0	0	0	0.5714	0	0	0
i	$\pi^{2D}_{1,3}$	0	0.5000	0	0	0.5000	0	0	0
t	$\pi^{2D}_{1,2}$	0	0	0.6000	0	0.4000	0	0	0
i	$\pi^{2D}_{2,1}$	0	0	0	0.8571	0	0.1429	0	0
a	$\pi^{2D}_{3,1}$	0	0	0	0.5000	0	0	0.5000	0
l	$\pi^{2D}_{4,1}$	0	0	0	0.9231	0	0	0	0.0769
(q)	$\pi^{2D}_{5,1}$	0	0	0	0.9375	0	0	0	0.0625

TABLE 4.4: Estimated steady-state vector for Fig. 4.7

$\pi^{2D}_{1,5} = \pi^{1D}_{q=1}$	0.0619
$\pi^{2D}_{1,4} = \pi^{1D}_{q=2}$	0.0902
$\pi^{2D}_{1,3} = \pi^{1D}_{q=3}$	0.1804
$\pi^{2D}_{1,2} = \pi^{1D}_{q=4}$	0.3007
$\pi^{2D}_{2,1} = \pi^{1D}_{q=5}$	0.3007
$\pi^{2D}_{3,1} = \pi^{1D}_{q=6}$	0.0430
$\pi^{2D}_{4,1} = \pi^{1D}_{q=7}$	0.0215
$\pi^{2D}_{5,1} = \pi^{1D}_{q=8}$	0.0018

The intermediate values for the outage results in Fig. 4.7 when $\overline{\gamma}_{SR_1} < \overline{\gamma}_{SR_2}$ and $\overline{\gamma}_{R_1D} = \overline{\gamma}_{R_2D}$,

TABLE 4.5: Estimated state transition matrix for Fig. 4.7

		F	i	n	a	l	(q)		
		$\pi^{2D}_{1,5}$	$\pi^{2D}_{1,4}$	$\pi^{2D}_{1,3}$	$\pi^{2D}_{1,2}$	$\pi^{2D}_{2,1}$	$\pi^{2D}_{3,1}$	$\pi^{2D}_{4,1}$	$\pi^{2D}_{5,1}$
I	$\pi^{2D}_{1,5}$	0.0625	0	0	0	0.9375	0	0	0
n	$\pi^{2D}_{1,4}$	0.0769	0	0	0	0.9231	0	0	0
i	$\pi^{2D}_{1,3}$	0	0.1000	0	0	0.9000	0	0	0
t	$\pi^{2D}_{1,2}$	0	0	0.1429	0	0.8571	0	0	0
i	$\pi^{2D}_{2,1}$	0	0	0	0.4000	0	0.6000	0	0
a	$\pi^{2D}_{3,1}$	0	0	0	0.9000	0	0	0.1000	0
l	$\pi^{2D}_{4,1}$	0	0	0	0.5714	0	0	0	0.4286
(q)	$\pi^{2D}_{5,1}$	0	0	0	0.6250	0	0	0	0.3750

TABLE 4.6: Estimated steady-state vector for Fig. 4.7

$\pi^{2D}_{1,5} = \pi^{1D}_{q=1}$	0.0004
$\pi^{2D}_{1,4} = \pi^{1D}_{q=2}$	0.0050
$\pi^{2D}_{1,3} = \pi^{1D}_{q=3}$	0.0500
$\pi^{2D}_{1,2} = \pi^{1D}_{q=4}$	0.3497
$\pi^{2D}_{2,1} = \pi^{1D}_{q=5}$	0.3497
$\pi^{2D}_{3,1} = \pi^{1D}_{q=6}$	0.2098
$\pi^{2D}_{4,1} = \pi^{1D}_{q=7}$	0.0210
$\pi^{2D}_{5,1} = \pi^{1D}_{q=8}$	0.0144

The intermediate values for the outage results in Fig. 4.7 when $\overline{\gamma}_{SR_1} = \overline{\gamma}_{SR_2}$ and $\overline{\gamma}_{R_1D} > \overline{\gamma}_{R_2D}$,

TABLE 4.7: Estimated state transition matrix for Fig. 4.7

		F	i	n	a	l	(q)		
		$\pi^{2D}_{1,5}$	$\pi^{2D}_{1,4}$	$\pi^{2D}_{1,3}$	$\pi^{2D}_{1,2}$	$\pi^{2D}_{2,1}$	$\pi^{2D}_{3,1}$	$\pi^{2D}_{4,1}$	$\pi^{2D}_{5,1}$
I	$\pi^{2D}_{1,5}$	0.3750	0	0	0	0.6250	0	0	0
n	$\pi^{2D}_{1,4}$	0.4286	0	0	0	0.5714	0	0	0
i	$\pi^{2D}_{1,3}$	0	0.5000	0	0	0.5000	0	0	0
t	$\pi^{2D}_{1,2}$	0	0	0.6000	0	0.4000	0	0	0
i	$\pi^{2D}_{2,1}$	0	0	0	0.8571	0	0.1429	0	0
a	$\pi^{2D}_{3,1}$	0	0	0	0.5000	0	0	0.5000	0
l	$\pi^{2D}_{4,1}$	0	0	0	0.9231	0	0	0	0.0769
(q)	$\pi^{2D}_{5,1}$	0	0	0	0.9375	0	0	0	0.0625

TABLE 4.8: Estimated steady-state vector for Fig. 4.7

$\pi^{2D}_{1,5} = \pi^{1D}_{q=1}$	0.0619
$\pi^{2D}_{1,4} = \pi^{1D}_{q=2}$	0.0902
$\pi^{2D}_{1,3} = \pi^{1D}_{q=3}$	0.1804
$\pi^{2D}_{1,2} = \pi^{1D}_{q=4}$	0.3007
$\pi^{2D}_{2,1} = \pi^{1D}_{q=5}$	0.3007
$\pi^{2D}_{3,1} = \pi^{1D}_{q=6}$	0.0430
$\pi^{2D}_{4,1} = \pi^{1D}_{q=7}$	0.0215
$\pi^{2D}_{5,1} = \pi^{1D}_{q=8}$	0.0018

The intermediate values for the outage results in Fig. 4.7 when $\overline{\gamma}_{SR_1} = \overline{\gamma}_{SR_2}$ and $\overline{\gamma}_{R_1D} < \overline{\gamma}_{R_2D}$,

TABLE 4.9: Estimated state transition matrix for Fig. 4.7

		F	i	n	a	l	(q)		
		$\pi^{2D}_{1,5}$	$\pi^{2D}_{1,4}$	$\pi^{2D}_{1,3}$	$\pi^{2D}_{1,2}$	$\pi^{2D}_{2,1}$	$\pi^{2D}_{3,1}$	$\pi^{2D}_{4,1}$	$\pi^{2D}_{5,1}$
I	$\pi^{2D}_{1,5}$	0.0625	0	0	0	0.9375	0	0	0
n	$\pi^{2D}_{1,4}$	0.0769	0	0	0	0.9231	0	0	0
i	$\pi^{2D}_{1,3}$	0	0.1000	0	0	0.9000	0	0	0
t	$\pi^{2D}_{1,2}$	0	0	0.1429	0	0.8571	0	0	0
i	$\pi^{2D}_{2,1}$	0	0	0	0.4000	0	0.6000	0	0
a	$\pi^{2D}_{3,1}$	0	0	0	0.9000	0	0	0.1000	0
l	$\pi^{2D}_{4,1}$	0	0	0	0.5714	0	0	0	0.4286
(q)	$\pi^{2D}_{5,1}$	0	0	0	0.6250	0	0	0	0.3750

TABLE 4.10: Estimated steady-state vector for Fig. 4.7

$\pi^{2D}_{1,5} = \pi^{1D}_{q=1}$	0.0004
$\pi^{2D}_{1,4} = \pi^{1D}_{q=2}$	0.0050
$\pi^{2D}_{1,3} = \pi^{1D}_{q=3}$	0.0500
$\pi^{2D}_{1,2} = \pi^{1D}_{q=4}$	0.3497
$\pi^{2D}_{2,1} = \pi^{1D}_{q=5}$	0.3497
$\pi^{2D}_{3,1} = \pi^{1D}_{q=6}$	0.2098
$\pi^{2D}_{4,1} = \pi^{1D}_{q=7}$	0.0210
$\pi^{2D}_{5,1} = \pi^{1D}_{q=8}$	0.0144

The system performance in terms of outage probability with the same states as above and the same transmission rate but with the harvesting time $\tau = 0.4$ seconds is analyzed in Fig. 4.8,

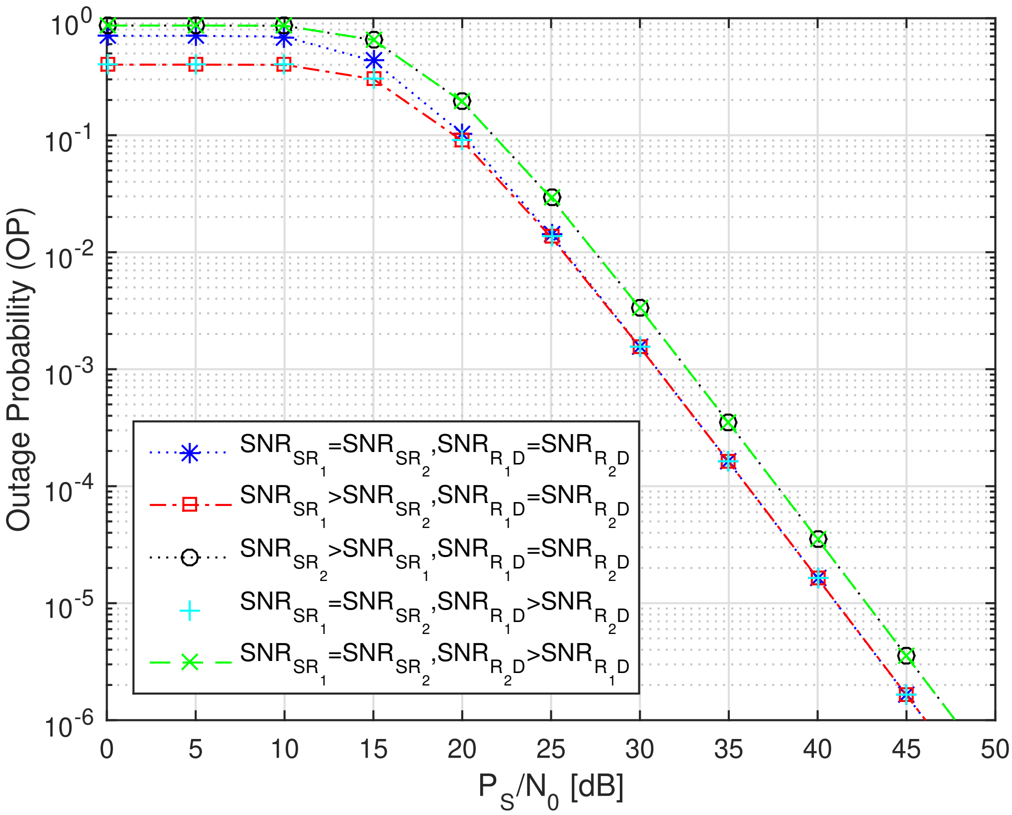

FIGURE 4.8: Results with 4 Energy states Quantization with variable average SNRs, harvesting time $\tau = 0.4$ seconds, where SNR on the legend is the average $\overline{\gamma}$ of the link.

The same observation done in Fig. 4.7 is also continued with an increased harvesting period in Fig. 4.8 to discover the effect of increasing harvesting time. The same conclusion that links with better SNRs perform better is drawn just like in Fig. 4.7 with an exception of a better performance for all of the variable SNR cases because of an increased transmit relay power from harvested energy due to a higher value of $E_0 = \frac{2}{n}$, where $n = 4$. The intermediate values for the outage results in Fig. 4.8 would be exactly the same as the values in Fig. 4.7 with only increase in the harvested energy.

Finally, for four states with the harvesting time increased to $\tau = 0.6$ seconds, the following results were obtained,

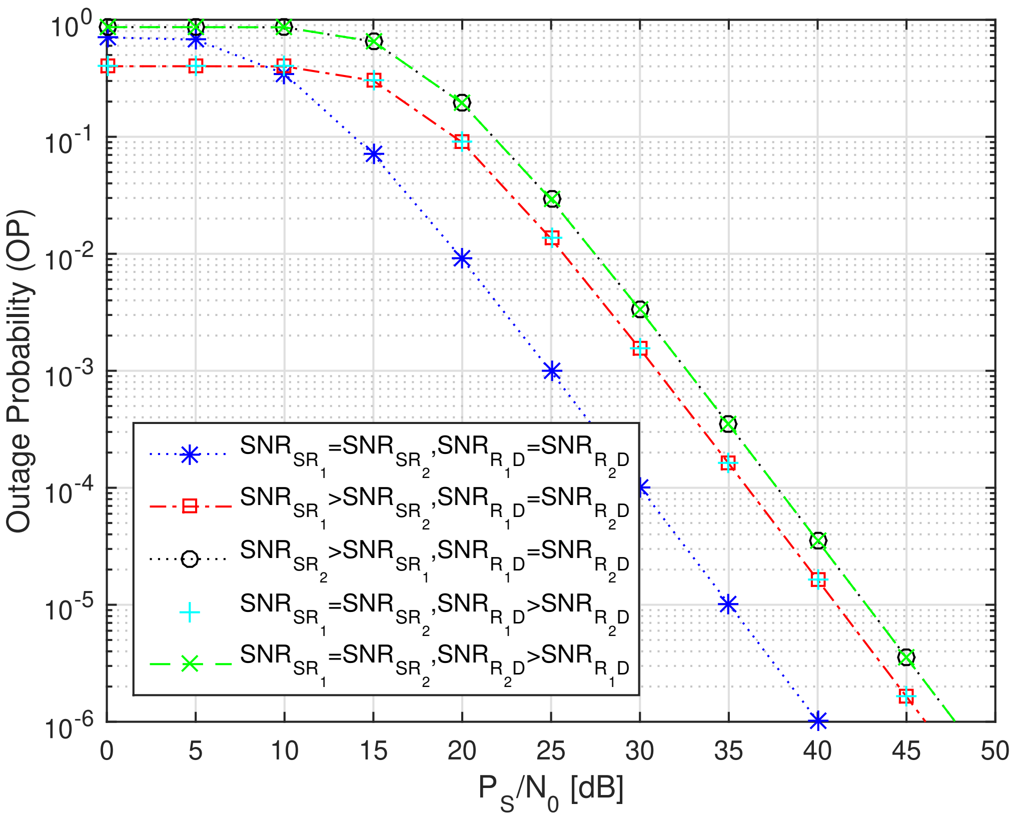

Figure 4.9: Results with 4 Energy states Quantization, harvesting time $\tau = 0.6$ seconds, where SNR on the legend is the average $\overline{\gamma}$ of the link.

The same conclusions just like in Fig. 4.7 and Fig. 4.8 are drawn except for a better performance due to an increased relay transmit power. All the results in Fig. 4.7, Fig. 4.8 and Fig. 4.9 are as expected because of increased relay energies meaning higher SNRs for longer harvesting times. The impacting energy step is due to a higher value of $E_0 = \frac{3}{n}$, where $n = 4$. The intermediate values for the outage results in Fig. 4.9 were also exactly the same as in Fig. 4.7 and Fig. 4.8 with an increased harvesting time up to 0.6 seconds.

To draw convincing conclusions on the impact of an increasing harvesting period, performances are compared under the fixed and equal average SNRs in Fig. 4.10. The same conditions are assumed in terms of bit rate, variance and the same average

SNRs, $\overline{\gamma}_{SR_k} = \overline{\gamma}_{R_kD}$ then the results in Fig. 4.10 were obtained for different harvesting times.

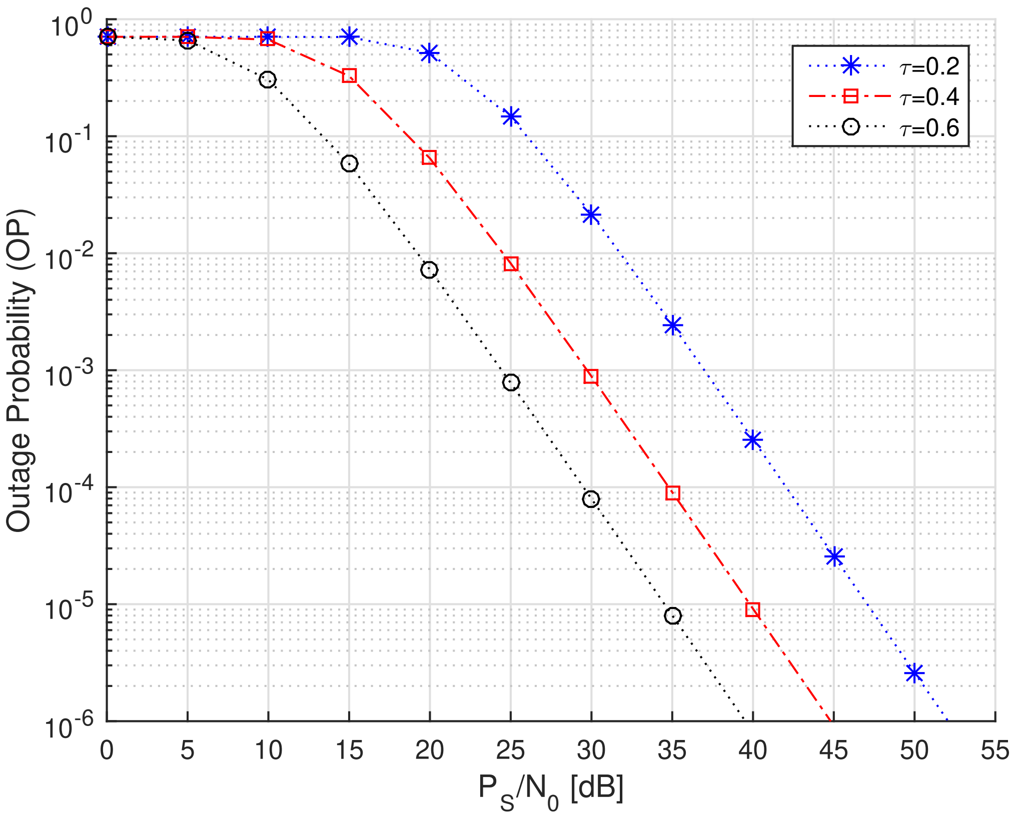

FIGURE 4.10: Results with 4 Energy states Quantization with different harvesting times $\tau = \{0.2, 0.4, 0.6\}$ seconds

The results in Fig. 4.10 are still embedded within Fig. 4.7, 4.8 and 4.9 but they cannot easily be distinguished because the conditions are not isolated. The results in 4.10 clearly show the impact of energy harvesting in cooperative communication when the most important factor which is harvesting time is being increased. Due to the energy and successful packet transmission trade-off, the harvesting time can be extended to limited fraction of the frame duration to allow enough time for packet transmission. The same analysis was also carried out for 3 energy states per relay to show the concept holds for any number of states n.

4.4.2 The performance analysis of Three System states

The same set of results were performed in line with those of four energy harvesting state but with three harvesting states. The simulation and analytical results were found to tightly match in Fig. 4.11. Just as deduced in Fig. 4.7 under four harvesting states, the same conclusion is drawn in Fig. 4.12 with three energy states. The intermediate values in terms of transition probabilities and steady-state probabilities were provided for affirmation.

For the following three energy states per relay:
$(\pi_{1,4}^{2D}, \pi_{1,3}^{2D}, \pi_{1,2}^{2D}, \pi_{2,1}^{2D}, \pi_{3,1}^{2D}, \pi_{4,1}^{2D})$, the following results 4.11 for the simulation and analytical were obtained,

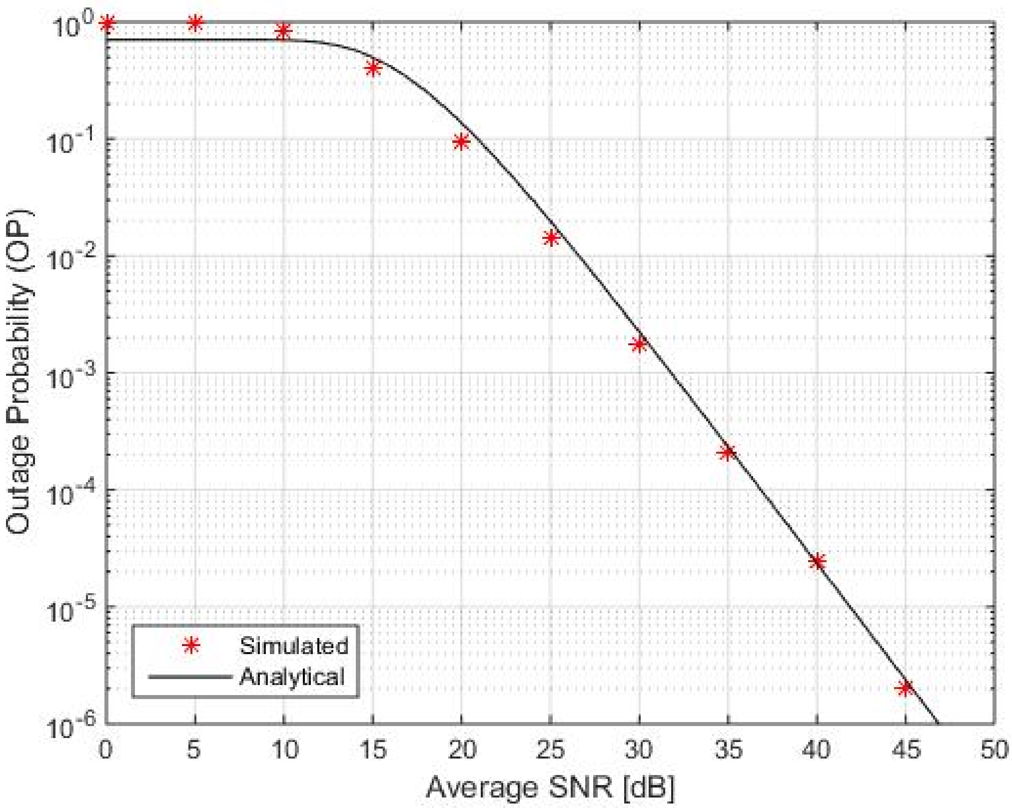

FIGURE 4.11: Results with 3 Energy states Quantization

The outage probability of the following three states ($\pi_{1,4}^{2D}, \pi_{1,3}^{2D}\pi_{1,2}^{2D}, \pi_{2,1}^{2D}, \pi_{3,1}^{2D}, \pi_{4,1}^{2D}$) with bit rate, $r = 1Bit/s$, harvesting time $\tau = 0.2$ seconds, the following results were obtained,

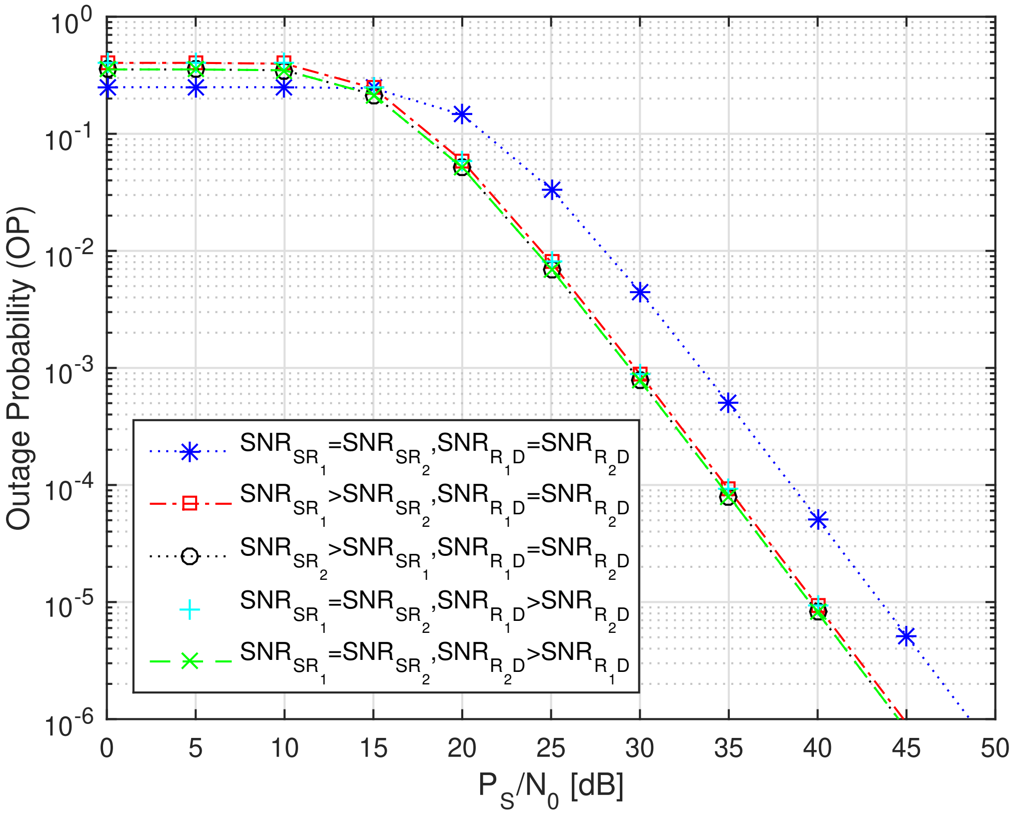

Figure 4.12: Results with 3 Energy states Quantization with different SNRs, harvesting time $\tau = 0.2$ seconds, where SNR on the legend is the average $\overline{\gamma}$ of the link.

The intermediate values for the outage results in Fig. 4.12 when $\overline{\gamma}_{SR_1} = \overline{\gamma}_{SR_2}$ and $\overline{\gamma}_{R_1D} = \overline{\gamma}_{R_2D}$,

Table 4.11: Estimated state transition matrix for Fig. 4.12

	$\pi^{2D}_{1,4}$	$\pi^{2D}_{1,3}$	$\pi^{2D}_{1,2}$	$\pi^{2D}_{2,1}$	$\pi^{2D}_{3,1}$	$\pi^{2D}_{4,1}$
$\pi^{2D}_{1,4}$	0.2000	0	0	0.8000	0	0
$\pi^{2D}_{1,3}$	0.2500	0	0	0.7500	0	0
$\pi^{2D}_{1,2}$	0	0.3333	0	0.6667	0	0
$\pi^{2D}_{2,1}$	0	0	0.6667	0	0.3333	0
$\pi^{2D}_{3,1}$	0	0	0.7500	0	0	0.2500
$\pi^{2D}_{4,1}$	0	0	0.8000	0	0	0.2000

Table 4.12: Estimated steady-state vector for Fig. 4.12

$\pi^{2D}_{1,4} = \pi^{1D}_{q=1}$	0.0362
$\pi^{2D}_{1,3} = \pi^{1D}_{q=2}$	0.1159
$\pi^{2D}_{1,2} = \pi^{1D}_{q=3}$	0.3478
$\pi^{2D}_{2,1} = \pi^{1D}_{q=4}$	0.3478
$\pi^{2D}_{3,1} = \pi^{1D}_{q=5}$	0.1159
$\pi^{2D}_{4,1} = \pi^{1D}_{q=6}$	0.0362

The intermediate values for the outage results in Fig. 4.12 when $\overline{\gamma}_{SR_1} > \overline{\gamma}_{SR_2}$ and $\overline{\gamma}_{R_1D} = \overline{\gamma}_{R_2D}$,

Table 4.13: Estimated state transition matrix for Fig. 4.12

	$\pi_{1,4}^{2D}$	$\pi_{1,3}^{2D}$	$\pi_{1,2}^{2D}$	$\pi_{2,1}^{2D}$	$\pi_{3,1}^{2D}$	$\pi_{4,1}^{2D}$
$\pi_{1,4}^{2D}$	0.4286	0	0	0.5714	0	0
$\pi_{1,3}^{2D}$	0.5000	0	0	0.5000	0	0
$\pi_{1,2}^{2D}$	0	0.6000	0	0.4000	0	0
$\pi_{2,1}^{2D}$	0	0	0.8571	0	0.1429	0
$\pi_{3,1}^{2D}$	0	0	0.5000	0	0	0.5000
$\pi_{4,1}^{2D}$	0	0	0.9231	0	0	0.0769

Table 4.14: Estimated steady-state vector for Fig. 4.12

$\pi_{1,4}^{2D} = \pi_{q=1}^{1D}$	0.1569
$\pi_{1,3}^{2D} = \pi_{q=2}^{1D}$	0.1794
$\pi_{1,2}^{2D} = \pi_{q=3}^{1D}$	0.2989
$\pi_{2,1}^{2D} = \pi_{q=4}^{1D}$	0.2989
$\pi_{3,1}^{2D} = \pi_{q=5}^{1D}$	0.0427
$\pi_{4,1}^{2D} = \pi_{q=6}^{1D}$	0.0231

The intermediate values for the outage results in Fig. 4.12 when $\overline{\gamma}_{SR_1} < \overline{\gamma}_{SR_2}$ and $\overline{\gamma}_{R_1D} = \overline{\gamma}_{R_2D}$,

TABLE 4.15: Estimated state transition matrix for Fig. 4.12

	$\pi^{2D}_{1,4}$	$\pi^{2D}_{1,3}$	$\pi^{2D}_{1,2}$	$\pi^{2D}_{2,1}$	$\pi^{2D}_{3,1}$	$\pi^{2D}_{4,1}$
$\pi^{2D}_{1,4}$	0.0769	0	0	0.9231	0	0
$\pi^{2D}_{1,3}$	0.1000	0	0	0.9000	0	0
$\pi^{2D}_{1,2}$	0	0.1429	0	0.8571	0	0
$\pi^{2D}_{2,1}$	0	0	0.4000	0	0.6000	0
$\pi^{2D}_{3,1}$	0	0	0.9000	0	0	0.1000
$\pi^{2D}_{4,1}$	0	0	0.5714	0	0	0.4286

TABLE 4.16: Estimated steady-state vector for Fig. 4.12

$\pi^{2D}_{1,4} = \pi^{1D}_{q=1}$	0.0054
$\pi^{2D}_{1,3} = \pi^{1D}_{q=2}$	0.0499
$\pi^{2D}_{1,2} = \pi^{1D}_{q=3}$	0.3492
$\pi^{2D}_{2,1} = \pi^{1D}_{q=4}$	0.3492
$\pi^{2D}_{3,1} = \pi^{1D}_{q=5}$	0.2095
$\pi^{2D}_{4,1} = \pi^{1D}_{q=6}$	0.0367

The intermediate values for the outage results in Fig. 4.12 when $\overline{\gamma}_{SR_1} = \overline{\gamma}_{SR_2}$ and $\overline{\gamma}_{R_1D} > \overline{\gamma}_{R_2D}$,

TABLE 4.17: Estimated state transition matrix for Fig. 4.12

	$\pi^{2D}_{1,4}$	$\pi^{2D}_{1,3}$	$\pi^{2D}_{1,2}$	$\pi^{2D}_{2,1}$	$\pi^{2D}_{3,1}$	$\pi^{2D}_{4,1}$
$\pi^{2D}_{1,4}$	0.4286	0	0	0.5714	0	0
$\pi^{2D}_{1,3}$	0.5000	0	0	0.5000	0	0
$\pi^{2D}_{1,2}$	0	0.6000	0	0.4000	0	0
$\pi^{2D}_{2,1}$	0	0	0.8571	0	0.1429	0
$\pi^{2D}_{3,1}$	0	0	0.5000	0	0	0.5000
$\pi^{2D}_{4,1}$	0	0	0.9231	0	0	0.0769

TABLE 4.18: Estimated steady-state vector for Fig. 4.12

$\pi^{2D}_{1,4} = \pi^{1D}_{q=1}$	0.1569
$\pi^{2D}_{1,3} = \pi^{1D}_{q=2}$	0.1794
$\pi^{2D}_{1,2} = \pi^{1D}_{q=3}$	0.2989
$\pi^{2D}_{2,1} = \pi^{1D}_{q=4}$	0.2989
$\pi^{2D}_{3,1} = \pi^{1D}_{q=5}$	0.0427
$\pi^{2D}_{4,1} = \pi^{1D}_{q=6}$	0.0231

The intermediate values for the outage results in Fig. 4.12 when $\overline{\gamma}_{SR_1} = \overline{\gamma}_{SR_2}$ and $\overline{\gamma}_{R_1D} < \overline{\gamma}_{R_2D}$,

TABLE 4.19: Estimated state transition matrix for Fig. 4.12

	$\pi^{2D}_{1,4}$	$\pi^{2D}_{1,3}$	$\pi^{2D}_{1,2}$	$\pi^{2D}_{2,1}$	$\pi^{2D}_{3,1}$	$\pi^{2D}_{4,1}$
$\pi^{2D}_{1,4}$	0.0769	0	0	0.9231	0	0
$\pi^{2D}_{1,3}$	0.1000	0	0	0.9000	0	0
$\pi^{2D}_{1,2}$	0	0.1429	0	0.8571	0	0
$\pi^{2D}_{2,1}$	0	0	0.4000	0	0.6000	0
$\pi^{2D}_{3,1}$	0	0	0.9000	0	0	0.1000
$\pi^{2D}_{4,1}$	0	0	0.5714	0	0	0.4286

TABLE 4.20: Estimated steady-state vector for Fig. 4.12

$\pi^{2D}_{1,4} = \pi^{1D}_{q=1}$	0.0054
$\pi^{2D}_{1,3} = \pi^{1D}_{q=2}$	0.0499
$\pi^{2D}_{1,2} = \pi^{1D}_{q=3}$	0.3492
$\pi^{2D}_{2,1} = \pi^{1D}_{q=4}$	0.3492
$\pi^{2D}_{3,1} = \pi^{1D}_{q=5}$	0.2095
$\pi^{2D}_{4,1} = \pi^{1D}_{q=6}$	0.0367

The performance behaviour of the system while increasing energy harvesting time to $\tau = 0.4$ seconds with the above three energy states is as shown below,

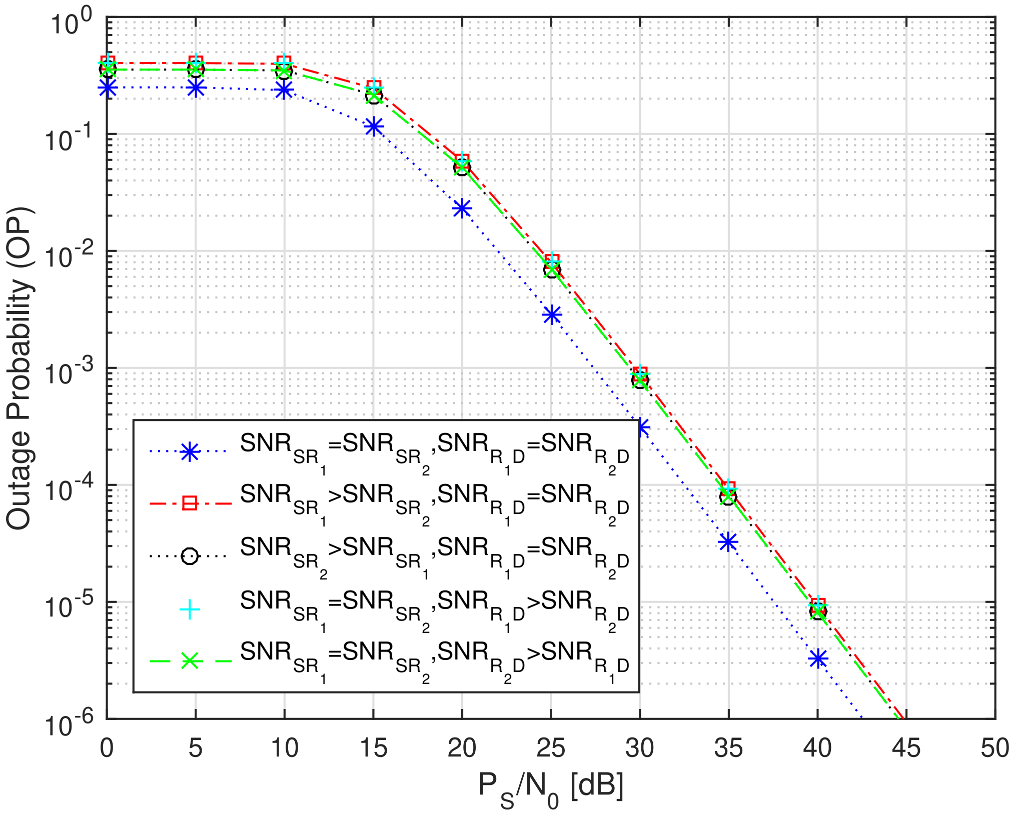

FIGURE 4.13: Results with 3 Energy states Quantization, harvesting time $\tau = 0.4$ seconds, where SNR on the legend is the average $\overline{\gamma}$ of the link.

The intermediate values for the above outage results in Fig. 4.13 were also exactly the same as in Fig. 4.12.

Outage probability for the above three states with harvesting time increased to $\tau = 0.6$ seconds, the following resulted in Fig. 4.14,

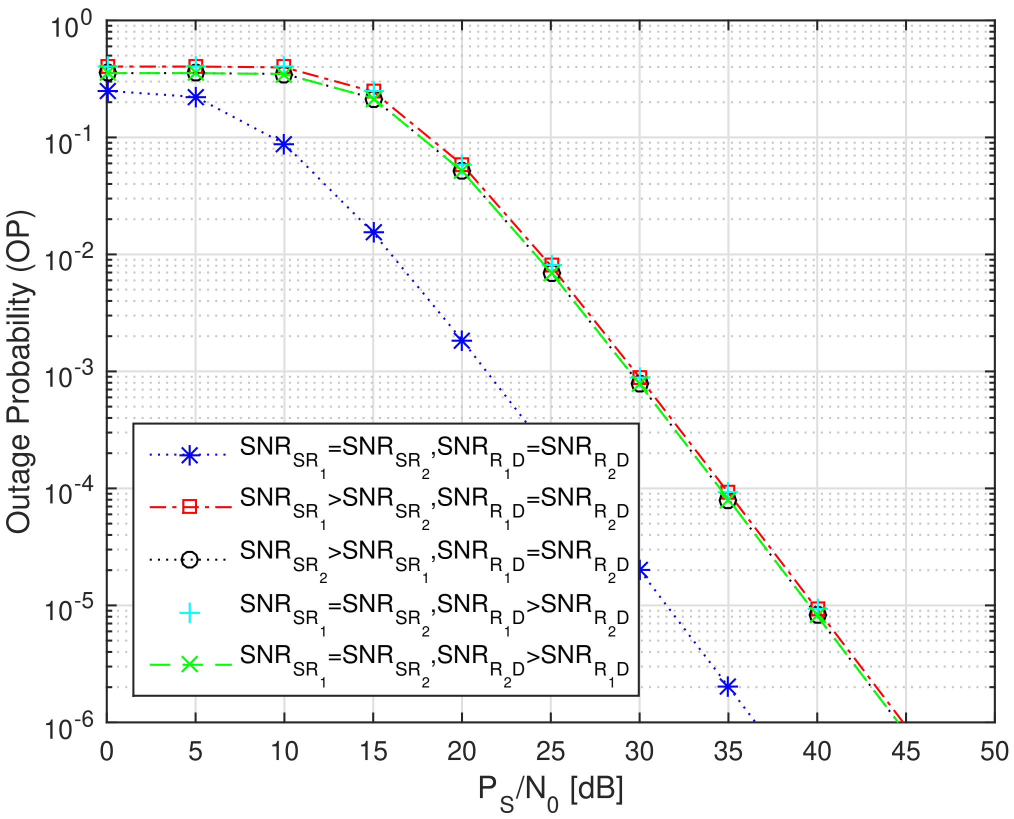

FIGURE 4.14: Results with 3 Energy states Quantization, harvesting time $\tau = 0.6$ seconds, where SNR on the legend is the average $\overline{\gamma}$ of the link.

The intermediate values for the above outage results in Fig. 4.14 were exactly the same as in figures 4.12 and 4.13.

To drive the point home about the comparisons of average SNRs, $\overline{\gamma}_{SR_k}$ and $\overline{\gamma}_{R_kD}$ with 3 energy states before making any final conclusions through a number of rates $\beta = \{0.6, 0.8, 1.2, 1.4, 1.6\}$ were assumed, where β is just a list of amplifaction factors.

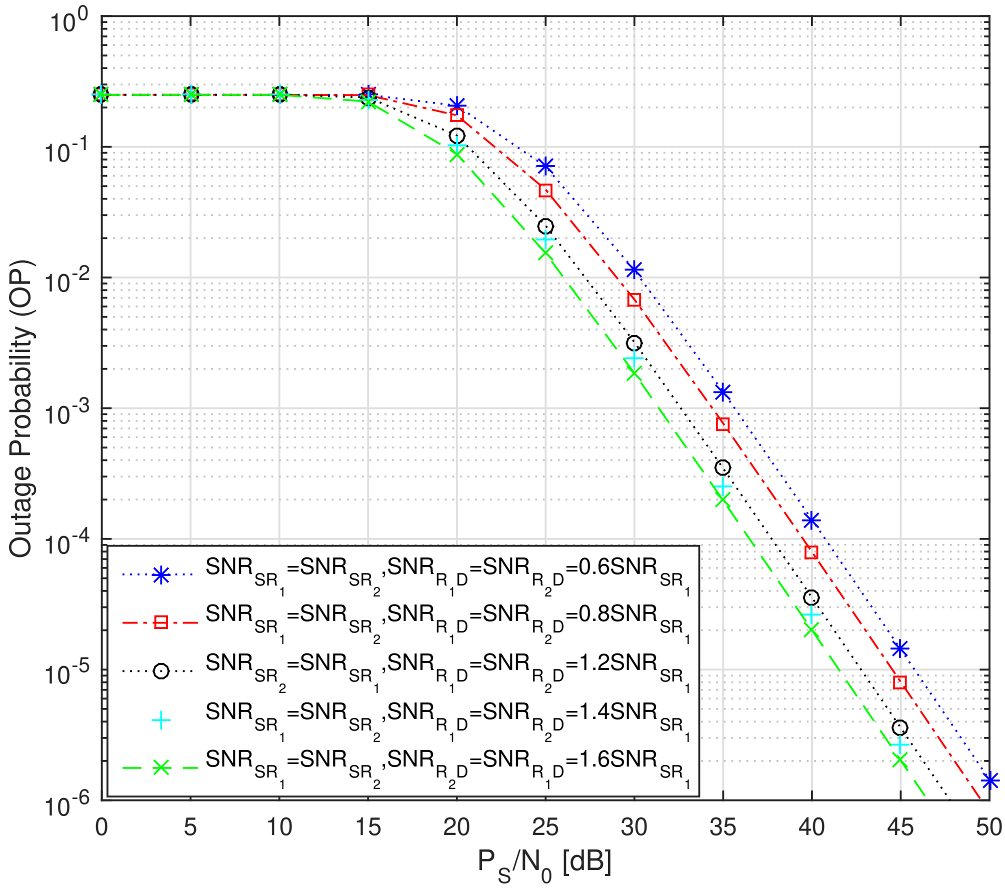

FIGURE 4.15: $\overline{\gamma}_{SR_1} = \overline{\gamma}_{SR_2}$, $\overline{\gamma}_{R_1D} = \overline{\gamma}_{R_2D} = \beta\overline{\gamma}_{SR_1}$, $\tau = 0.2$ seconds, where SNR on the legend is the average $\overline{\gamma}$ of the link.

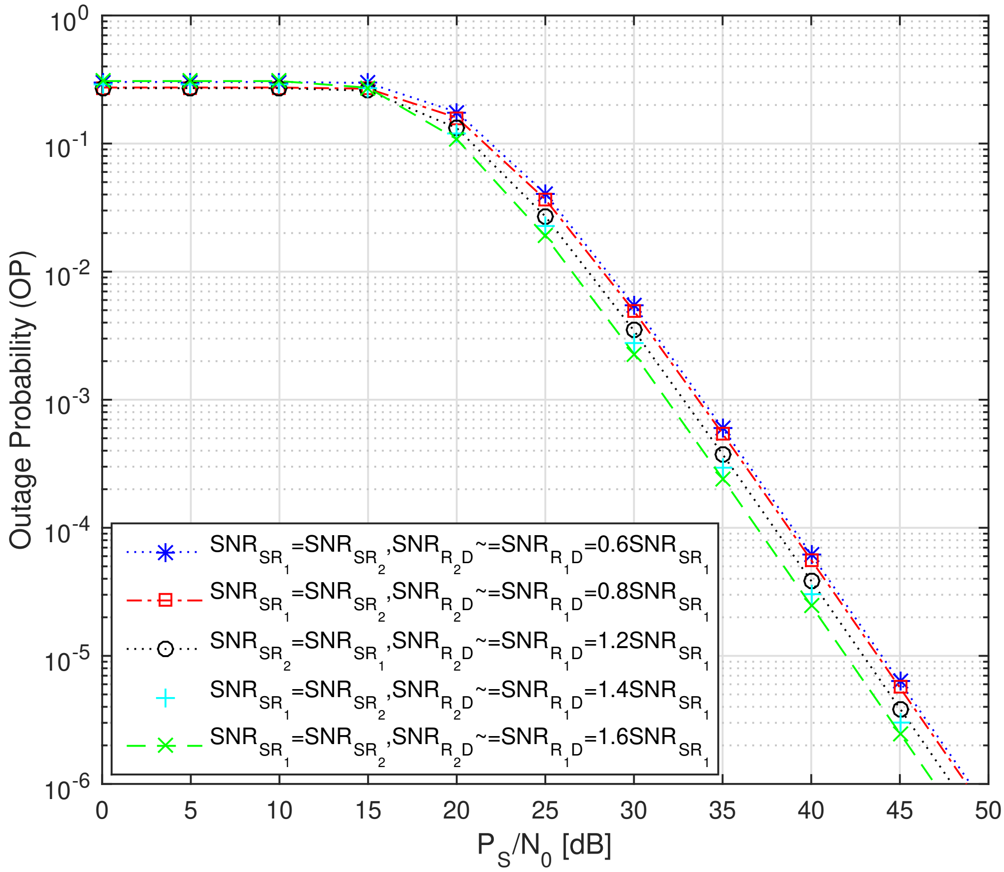

FIGURE 4.16: $\overline{\gamma}_{SR_1} = \overline{\gamma}_{SR_2}$, $\overline{\gamma}_{R_2D} \neq \overline{\gamma}_{R_1D} = \beta\overline{\gamma}_{SR_1}$, $\tau = 0.2$ seconds, where SNR on the legend is the average $\overline{\gamma}$ of the link.

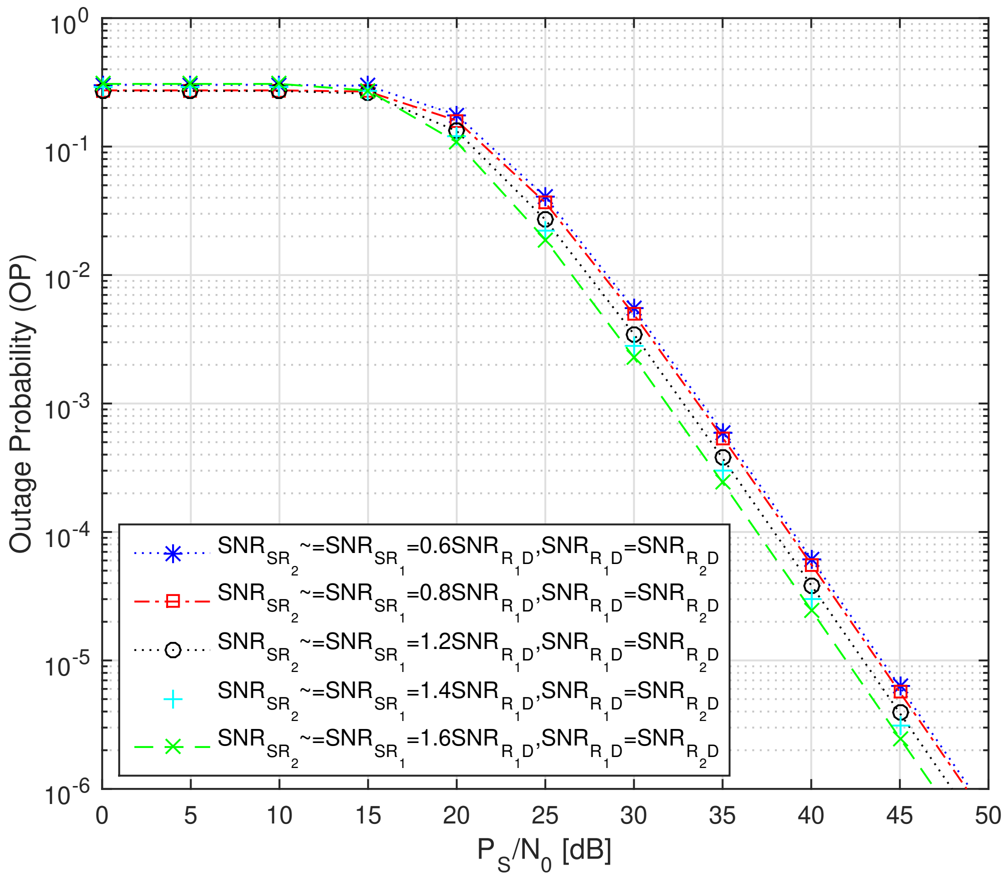

FIGURE 4.17: $\overline{\gamma}_{SR_2} \neq \overline{\gamma}_{SR_1} = \beta\overline{\gamma}_{R_1D}$, $\overline{\gamma}_{R_1D} = \overline{\gamma}_{R_2D}$, $\tau = 0.2$ seconds, where SNR on the legend is the average $\overline{\gamma}$ of the link.

From the results shown in Fig. 4.15, 4.16 and 4.17 it is clearly evident that links with higher average SNRs perform better and this is seen as β is increasing from 0.6 to 1.6. Since the selection scheme is reactive then the higher the $\overline{\gamma}_{R_kD}$ the lower the outage.

The above results in Fig. 4.6 for four states attested a very strong correlation between the simulated and analytical curves can be seen which validates the proposed analytical framework. According to Fig. 4.17, it can be seen that plots with $\overline{\gamma}_{SR_1}$ or $\overline{\gamma}_{R_1D}$ as maximum match one another just like plots with $\overline{\gamma}_{SR_2}$ and $\overline{\gamma}_{R_1D}$ as greater matching perfectly. When average SNRs are equal at low harvesting times performance might be poor but greatly improves as harvesting time increases as seen in Fig.

4.8 and 4.9 just because at those times both relay SNRs are higher and probability of outage due to R_1 and R_2 is very low. The Fig. 4.10 vividly shows that as energy harvesting time τ is increasing the probability of the system being in outage drops significantly. It was therefore found out that an increase of time to harvest from 0.2 seconds to 0.6 seconds adds a gain of more than 10 dB to the system which means an improvement in performance and thus supported our claim by quantified results that energy harvesting indeed enhances performances.

4.5 Conclusion

The work in this chapter has presented reactive opportunistic relay selection in energy harvesting networks in an attempt to solve the problem of coverage and limited transmit power/energy. This chapter investigated performance of cooperative networks aided by energy harvesting relays in terms of outage behaviour. An n x n Markov model was proposed to quantify the energy of relays from the harvested energy flow. The work may be further extended in the future by analysing the same scheme when the relay cluster is formed by more than two relays ($K > 2$) which is currently observed as an open issue. From this work, the effect of energy harvesting in cooperative communication has been modelled and formulated as a Markov decision process (MDP), the model was simulated and the analysis indeed shows harvested energy improves relay transmit power. This increased transmit power is very essential in improving relay-destination SNRs although there may be increased interferences as well calling for cancellation schemes at the destination but this exceeds the scope of this work.

The outage analysis of the proposed scheme as illustrated in Fig. 4.7, 4.8 and 4.9 performs much better as compared to a non-cooperative direct source destination communication, theoretical single relay communication [48] and two relays using ORS selection in [67]. The outage probability performance of a non-cooperative suffers because it lacks the benefit of receiving replicated information from relays with higher SNR levels and available for the cooperative communication model. Therefore, the proposed scheme has better gains than all the compared schemes above in the literature by a minimum of approximately 5dB, indicating its robustness to unfriendly wireless environments. Achieving an outage of 10^{-2} the proposed scheme uses an SNR of $\leq$ 20dB(goes down with higher harvesting periods) with a harvesting period of 0.4 seconds as compared to the SNR($\geq$ 25dB) as required by other schemes. The proposed selection scheme does not only benefits the unselected relays which will be harvesting energy for the entire slot of the source frame transmission but even the participating relays conserve energy by first harvesting before transmission.

A dual-relay selection scheme with better SNR gains from accumulating harvested RF energy delivers better performances as established by the outage analysis and achieves a promising diversity with minimal complexity. The proposed relay selection capitalises on the RF energy to transmit with better SNRs towards the receiver and it also has the added advantage of conserving energy of unselected relays for future transmissions. A Markov chain approach to analyse the state transition matrix that models the energy evolutions in the relay batteries was designed. Analytical expressions for the outage probability and for the steady-state probability vector were also obtained. The analytical and simulation results demonstrate that the proposed relaying scheme has a better performance over the conventional scheme.

Chapter 5

Opportunistic RF Harvesting in Buffer-Aided Relay Selection

5.1 Introduction

The main theme of this chapter is to present the potential buffer-aided relaying coupled with energy harvesting in cooperative wireless communication. It is organized as giving a brief introduction about buffer-aided relay methods and highlights the rationale behind their operation in energy harvesting networks. The analysis is based on a system model setting in Section 5.2, performance analysis in terms of outage analysis is also presented with recommendations to conclude the research findings.

In this chapter, the benefits and the determination of the solution of using buffer-aided relaying in energy harvesting networks are assessed. The system in consideration consisted of a source, two relays and a destination. In this system only the relays have energy harvesting capabilities. The relay selection among the two relays is performed on the network parameters basis and buffer states. The network parameters, mainly the SNRs regulate packet arrivals at the relays. The amount of energy harvested and in the batteries ensures a stable data queue in relays by maintaining a stable service rate [37][74].

Initially, the catch lies in primarily evaluating the outage conditions on the relays which would lead to the system outage as there is no direct link between the source and the destination. These outage conditions are a result of relays not having enough storage resources for incoming packets and having null packets to deliver as outgoing packets to the destination [36], and the last condition would be relays not having enough power resources to transmit outgoing packets.

To solve the above stated problems, an introduction of a solution that makes use of a hybrid relay selection scheme [12] and a time-switching energy harvesting protocol is therefore considered. The hybrid relay selection is a composite scheme of the most popular opportunistic and max-max relay selection schemes. The time-switching is decided upon the power-splitting because all network nodes in this cooperative network are single antenna, meaning the same RF antenna is used to harvest energy from the source signal and then cooperate by transmitting the same signal afterwards.

5.2 System Model

In this chapter much like the previous chapter, a consideration of a relay network with one source node S, one destination node, D, and two half-duplex relays, $\{R_1, R_2\}$ is achieved. All relays are equipped with buffers for data and energy harvesting modules to harvest and store in the battery. The best relay receives a packet in the first time slot in its buffer. In the second time slot, the best relay chosen for transmission would forward a packet from the buffer to the receiving end node.

As in accordance with Fig. 5.1, the direct link is assumed to be in deep fade and thus no direct communication between the source and destination, in the same note all relaying devices do not communicate with each other. Moreover, all transmissions are packetized while channels would be constant for a packet duration with independent variations from packet to packet just like in the block fading model.

The channel coefficients h_{SR_k} and h_{R_kD} are mutually independent zero-mean complex Gaussian random variables (Rayleigh fading). Transmissions are organized in packets while channels are constant for the duration of a packet and vary independently from one packet to another.

The first half phase information transmitted from S to R_k and the received signal at the relay is,

$$y_{SR_k}(t) = \sqrt{P_S} h_{SR_k}(t) x_S(t) + n_{R_k}(t) \tag{5.1}$$

Where P_S is the source transmit power, $n_{R_k}(t)$ the additive noise at R_k, and $h_{SR_k}(t)$ denotes the fading coefficient between S and R_k.

In the second half phase, the received information at the relay retransmitted from R_k to D is,

$$y_{R_kD}(t) = \sqrt{P_{R_k}} h_{R_kD}(t) x_{R_k}(t) + n_D(t), \tag{5.2}$$

where $x_{R_k}(t)$ denotes the retransmit signal at R_k and P_{R_k} is the transmit power at R_k. h_{R_kD} is the channel fading coefficient between R_k and D.

γ_{SR_k} denotes the signal-to-noise ratio between the source and R_k and is given by equation 5.3

$$\gamma_{SR_k}(t) = \frac{|h_{SR_k}|^2 E_S(t)}{N_0}, \tag{5.3}$$

where E_S is energy of the source.

γ_{R_kD} denotes the signal-to-noise ratio between the R_k and D and is given by equation 5.4

$$\gamma_{R_kD}(t) = \frac{|h_{R_kD}|^2 E_{R_k}(t)}{N_0}, \tag{5.4}$$

where E_{R_k} is energy of the relay R_k.

The harvested transmit symbol energy for the k^{th} relay as a function of time would be exactly the same as expressed in equation 4.12. Likewise, the transmit power of the k^{th} relay as a function of time is as defined by equation 4.14.

5.2.1 Relay Selection Scheme

There is a slight difference in the relay selection criteria of this buffer-aided relaying which considers a hybrid selection scheme of ORS and MMRS to the reactive relay selection in chapter 4. The best k^{th} relay to receive, b^*_{rx}, would be selected from the best S-R links whilst the best relay to transmit, b^*_{tx}, would be chosen from the best R-D links. There are four possible events in this selection, either the relay is chosen to receive, not receive, transmit or not transmit, events $= \{Receive, Receive^{\complement}, Transmit, Transmit^{\complement}\}$. Where $\complement$ is the complement of being chosen to receive or transmit.

The best relay to receive b^*_{rx} as a function of channel strength on the $S \rightarrow R_k$ link amongst a cluster of (R_1, R_2) is,

$$b^*_{rx} = \arg \max_{k \in \ \{1,2\}} (\gamma_{SR_k}). \tag{5.5}$$

The best relay to transmit b^*_{tx}, $R_k \rightarrow D$ is defined as

$$b^*_{tx} = \arg \max_{k \in \ \{1,2\}} (\gamma_{R_k D}). \tag{5.6}$$

The system model for Opportunistic RF Harvesting in Buffer-Aided Relay Selection is as illustrated in Fig. 5.1.

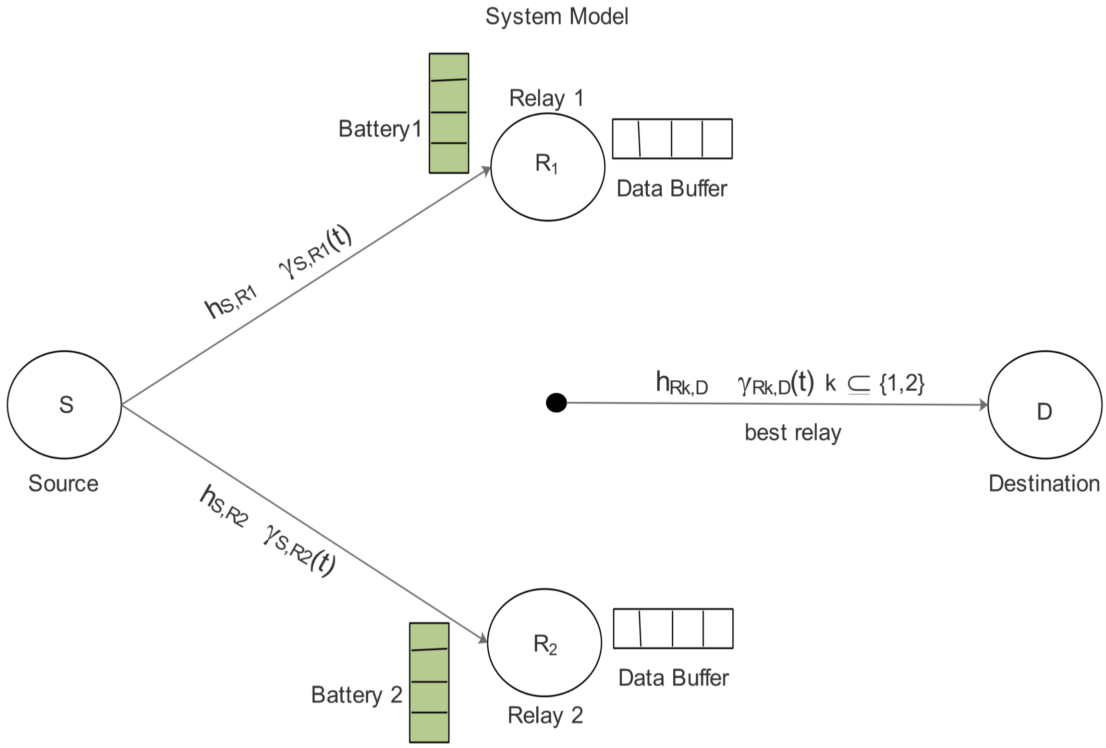

FIGURE 5.1: Cooperative Diversity Network for Relays with Buffers and Energy Harvesting Modules

The above figure 5.1 illustrates the system model for energy harvesting relay-aided cooperative network with buffers in consideration. It consists of one source node, one destination node and $k(1 \leq k \leq 2)$ relay nodes such that they are denoted in order as S, D and $R_k(1 \leq k \leq 2)$. Information flows from S to D while S is powered by stabilized traditional power P_S. The relay R_k is mono-antennary and powered by the energy harvested from a constant power P_S of S. **Assumption**: All buffers have equal elements of size B and each element can store one packet for simplicity of analysis.

5.2.2 Markovian Analysis of the System

5.2.2.1 Buffer Evolution

According to the system model in Fig. 5.1 only one packet is being transmitted in an interval, thus a single packet is received / transmitted per time slot. The buffer state is regarded at the end of harvesting period just before the beginning of information decoding and also just before the transmission period to the destination. For i which represents the buffer packets in relay 1 and j which represents the number of relay 2 buffer packets then a table to resemble the number of buffer packets of both relays is derived for which its columns are always found be the sum of $i + j$ as shown below.

Relay 2 packets

j

0,B	1,B	2,B	3,B	4,B	...	B,B
...						...
0,4	1,4	2,4	3,4	4,4		B,4
0,3	1,3	2,3	3,3	4,3		B,3
0,2	1,2	2,2	3,2	4,2		B,2
0,1	1,1	2,1	3,1	4,1		B,1
0,0	1,0	2,0	3,0	4,0	...	B,0

i

Relay 1 packets

FIGURE 5.2: Buffer Table for the system depicting packet evolutions of R_1 buffer and R_2 buffer in the format (R_1,R_2)

From the above buffer states of R_1 and R_2 in Table 5.2, the state $(0, 0)$(both relays empty) and (B, B)(both relays full) are the state limits for both R_1 and R_2. A buffer state $(0, 0)$ would mean both relays are empty and on the other hand the buffer state (B, B) would mean both relays are full. The freedom of relays in packet reception and transmission introduces an interesting evolution in the number of packets in the relay buffers worth studying. These evolutions result if one relay receives and transmits, then a number of packets of both relays remains unaltered at the end of the time frame. Be that as it may, if one relay receives and the other transmits, then a change is such that one buffer decreases (transmitting relay) with the same amount another increases (receiving relay) with. This poses a few challenges in avoiding buffer overflows and packet starvation. All packet evolutions have a mutualistic relationship because as one relay is receiving the other is not, and in the same manner as the other is transmitting the other relay is not. For example, with one packet reception and two helping relays there can only be two alternate states $(0, 1)$ and $(1, 0)$. The system state $(0, 1)$ means 0 packets in R_2's buffer and 1 packet in R_1's buffer, and on the contrary, state $(1, 0)$ means 1 packet in R_1 and 0 packets in R_2. The possible system state transitions from state $(0, 1)$ to state $(1, 0)$ would result when R_1 receives a packet and R_2 transmits while the opposite transition would result when R_2 receives a packet and R_1 transmits.

Suppose it is assumed that there are 4 packets in a combined system such that each relay has a buffer size of 4. All the possible states with two relays of buffer size 4 will correspond to the highlighted diagonal as shown on Table 5.3 chosen to be the main diagonal of operation for all the five alternating system states which could be attained based on the following events: {Relay 1 receives, Relay 1 transmits}, {Relay 1 receives, Relay 2 transmits}, {Relay 2 receives, Relay 1 transmits} and {Relay 2 receives, Relay 2 transmits}. A shortened version of these events which has been frequently used is as follows:
$\{R_1, R_1\}, \{R_1, R_2\}, \{R_2, R_1\}$ and $\{R_2, R_2\}$.

The buffer table for the buffer size of R_1, R_2 as $max(i) = 4, max(j) = 4$ with the diagonal of operation highlighted is as shown in Fig. 5.3.

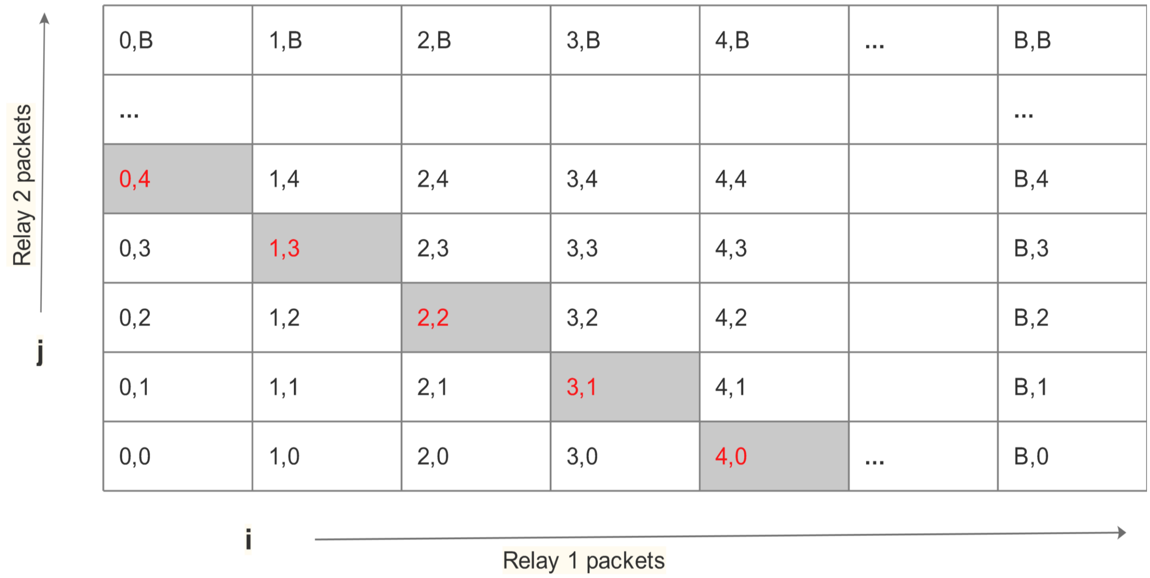

FIGURE 5.3: Buffer Table for the system showing packet evolutions of R_1 buffer and R_2 buffer for a maximum number of 4 packets

5.2.2.2 Combined Buffer and Energy Model

Now that the buffer states of both R_1 and R_2 have been defined and formulated, the system state was formulated and determined as a function of both buffer states and energy states of both R_1 and R_2 as done previously in Chapter 4 with energy of relays. Nevertheless, the energy model in Fig. 4.4 is still conceived for the model in Fig. 5.1. This simply means the system state is now defined by four fundamental components being: {Relay 1 buffer, Relay 2 buffer, Relay 1 Energy, Relay 2 Energy} as clearly portrayed in Fig. 5.4.

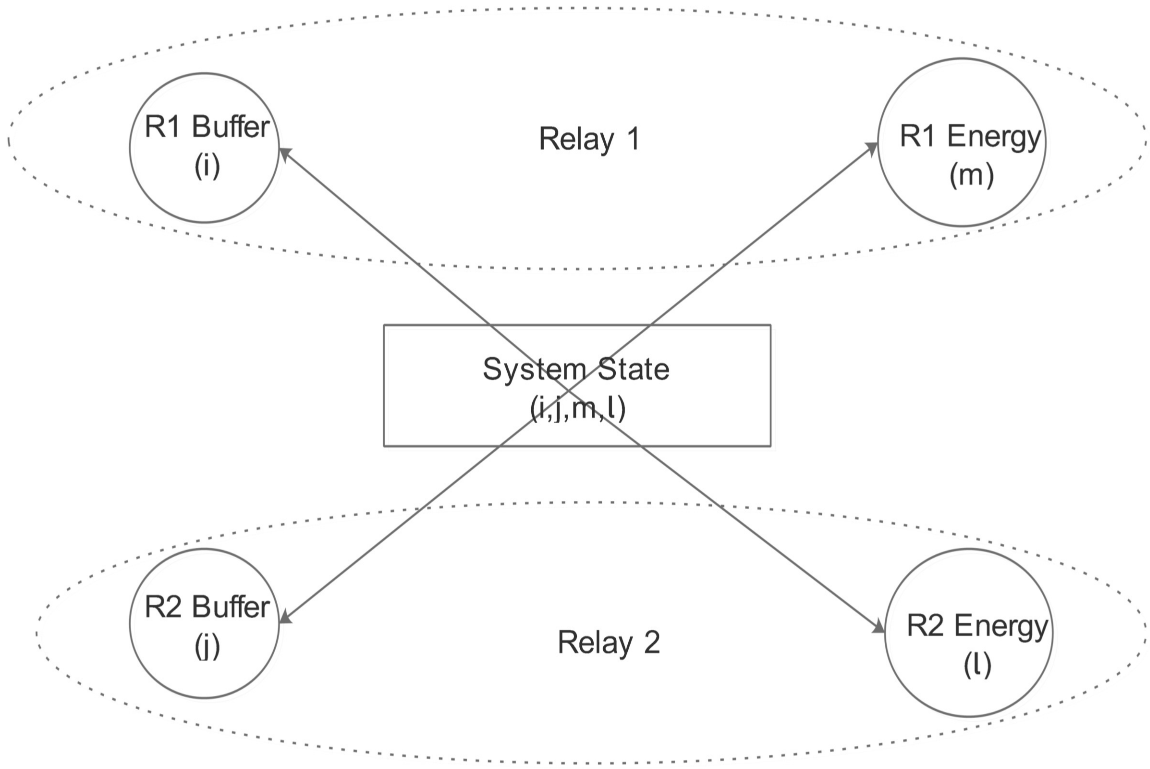

FIGURE 5.4: Buffer-Aided relaying model system state components

Since the buffers are independent of energy, construction of buffer to energy states mappings when the maximum energy harvesting state is $n = 2$ for the battery to be full is necessary to fully define the system state. The following 10 states were attained as a result of the mapping process as shown in Fig. 5.5.

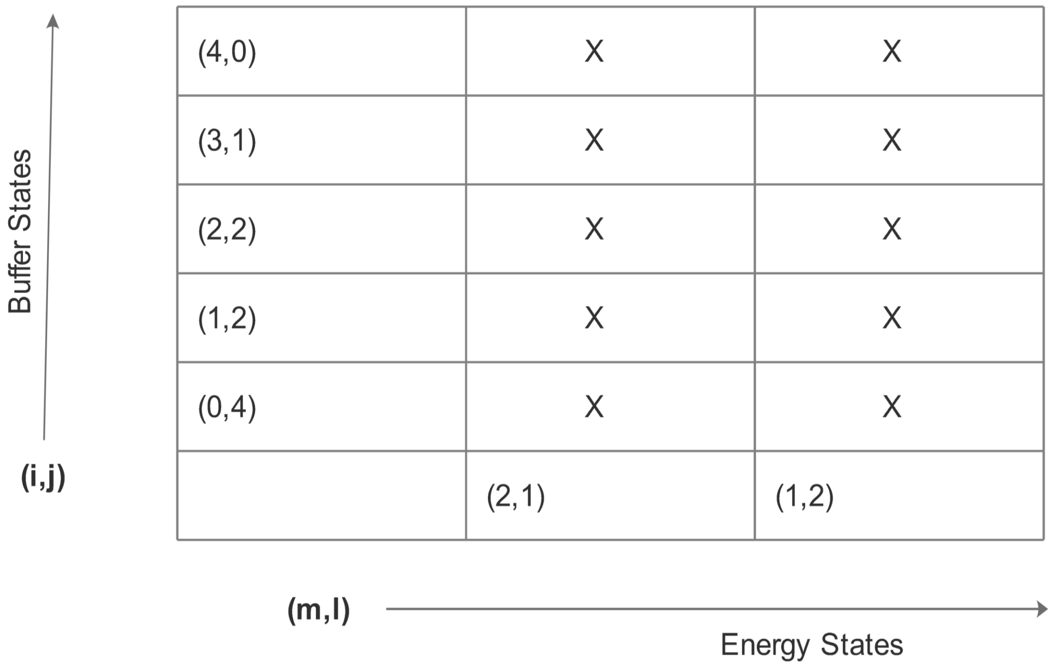

FIGURE 5.5: System states generated by buffer to energy mappings when $max(i) = 4, max(j) = 4$ and maximum n^{th} energy state is 1

The notation of relay reception and transmission is formulated such that it is $R_x R_y$ where $x \subseteq \{1, 2\}, y \subseteq \{1, 2\}$. R_x is the receiving relay and R_y is the transmitting relay.

The buffer to energy states mappings when the maximum n^{th} harvesting state that could be reached is $n = 2$ with the same buffer sizes $max(i) = 4, max(j) = 4$ are also shown below in Fig. 5.6.

(4,0)	X	X	X	X
(3,1)	X	X	X	X
(2,2)	X	X	X	X
(1,3)	X	X	X	X
(0,4)	X	X	X	X
	(3,1)	(2,1)	(1,2)	(1,3)

Buffer States (i,j)

(m,l) Energy States

FIGURE 5.6: System states generated by buffer to energy mappings when $max(i) = 4, max(j) = 4$ and maximum n^{th} harvesting state is 2.

The system states diagram for $m = 1$ and $l \neq 1$,

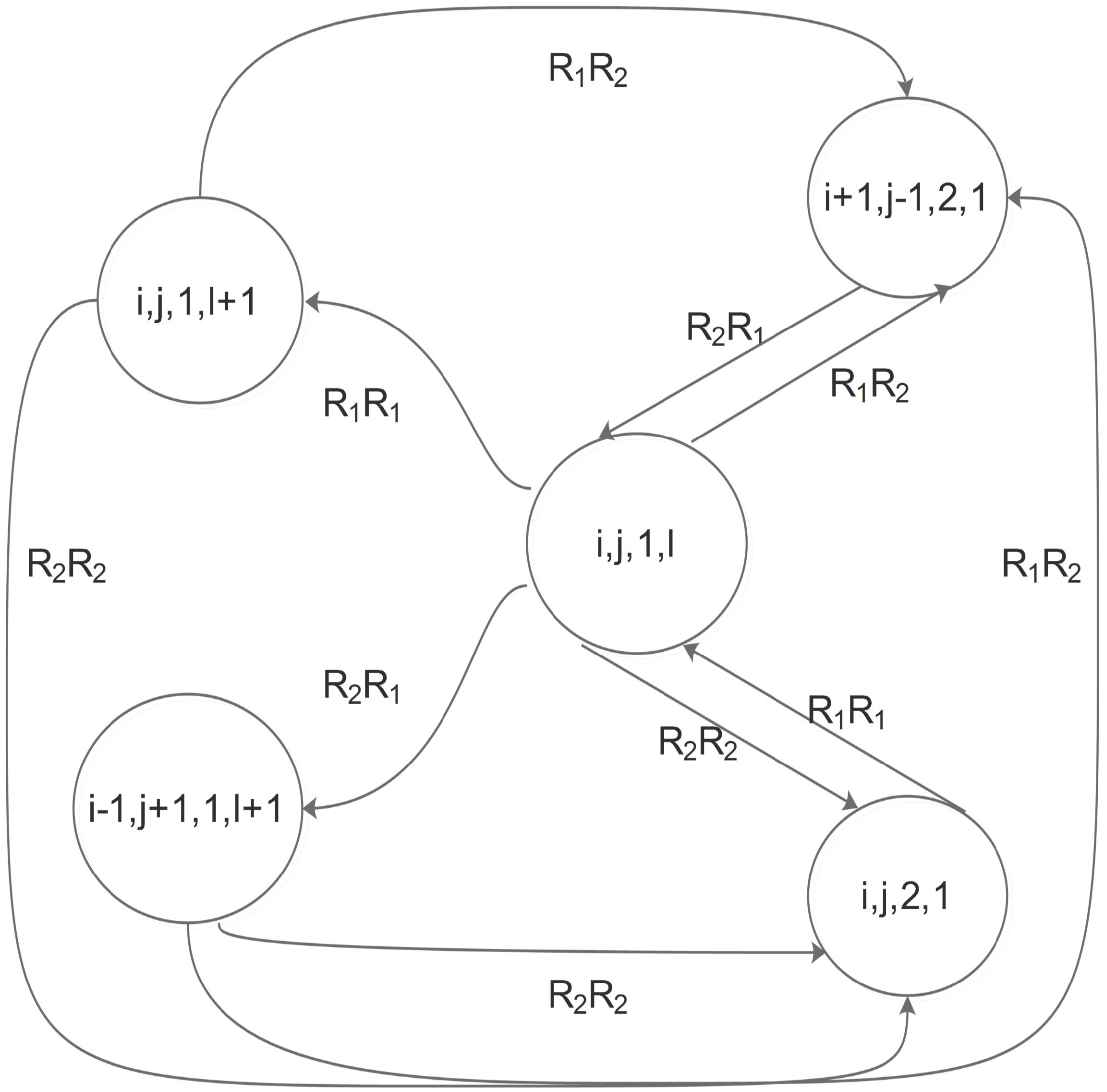

FIGURE 5.7: Markov diagram of the System for $m = 1, l \neq 1$

The system state is a function of 4 parameters (i, j, m, l) such that i is R_1's buffer, j is R_2's buffer, m is relay R_1's energy and l the relay R_2's energy. The above diagram 5.7 shows all system states and transitions when relay R_1 has energy 1 and relay R_2 has energy not equal to 1.

Definition of States:

The state is represented as $S_{i,j,m,l}$ where $i \Rightarrow$ Relay 1 buffer state and $j \Rightarrow$ Relay 2 buffer state, $m \Rightarrow$ Relay R_1 energy state and $l \Rightarrow$ Relay R_2 energy state. For example $S_{1,1,1,2}$ means relay R_1 has 1 packet in its buffer and $1E_0$ unit of energy while relay R_2 has 1 buffer packet and $2E_0$ energy units.

Transition Probabilities for the System at state $(i, j, 1, l)$ are shown in figure 5.8:

| i,j,1,l | $\longrightarrow$ | i,j,1,l+1 |

Transition probability from state $(i, j, 1, l)$ to state $(i, j, 1, l+1)$, $\phi_{((i,j,1,l),(i,j,1,l+1))}$ is a result of relay R_2 being chosen to receive and R_1 to transmit while the system was at state $(i, j, 1, l)$.

| i,j,1,l | $\longrightarrow$ | i,j,2,1 |

Transition probability from state $(i, j, 1, l)$ to state $(i, j, 2, 1)$, $\phi_{((i,j,1,l),(i,j,2,1))}$ is a result of relay R_1 being chosen to receive and R_2 transmit while the system was at state $(i, j, 1, l)$.

| i,j,1,l | $\longrightarrow$ | i+1,j-1,2,1 |

Transition probability from state $(i, j, 1, l)$ to state $(i + 1, j - 1, 2, 1)$, $\phi_{((i,j,1,l),(i+1,j-1,2,1))}$ is a result of relay R_1 being chosen to receive and relay R_2 to transmit while the system was at state $(i, j, 1, l)$.

| i,j,1,l | $\longrightarrow$ | i-1,j+1,1,l+1 |

Transition probability from state $(i, j, 1, l)$ to state $(i - 1, j + 1, 1, l + 1)$, $\phi_{((i,j,1,l),(i-1,j+1,1,l+1))}$ is a result of relay R_2 being chosen to receive and relay R_1 to transmit while the system was at state $(i, j, 1, l)$.

The system states diagram when $m \neq 1$ and $l = 1$,

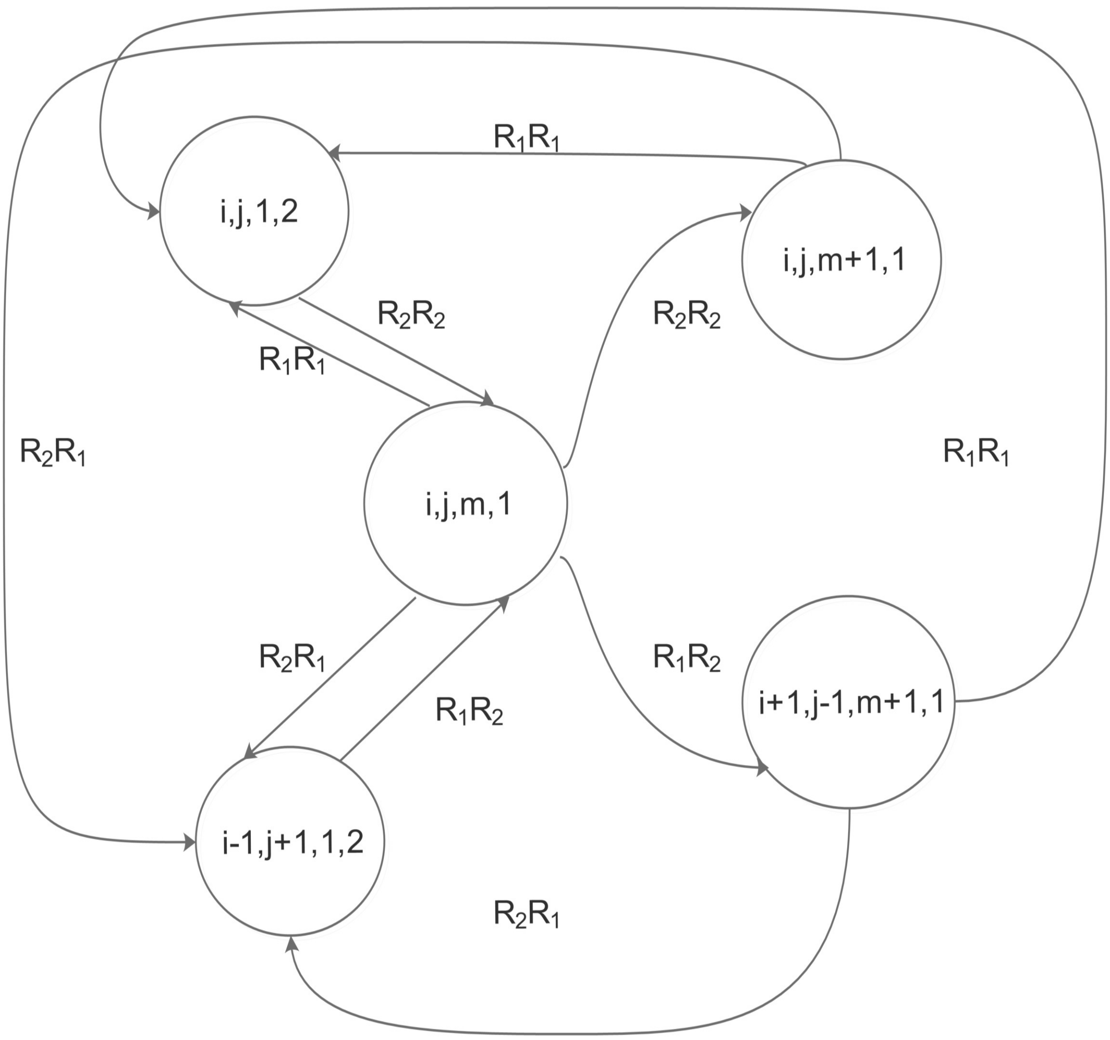

FIGURE 5.8: Markov diagram of the System for $m \neq 1, l = 1$

The above diagram Fig 5.8 shows all system states and transitions when relay R_2 has energy equal to 1 and relay R_1 not equal to 1. As observed in Fig. 5.7 and 5.8, the only possible energy states are $(1, l)$ and (m, l) while holdoning the literature concept that all energy is expended during transmission.

Transition Probabilities for the System at state $(i, j, m, 1)$, as seen in figure 5.1:

$\boxed{\text{i,j,m,1}} \longrightarrow \boxed{\text{i,j,m+1,1}}$ Transition probability from state $(i, j, m, 1)$ to state $(i, j, m + 1, 1)$, $\phi_{((i,j,m,1),(i,j,m+1,1))}$ is a result of relay R_2 being chosen to receive and transmit while the system was at state $(i, j, m, 1)$.

i,j,m,1	$\longrightarrow$	i,j,1,2	Transition probability from state $(i, j, m, 1)$ to state

$(i, j, 1, 2)$, $\phi_{((i,j,m,1),(i,j,1,2))}$ is a result of relay R_1 being chosen to receive and transmit while the system was at state $(i, j, m, 1)$.

i,j,m,1	$\longrightarrow$	i-1,j+1,1,2	Transition probability from state $(i, j, m, 1)$ to state

$(i - 1, j + 1, 1, 2)$, $\phi_{((i,j,m,1),(i-1,j+1,1,2))}$ is a result of relay R_2 being chosen to receive and relay R_1 to transmit while the system was at state $(i, j, m, 1)$.

i,j,m,1	$\longrightarrow$	i+1,j-1,m+1,1	Transition probability from state $(i, j, m, 1)$ to state

$(i + 1, j - 1, m + 1, 1)$, $\phi_{((i,j,m,1),(i+1,j-1,m+1,1))}$ is a result of relay R_1 being chosen to receive and relay R_2 to transmit while the system was at state $(i, j, m, 1)$.

5.2.2.3 Derivation of Transitional Matrices

If introducing a new notation R_1R_2 such that R_1 is the receiving relay node in the first time slot and R_2 the transmitting relay node in the second time slot, then the transition matrices could simply be denoted as shown below in Fig. 5.9 for 10 states and in Fig. 5.10 for 20 states.

Selection events for a relay to receive are as follows:

- Source-relay channel should be greater, $\gamma_{SR_k} = max(\gamma_{SR_1}, \gamma_{SR_2})$, for $k \subseteq \{1, 2\}$
- The buffer of the relay should be less than the maximum capacity of the buffer to accommodate a new packet, $Q_{R_k} < Q_{max}$

Selection events for a relay to transmit are as follows:

- The maximum relay-destination channel is given priority, $\gamma_{R_kD} = max(\gamma_{R_1D}, \gamma_{R_2D})$, for $k \subseteq \{1, 2\}$
- The buffer of the relay should be greater than 0 to avoid transmitting null packets to the destination node, $Q_{R_k} > 0,$ for $k \subseteq \{1, 2\}$

The transition matrix of the system when buffers of R_1 and R_2 are such that $max(i) = 4, max(j) = 4$ with two energy states $\{(2, 1), (1, 2)\}$ in accordance with Fig. 5.5 is:

		F	i	n	a	l	S	t	a	t	e
		(4,0,2,1)	(4,0,1,2)	(3,1,2,1)	(3,1,1,2)	(2,2,2,1)	(2,2,1,2)	(1,3,2,1)	(1,3,1,2)	(0,4,2,1)	(0,4,1,2)
I	(4,0,2,1)	R_2R_2	0	0	R_2R_1	0	0	0	0	0	0
n	(4,0,1,2)	R_2R_2	0	0	R_2R_1	0	0	0	0	0	0
i	(3,1,2,1)	R_1R_2	0	R_2R_2	R_1R_1	0	R_2R_1	0	0	0	0
t	(3,1,1,2)	R_1R_2	0	R_2R_2	R_1R_1	0	R_2R_1	0	0	0	0
i	(2,2,2,1)	0	0	R_1R_2	0	R_2R_2	R_1R_1	0	R_2R_1	0	0
a	(2,2,1,2)	0	0	R_1R_2	0	R_2R_2	R_1R_1	0	R_2R_1	0	0
l	(1,3,2,1)	0	0	0	0	R_1R_2	0	R_2R_2	R_1R_1	0	R_2R_1
	(1,3,1,2)	0	0	0	0	R_1R_2	0	R_2R_2	R_1R_1	0	R_2R_1
	(0,4,2,1)	0	0	0	0	0	0	R_1R_2	0	0	R_1R_1
	(0,4,1,2)	0	0	0	0	0	0	R_1R_2	0	0	R_1R_1

FIGURE 5.9: Transition matrix of the system with buffers at $max(i) = 4, max(j) = 4$ and 1 energy state $\{(2, 1), (1, 2)\}$

The transmission matrix of the system when buffers of R_1 and R_2 are such that $max(i) = 4, max(j) = 4$ with four energy states $\{(3,1),(2,1),(1,2),(1,3)\}$ in accordance with Fig. 5.6 is:

		F	i	n	a	l	S	t	a	t	e	s									
		(4,0,3,1)	(4,0,2,1)	(4,0,1,2)	(4,0,1,3)	(3,1,3,1)	(3,1,2,1)	(3,1,1,2)	(3,1,1,3)	(2,2,3,1)	(2,2,2,1)	(2,2,1,2)	(2,2,1,3)	(1,3,3,1)	(1,3,2,1)	(1,3,1,2)	(1,3,1,3)	(0,4,3,1)	(0,4,2,1)	(0,4,1,2)	(0,4,1,3)
I	(4,0,3,1)	R_2R_2	0	0	0	0	0	R_2R_1	0	0	0	0	0	0	0	0	0	0	0	0	0
n	(4,0,2,1)	R_2R_2	0	0	0	0	0	R_2R_1	0	0	0	0	0	0	0	0	0	0	0	0	0
i	(4,0,1,2)	0	R_2R_2	0	0	0	0	0	R_2R_1	0	0	0	0	0	0	0	0	0	0	0	0
t	(4,0,1,3)	0	R_2R_2	0	0	0	0	0	R_2R_1	0	0	0	0	0	0	0	0	0	0	0	0
i	(3,1,3,1)	R_1R_2	0	0	0	R_2R_2	0	R_1R_1	0	0	0	R_2R_1	0	0	0	0	0	0	0	0	0
a	(3,1,2,1)	R_1R_2	0	0	0	R_2R_2	0	R_1R_1	0	0	0	R_2R_1	0	0	0	0	0	0	0	0	0
l	(3,1,1,2)	0	R_1R_2	0	0	0	R_2R_2	0	R_1R_1	0	0	0	R_2R_1	0	0	0	0	0	0	0	0
S	(3,1,1,3)	0	R_1R_2	0	0	0	R_2R_2	0	R_1R_1	0	0	0	R_2R_1	0	0	0	0	0	0	0	0
t	(2,2,3,1)	0	0	0	0	R_1R_2	0	0	0	R_2R_2	0	R_1R_1	0	0	0	R_2R_1	0	0	0	0	0
a	(2,2,2,1)	0	0	0	0	R_1R_2	0	0	0	R_2R_2	0	R_1R_1	0	0	0	R_2R_1	0	0	0	0	0
t	(2,2,1,2)	0	0	0	0	0	R_1R_2	0	0	0	R_2R_2	0	R_1R_1	0	0	0	R_2R_1	0	0	0	0
e	(2,2,1,3)	0	0	0	0	0	R_1R_2	0	0	0	R_2R_2	0	R_1R_1	0	0	0	R_2R_1	0	0	0	0
s	(1,3,3,1)	0	0	0	0	0	0	0	0	R_1R_2	0	0	0	R_2R_2	0	R_1R_1	0	0	0	R_2R_1	0
	(1,3,2,1)	0	0	0	0	0	0	0	0	R_1R_2	0	0	0	R_2R_2	0	R_1R_1	0	0	0	R_2R_1	0
	(1,3,1,2)	0	0	0	0	0	0	0	0	0	R_1R_2	0	0	0	R_2R_2	0	R_1R_1	0	0	0	R_2R_1
	(1,3,1,3)	0	0	0	0	0	0	0	0	0	R_1R_2	0	0	0	R_2R_2	0	R_1R_1	0	0	0	R_2R_1
	(0,4,3,1)	0	0	0	0	0	0	0	0	0	0	0	0	R_1R_2	0	0	0	0	0	R_1R_1	0
	(0,4,2,1)	0	0	0	0	0	0	0	0	0	0	0	0	R_1R_2	0	0	0	0	0	R_1R_1	0
	(0,4,1,2)	0	0	0	0	0	0	0	0	0	0	0	0	0	R_1R_2	0	0	0	0	0	R_1R_1
	(0,4,1,3)	0	0	0	0	0	0	0	0	0	0	0	0	0	R_1R_2	0	0	0	0	0	R_1R_1

FIGURE 5.10: Transition matrix of the system with buffers at $max(i) = 4, max(j) = 4$ and 2 energy states $\{(3,1),(2,1),(1,2),(1,3)\}$

5.2.3 Reduction from $4D$ State to a $2D$ State Markov

The buffer states of both R_1 and R_2 form a one state (i, j) where i is the number of packets in the R_1 buffer and j of R_2 buffer. This two-dimensional state (i, j) is also mapped into a common state called p such that,

$$p = i + 1, \text{ If relay 1 is receiving} \tag{5.7}$$

and

$$p = (B + 1) - j, \text{ If relay 2 is transmitting} \tag{5.8}$$

Where $B \equiv$ Buffer size.

The two dimensional state (m, l) represents the system energy state which is also expressed as a function of a common state called q in a similar manner to the buffer state, p above. A one dimensional energy state q is expressed in terms of energies of relay R_1, m and relay R_2, l such that,

$$q = \begin{cases} n + (l - 2), & \text{if } m = 1 \\ n + (1 - m), & \text{if } l = 1 \end{cases} \tag{5.9}$$

Where $E_{max} = nE_0$ is the total number of states per relay in an n-state Markov model.

Applying reduction equations in 5.7, 5.8 and 5.9 to simplify the $4D$ buffer and energy mapping into $2D$. For example the Table in Fig. 5.5 has now been simplified as shown in Fig. 5.11.

Buffer States

(4,0)------>(p=5)	X	X
(3,1)------>(p=4)	X	X
(2,2)------>(p=3)	X	X
(1,2)------>(p=2)	X	X
(0,4)------>(p=1)	X	X
	(2,1)------>(q=1)	(1,2)------>(q=2)

(i,j) → p

(m,l) → q

Energy States

FIGURE 5.11: Reduced Buffer to Energy mappings to $2D$ at $max(i) = 4, max(j) = 4$ and 1 energy state per relay $\{(2,1),(1,2)\}$

The Table in Fig. 5.6 in the same manner is reduced to $2D$ as shown in Fig. 5.12.

Buffer States

(4,0)------>(p=5)	X	X	X	X
(3,1)------>(p=4)	X	X	X	X
(2,2)------>(p=3)	X	X	X	X
(1,3)------>(p=2)	X	X	X	X
(0,4)------>(p=1)	X	X	X	X
	(3,1)------>(q=1)	(2,1)------>(q=2)	(1,2)------>(q=3)	(1,3)------>(q=4)

(i,j) → p

(m,l) → q

Energy States

FIGURE 5.12: Reduced Buffer to Energy mappings to $2D$ at $max(i) = 4, max(j) = 4$ and 2 energy states per relay $\{(3,1),(2,1),(1,2),(1,3)\}$

Therefore, the reduced transition matrix in Fig. 5.9 into a $2D$ format is as represented in Fig. 5.13.

		F	i	n	a	l	(p,q)				
		(5,1)	(5,2)	(4,1)	(4,2)	(3,1)	(3,2)	(2,1)	(2,2)	(1,1)	(1,2)
I	(5,1)	R_2R_2	0	0	R_2R_1	0	0	0	0	0	0
n	(5,2)	R_2R_2	0	0	R_2R_1	0	0	0	0	0	0
i	(4,1)	R_1R_2	0	R_2R_2	R_1R_1	0	R_2R_1	0	0	0	0
t	(4,2)	R_1R_2	0	R_2R_2	R_1R_1	0	R_2R_1	0	0	0	0
i	(3,1)	0	0	R_1R_2	0	R_2R_2	R_1R_1	0	R_2R_1	0	0
a	(3,2)	0	0	R_1R_2	0	R_2R_2	R_1R_1	0	R_2R_1	0	0
l	(2,1)	0	0	0	0	R_1R_2	0	R_2R_2	R_1R_1	0	R_2R_1
(p,q)	(2,2)	0	0	0	0	R_1R_2	0	R_2R_2	R_1R_1	0	R_2R_1
	(1,1)	0	0	0	0	0	0	R_1R_2	0	0	R_1R_1
	(1,2)	0	0	0	0	0	0	R_1R_2	0	0	R_1R_1

FIGURE 5.13: $2D$ form transition matrix of the system with buffers at $max(i) = 4, max(j) = 4$ and 1 energy state per relay $\{(2,1),(1,2)\}$

The reduced transition matrix in Fig. 5.10 into a $2D$ format is as represented in Fig. 5.14.

		F	i	n	a	l	S	t	a	t	e	(p,q)									
		(5,1)	(5,2)	(5,3)	(5,4)	(4,1)	(4,2)	(4,3)	(4,4)	(3,1)	(3,2)	(3,3)	(3,4)	(2,1)	(2,2)	(2,3)	(2,4)	(1,1)	(1,2)	(1,3)	(1,4)
I	(5,1)	R_2R_2	0	0	0	0	0	R_2R_1	0	0	0	0	0	0	0	0	0	0	0	0	0
n	(5,2)	R_2R_2	0	0	0	0	0	R_2R_1	0	0	0	0	0	0	0	0	0	0	0	0	0
i	(5,3)	0	R_2R_2	0	0	0	0	0	R_2R_1	0	0	0	0	0	0	0	0	0	0	0	0
t	(5,4)	0	R_2R_2	0	0	0	0	0	R_2R_1	0	0	0	0	0	0	0	0	0	0	0	0
i	(4,1)	R_1R_2	0	0	0	R_2R_2	0	R_1R_1	0	0	0	R_2R_1	0	0	0	0	0	0	0	0	0
a	(4,2)	R_1R_2	0	0	0	R_2R_2	0	R_1R_1	0	0	0	R_2R_1	0	0	0	0	0	0	0	0	0
l	(4,3)	0	R_1R_2	0	0	0	R_2R_2	0	R_1R_1	0	0	0	R_2R_1	0	0	0	0	0	0	0	0
S	(4,4)	0	R_1R_2	0	0	0	R_2R_2	0	R_1R_1	0	0	0	R_2R_1	0	0	0	0	0	0	0	0
t	(3,1)	0	0	0	0	R_1R_2	0	0	0	R_2R_2	0	R_1R_1	0	0	0	R_2R_1	0	0	0	0	0
a	(3,2)	0	0	0	0	R_1R_2	0	0	0	R_2R_2	0	R_1R_1	0	0	0	R_2R_1	0	0	0	0	0
t	(3,3)	0	0	0	0	0	R_1R_2	0	0	0	R_2R_2	0	R_1R_1	0	0	0	R_2R_1	0	0	0	0
e	(3,4)	0	0	0	0	0	R_1R_2	0	0	0	R_2R_2	0	R_1R_1	0	0	0	R_2R_1	0	0	0	0
(p,q)	(2,1)	0	0	0	0	0	0	0	0	R_1R_2	0	0	0	R_2R_2	0	R_1R_1	0	0	0	R_2R_1	0
	(2,2)	0	0	0	0	0	0	0	0	R_1R_2	0	0	0	R_2R_2	0	R_1R_1	0	0	0	R_2R_1	0
	(2,3)	0	0	0	0	0	0	0	0	0	R_1R_2	0	0	0	R_2R_2	0	R_1R_1	0	0	0	R_2R_1
	(2,4)	0	0	0	0	0	0	0	0	0	R_1R_2	0	0	0	R_2R_2	0	R_1R_1	0	0	0	R_2R_1
	(1,1)	0	0	0	0	0	0	0	0	0	0	0	0	R_1R_2	0	0	0	0	0	R_1R_1	0
	(1,2)	0	0	0	0	0	0	0	0	0	0	0	0	R_1R_2	0	0	0	0	0	R_1R_1	0
	(1,3)	0	0	0	0	0	0	0	0	0	0	0	0	0	R_1R_2	0	0	0	0	0	R_1R_1
	(1,4)	0	0	0	0	0	0	0	0	0	0	0	0	0	R_1R_2	0	0	0	0	0	R_1R_1

FIGURE 5.14: $2D$ form transition matrix of the system with buffers at $max(i) = 4, max(j) = 4$ and 2 energy state per relay $\{(3,1),(2,1),(1,2),(1,3)\}$

5.3 Performance Analysis

5.3.1 Derivation of steady-state Probabilities

The system state in this chapter is a combined (buffer, energy) unlike in Chapter 4 where the system is confined only to harvested energy. The steady-states $\pi_{p,q}$ are formulated as a function of two-dimensional states (p, q) from a reduced four-dimensional state (i, j, m, l).

To determine the system states by usage of steady-state equation,

$$\begin{aligned} \pi_{p,q}\phi_{transition} &= \pi_{p,q} \\ \text{Where} \quad \sum_{p=1}^{B=Buffersize} \sum_{q=1}^{n} \pi_{p,q} &= 1 \end{aligned} \tag{5.10}$$

Where $\pi_{p,q}$ is the steady-state vector and $\phi_{transition}$ is the probability transition matrix, hence determining the system state at the steady state. The stationary distribution $\pi_{p,q}$ is a vector whose entries are non-negative and sum to 1.

5.3.2 Outage Probability Analysis

Conditions that lead to outage in a buffer-aided relay cooperative network:

1. For a selected receiving relay node:
   - There will be outage when the source-to-relay SNR link is less than the threshold SNR, $\gamma_{SR_k} < \gamma_{th}$.
2. For a chosen transmitting relay node:
   - Outage will result when the relay-to-destination SNR link is less than the threshold SNR, $\gamma_{R_kD} < \gamma_{th}$.

To find an outage expression, an equation 4.10 was followed and useful. If the system is at state $(i, j, m, 1)$ where R_2 has energy of E_0 in the battery while R_1 has energy of mE_0 at any buffer sizes (i, j). According to our main assumption as used in the literature, energy is only used for transmitting and not for receiving.

Therefore, the link outage of the Source-R_1 (SR_1), the receiving link when the system is in state $(i, j, m, 1)$ is

$$\begin{aligned} P_{SR_1}|_{(i,j,m,1)} &= 1 - \exp\left(\frac{-\gamma_{th}}{\overline{\gamma}_{SR_1}}\right) \\ &= 1 - \exp\left(\frac{-\gamma_{th}}{\frac{\frac{P_S \mathbb{E}\{|h_{SR_1}|^2\} N_0}{((1-\tau)T)}}{2}}\right) \\ &= 1 - \exp\left(\frac{-2\gamma_{th}}{P_S((1-\tau)T)\mathbb{E}\{|h_{SR_1}|^2\} N_0}\right) \end{aligned} \tag{5.11}$$

The Source-R_2 (SR_2) link outage when the system is in state $(i, j, 1, l)$ is as follows

$$\begin{aligned} P_{SR_2}|_{(i,j,1,l)} &= 1 - \exp\left(\frac{-\gamma_{th}}{\overline{\gamma}_{SR_2}}\right) \\ &= 1 - \exp\left(\frac{-\gamma_{th}}{\frac{\frac{P_S \mathbb{E}\{|h_{SR_2}|^2\} N_0}{((1-\tau)T)}}{2}}\right) \\ &= 1 - \exp\left(\frac{-2\gamma_{th}}{P_S((1-\tau)T)\mathbb{E}\{|h_{SR_2}|^2\} N_0}\right) \end{aligned} \tag{5.12}$$

The outage of the R_1-Destination (R_1D) transmitting link when the system is in state $(i, j, m, 1)$ can be expressed as,

$$\begin{aligned} P_{R_1D}|_{(i,j,m,1)} &= 1 - \exp\left(\frac{-\gamma_{th}}{\overline{\gamma}_{R_1D}}\right) \\ &= 1 - \exp\left(\frac{-\gamma_{th}}{\frac{\frac{mE_0\mathbb{E}\{|h_{R_1D}|^2\}N_0}{((1-\tau)T)}}{2}}\right) \\ &= 1 - \exp\left(\frac{-2\gamma_{th}}{mE_0((1-\tau)T)\mathbb{E}\{|h_{R_1D}|^2\}N_0}\right) \end{aligned} \tag{5.13}$$

The outage of the R_2-Destination (R_2D) link when the system is in state $(i, j, 1, l)$ can be expressed as,

$$\begin{aligned} P_{R_2D}|_{(i,j,1,l)} &= 1 - \exp\left(\frac{-\gamma_{th}}{\overline{\gamma}_{R_2D}}\right) \\ &= 1 - \exp\left(\frac{-\gamma_{th}}{\frac{\frac{lE_0\mathbb{E}\{|h_{R_2D}|^2\}N_0}{((1-\tau)T)}}{2}}\right) \\ &= 1 - \exp\left(\frac{-2\gamma_{th}}{lE_0((1-\tau)T)\mathbb{E}\{|h_{R_2D}|^2\}N_0}\right) \end{aligned} \tag{5.14}$$

5.3.3 Derivation of Overall System Outage

The system outage would result due to outage of either or both $S - R_1$ link and $S - R_2$ link in relay R_1, either or both $R_1 - D$ and $R_2 - D$ links in relay R_2. It is given by computation of outage in the best receive and/or transmit relay channels.

The best relay to receive from the source S is given by a maximum $S - R_k$ link as shown below,

$$\gamma_{b^*_{rx}} = \max_{k \in \{1,2\}} (\gamma_{SR_k}).$$

While the best relay to transmit to the destination D is the one with highest $R_k - D$ link as computed using

$$\gamma_{b^*_{tx}} = \max_{k\in \{1,2\}} (\gamma_{R_k D}).$$

The system outage is therefore a result of best receiving $S - R_k$ link being in outage or the best transmitting $R_k - D$ link in outage or both. Thus there would be outage if the selected relay either R_1 or R_2 is in outage. For relay R_1 to be outage, the SNR of links $S - R_1$, $R_1 - D$ or both would be less than the threshold SNR. Likewise for R_2 to be in outage one or both of the links $S - R_2$, $R_2 - D$ would be less than the threshold SNR.

The outage probability of the system due to relay R_1 is,

$$\begin{aligned} P_{out_1|(p,q)} &= Pr(\gamma_{SR_1} < \gamma_{th}) + Pr(\gamma_{R_1D} < \gamma_{th}) \\ &= \left[1 - \exp\left(\frac{-\gamma_{th}}{\overline{\gamma}_{SR_1}}\right)\right] + \left[1 - \exp\left(\frac{-\gamma_{th}}{\overline{\gamma}_{R_1D}}\right)\right] \\ &= \left[1 - \exp\left(\frac{-2\gamma_{th}}{P_S((1-\tau)T)\mathbb{E}\{|h_{SR_1}|^2\}N_0}\right)\right] + \\ &\left[1 - \exp\left(\frac{-2\gamma_{th}}{(E_{max} + (1-q))E_0((1-\tau)T)\mathbb{E}\{|h_{R_1D}|^2\}N_0}\right)\right] \end{aligned} \tag{5.15}$$

The probability outage of the system due to relay R_2 is,

$$\begin{aligned} P_{out_2|(p,q)} &= Pr(\gamma_{SR_2} < \gamma_{th}) + Pr(\gamma_{R_2D} < \gamma_{th}) \\ &= \left[1 - \exp\left(\frac{-\gamma_{th}}{\overline{\gamma}_{SR_2}}\right)\right] + \left[1 - \exp\left(\frac{-\gamma_{th}}{\overline{\gamma}_{R_2D}}\right)\right] \\ &= \left[1 - \exp\left(\frac{-2\gamma_{th}}{P_S((1-\tau)T)\mathbb{E}\{|h_{SR_2}|^2\}N_0}\right)\right] + \\ &\left[1 - \exp\left(\frac{-2\gamma_{th}}{(q-1)E_0((1-\tau)T)\mathbb{E}\{|h_{R_2D}|^2\}N_0}\right)\right] \end{aligned} \tag{5.16}$$

The system outage probability due to R_1 for receiving and R_2 for transmitting,

$$\begin{aligned}
P_{out_1|(p,q)} &= Pr(\gamma_{SR_1} < \gamma_{th}) + Pr(\gamma_{R_2D} < \gamma_{th}) \\
&= \left[1 - \exp\left(\frac{-\gamma_{th}}{\overline{\gamma}_{SR_1}}\right)\right] + \left[1 - \exp\left(\frac{-\gamma_{th}}{\overline{\gamma}_{R_2D}}\right)\right] \\
&= \left[1 - \exp\left(\frac{-2\gamma_{th}}{P_S((1-\tau)T)\mathbb{E}\{|h_{SR_1}|^2\}N_0}\right)\right] + \\
&\left[1 - \exp\left(\frac{-2\gamma_{th}}{(E_{max} + (1-q))E_0((1-\tau)T)\mathbb{E}\{|h_{R_2D}|^2\}N_0}\right)\right]
\end{aligned} \tag{5.17}$$

The system outage due to R_2 receiving and R_1 transmitting is,

$$\begin{aligned}
P_{out_2|(p,q)} &= Pr(\gamma_{SR_2} < \gamma_{th}) + Pr(\gamma_{R_1D} < \gamma_{th}) \\
&= \left[1 - \exp\left(\frac{-\gamma_{th}}{\overline{\gamma}_{SR_2}}\right)\right] + \left[1 - \exp\left(\frac{-\gamma_{th}}{\overline{\gamma}_{R_1D}}\right)\right] \\
&= \left[1 - \exp\left(\frac{-2\gamma_{th}}{P_S((1-\tau)T)\mathbb{E}\{|h_{SR_2}|^2\}N_0}\right)\right] + \\
&\left[1 - \exp\left(\frac{-2\gamma_{th}}{(q-1)E_0((1-\tau)T)\mathbb{E}\{|h_{R_1D}|^2\}N_0}\right)\right]
\end{aligned} \tag{5.18}$$

The overall outage probability of the system as a function of R_1 and R_2 is,

$$\begin{aligned}
P_{out|(p,q)} &= Pr(min\{\gamma_{b^*_{rx}}, \gamma_{b^*_{tx}}\} < \gamma_{th}) \\
&= P_{out_1|(p,q)}\pi_{p,q} + P_{out_2|(p,q)}\pi_{p,q} \\
&= \sum_{p=1}^{B}\sum_{q=1}^{E_{max}} \left[1 - \exp\left(\frac{-2\gamma_{th}}{P_S((1-\tau)T)\mathbb{E}\{|h_{SR_2}|^2\}N_0}\right)\right]\pi_{p,q} \\
&+ \sum_{p=1}^{B}\sum_{q=1}^{E_{max}} \left[1 - \exp\left(\frac{-2\gamma_{th}}{(q-1)E_0((1-\tau)T)\mathbb{E}\{|h_{R_2D}|^2\}N_0}\right)\right]\pi_{p,q}
\end{aligned} \tag{5.19}$$

5.4 Numerical Results and Simulations

This section illustrates the results developed for a buffer-aided model by numerical simulations. Without loss of generality, it was assumed that the minimum acceptable rate r is 1 bps just like in the reactive scheme in Chapter 4. Moreover, the number of relays K is 2, each with two packets in its buffer of the maximum size of four.

The analysis is done with variance N_0 and average SNRs $\overline{\gamma}_{SR_k} = \frac{\mathbb{E}\{|h^2_{SR_k}|\}E_S}{N_0}$, $\overline{\gamma}_{R_kD} = \frac{\mathbb{E}\{|h^2_{R_kD}|\}E_{R_k}}{N_0}$ for harvesting times $\tau = 0.2$, 0.4 and 0.6 seconds. The transition matrix is calculated from SNR values of the two relays depending on which was selected when the other was harvesting. Fig. 5.15 illustrates the outage probability of a buffer-aided harvesting relaying network as a function of SNR when the relays are harvesting energy for $\tau = 0.2$ seconds with five buffer states and four energy states. Fig. 5.16 exemplifies results for the same five buffer states and two energy states under the same conditions. The analytical simulations are aligned with the Monte Carlo simulations for both 20 and 10 system states accordingly.

In Fig. 5.15 the analytical framework simulations being aligned with Monte Carlo simulations for 5 buffer states with 2 discretized energy states per relay with relays harvesting for 0.2 seconds is shown. This indeed shows our analytical model is practically realizable because it matches the simulation framework.

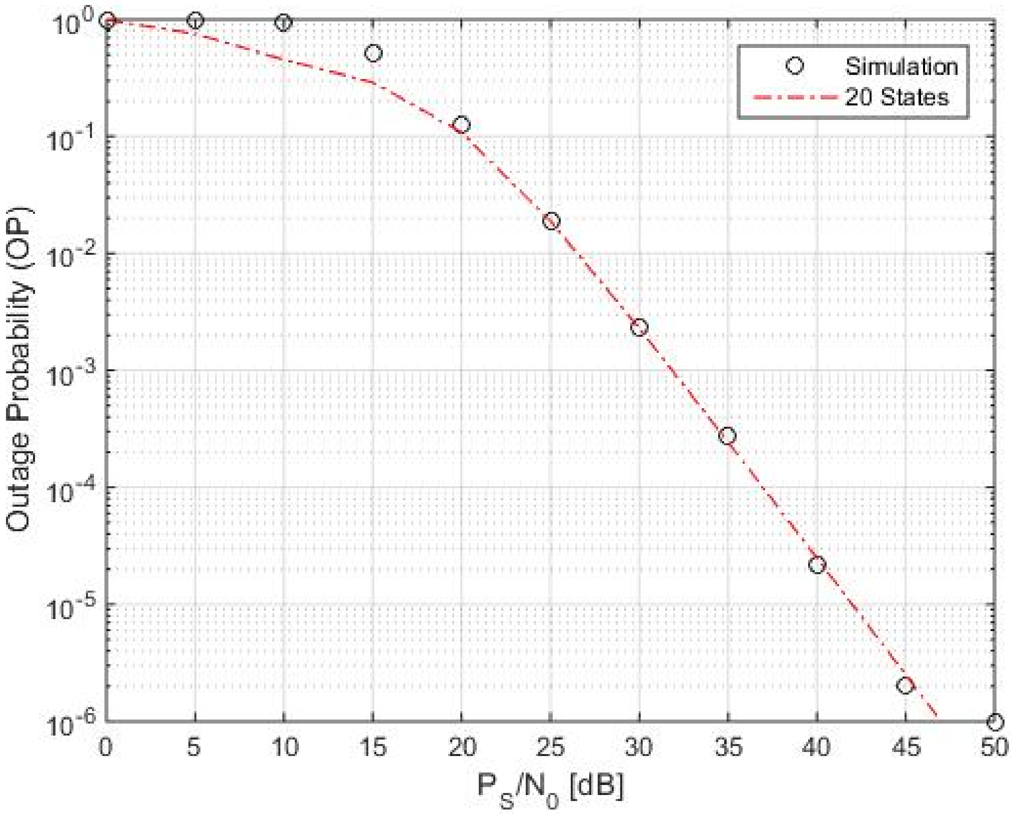

FIGURE 5.15: Monte Carlo simulation and analytical results for 5 buffer states with 2 energy states (per relay) quantization

The results in Fig. 5.16 show the outage behaviour of 5 buffer states and 2 discretized energy states with relays harvesting for 0.2 seconds under different average SNRs conditions. All the possible scenarios for $\overline{\gamma}_{SR_1} > \overline{\gamma}_{SR_2}$,$\overline{\gamma}_{R_1D} = \overline{\gamma}_{R_2D}$, and $\overline{\gamma}_{SR_1} < \overline{\gamma}_{SR_2}$, $\overline{\gamma}_{R_1D} = \overline{\gamma}_{R_2D}$, and $\overline{\gamma}_{SR_1} = \overline{\gamma}_{SR_2}$,$\overline{\gamma}_{R_1D} > \overline{\gamma}_{R_2D}$, and, $\overline{\gamma}_{SR_1} = \overline{\gamma}_{SR_2}$ $\overline{\gamma}_{R_1D} < \overline{\gamma}_{R_2D}$ were observed and plotted.

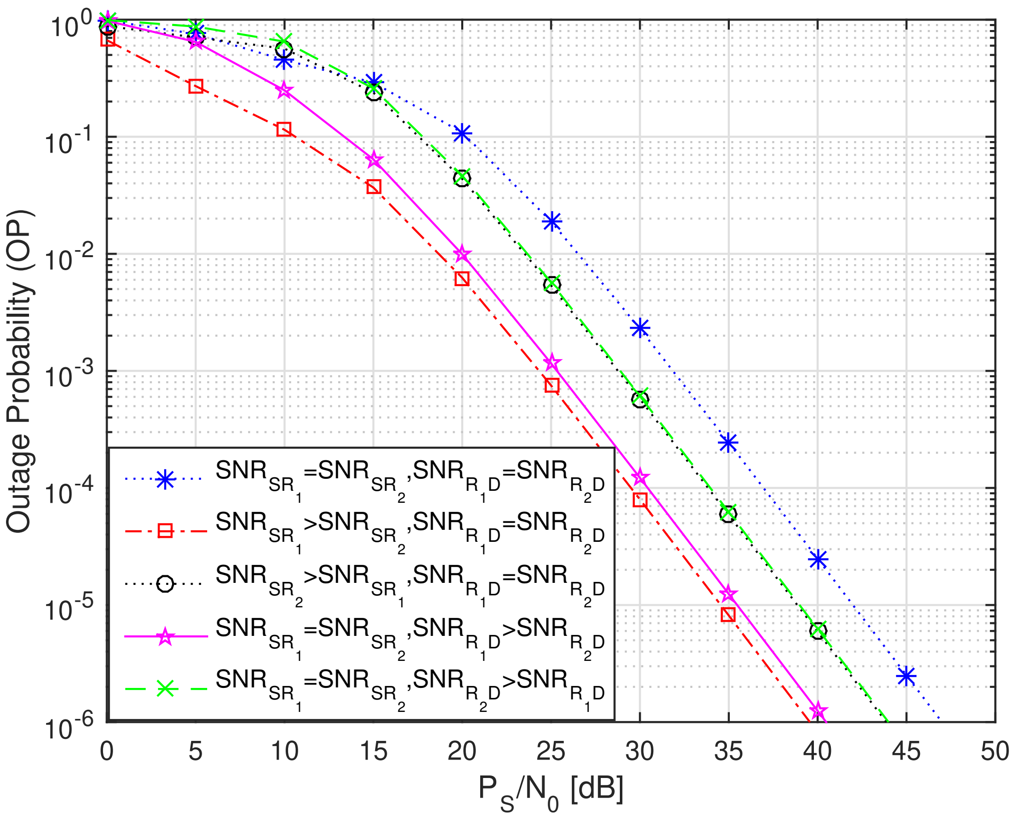

FIGURE 5.16: Results for 5 buffer states with 2 energy states (per relay) quantization with variable SNRs, where SNR on the legend is the average $\overline{\gamma}$ of the link.

From the results in Fig. 5.16 , it was also found that the S-R and R-D links with higher average SNRs perform much better. This is all because the selection is now considered at both source-relay and relay-destination links. As compared to results in Fig. 4.7 of Chapter 4 it can clearly be seen that indeed buffers add performance because Fig. 5.16 with less energy states, except the addition of buffers performs better than Fig. 4.7.

The intermediate results, transition probabilities and steady-state probabilities were also presented respectively based on the provided cases. For all equal SNRs, the results show symmetry of equal state probabilities of either choosing R_1 or R_2. For $\overline{\gamma}_{SR_1} > \overline{\gamma}_{SR_2}$ and $\overline{\gamma}_{R_1D} > \overline{\gamma}_{R_2D}$, the state probabilities values of using R_1 for relaying are higher than of R_2. Likewise, for cases $\overline{\gamma}_{SR_1} < \overline{\gamma}_{SR_2}$ and $\overline{\gamma}_{R_1D} < \overline{\gamma}_{R_2D}$, the state probabilities of using R_2 for relaying are much higher than R_1 as expected.

The intermediate values for the above outage results in Fig. 5.16: $\overline{\gamma}_{SR_1} = \overline{\gamma}_{SR_2}$ and $\overline{\gamma}_{R_1D} = \overline{\gamma}_{R_2D}$,

TABLE 5.1: Estimated state transition matrix for Fig. 5.16

		F	i	n	a	l	S	t	a	t	e	(p,q)									
		(5,1)	(5,2)	(5,3)	(5,4)	(4,1)	(4,2)	(4,3)	(4,4)	(3,1)	(3,2)	(3,3)	(3,4)	(2,1)	(2,2)	(2,3)	(2,4)	(1,1)	(1,2)	(1,3)	(1,4)
I	(5,1)	0.2500	0	0	0	0	0	0.2500	0	0	0	0	0	0	0	0	0	0	0	0	0
n	(5,2)	0.2500	0	0	0	0	0	0.2500	0	0	0	0	0	0	0	0	0	0	0	0	0
i	(5,3)	0	0.2500	0	0	0	0	0	0.2500	0	0	0	0	0	0	0	0	0	0	0	0
t	(5,4)	0	0.2500	0	0	0	0	0	0.2500	0	0	0	0	0	0	0	0	0	0	0	0
i	(4,1)	0.2500	0	0	0	0.2500	0	0.2500	0	0	0	0.2500	0	0	0	0	0	0	0	0	0
a	(4,2)	0.2500	0	0	0	0.2500	0	0.2500	0	0	0	0.2500	0	0	0	0	0	0	0	0	0
l	(4,3)	0	0.2500	0	0	0	0.2500	0	0.2500	0	0	0	0.2500	0	0	0	0	0	0	0	0
S	(4,4)	0	0.2500	0	0	0	0.2500	0	0.2500	0	0	0	0.2500	0	0	0	0	0	0	0	0
t	(3,1)	0	0	0	0	0.2500	0	0	0	0.2500	0	0.2500	0	0	0	0.2500	0	0	0	0	0
a	(3,2)	0	0	0	0	0.2500	0	0	0	0.2500	0	0.2500	0	0	0	0.2500	0	0	0	0	0
t	(3,3)	0	0	0	0	0	0.2500	0	0	0	0.2500	0	0.2500	0	0	0	0.2500	0	0	0	0
e	(3,4)	0	0	0	0	0	0.2500	0	0	0	0.2500	0	0.2500	0	0	0	0.2500	0	0	0	0
(p,q)	(2,1)	0	0	0	0	0	0	0	0	0.2500	0	0	0	0.2500	0	0.2500	0	0	0	0.2500	0
	(2,2)	0	0	0	0	0	0	0	0	0.2500	0	0	0	0.2500	0	0.2500	0	0	0	0.2500	0
	(2,3)	0	0	0	0	0	0	0	0	0	0.2500	0	0	0	0.2500	0	0.2500	0	0	0	0.2500
	(2,4)	0	0	0	0	0	0	0	0	0	0.2500	0	0	0	0.2500	0	0.2500	0	0	0	0.2500
	(1,1)	0	0	0	0	0	0	0	0	0	0	0	0	0.2500	0	0	0	0	0	0.2500	0
	(1,2)	0	0	0	0	0	0	0	0	0	0	0	0	0.2500	0	0	0	0	0	0.2500	0
	(1,3)	0	0	0	0	0	0	0	0	0	0	0	0	0	0.2500	0	0	0	0	0	0.2500
	(1,4)	0	0	0	0	0	0	0	0	0	0	0	0	0	0.2500	0	0	0	0	0	0.2500

TABLE 5.2: Estimated steady-state vector $\pi_{p,q}$ for Fig. 5.16

	q=1	q=2	q=3	q=4
p=5	0.0691	0.0264	0	0
p=4	0.0854	0.0691	0.0691	0.0264
p=3	0.0691	0.0854	0.0854	0.0691
p=2	0.0264	0.0691	0.0691	0.0854
p=1	0	0	0.0264	0.0691

The intermediate values for the outage results in Fig. 5.16 when $\overline{\gamma}_{SR_1} > \overline{\gamma}_{SR_2}$ and $\overline{\gamma}_{R_1D} = \overline{\gamma}_{R_2D}$,

TABLE 5.3: Estimated state transition matrix for Fig. 5.16

		F	i	n	a	l	S	t	a	t	e	(p,q)									
		(5,1)	(5,2)	(5,3)	(5,4)	(4,1)	(4,2)	(4,3)	(4,4)	(3,1)	(3,2)	(3,3)	(3,4)	(2,1)	(2,2)	(2,3)	(2,4)	(1,1)	(1,2)	(1,3)	(1,4)
I	(5,1)	0.0625	0	0	0	0	0	0.1875	0	0	0	0	0	0	0	0	0	0	0	0	0
n	(5,2)	0.0625	0	0	0	0	0	0.1875	0	0	0	0	0	0	0	0	0	0	0	0	0
i	(5,3)	0	0.0625	0	0	0	0	0	0.1875	0	0	0	0	0	0	0	0	0	0	0	0
t	(5,4)	0	0.0625	0	0	0	0	0	0.1875	0	0	0	0	0	0	0	0	0	0	0	0
i	(4,1)	0.1875	0	0	0	0.0625	0	0.5625	0	0	0	0.1875	0	0	0	0	0	0	0	0	0
a	(4,2)	0.1875	0	0	0	0.0625	0	0.5625	0	0	0	0.1875	0	0	0	0	0	0	0	0	0
l	(4,3)	0	0.1875	0	0	0	0.0625	0	0.5625	0	0	0	0.1875	0	0	0	0	0	0	0	0
S	(4,4)	0	0.1875	0	0	0	0.0625	0	0.5625	0	0	0	0.1875	0	0	0	0	0	0	0	0
t	(3,1)	0	0	0	0	0.1875	0	0	0	0.0625	0	0.5625	0	0	0	0.1875	0	0	0	0	0
a	(3,2)	0	0	0	0	0.1875	0	0	0	0.0625	0	0.5625	0	0	0	0.1875	0	0	0	0	0
t	(3,3)	0	0	0	0	0	0.1875	0	0	0	0.0625	0	0.5625	0	0	0	0.1875	0	0	0	0
e	(3,4)	0	0	0	0	0	0.1875	0	0	0	0.0625	0	0.5625	0	0	0	0.1875	0	0	0	0
(p,q)	(2,1)	0	0	0	0	0	0	0	0	0.1875	0	0	0	0.0625	0	0.5625	0	0	0	0.1875	0
	(2,2)	0	0	0	0	0	0	0	0	0.1875	0	0	0	0.0625	0	0.5625	0	0	0	0.1875	0
	(2,3)	0	0	0	0	0	0	0	0	0	0.1875	0	0	0	0.0625	0	0.5625	0	0	0	0.1875
	(2,4)	0	0	0	0	0	0	0	0	0	0.1875	0	0	0	0.0625	0	0.5625	0	0	0	0.1875
	(1,1)	0	0	0	0	0	0	0	0	0	0	0	0	0.1875	0	0	0	0	0	0.5625	0
	(1,2)	0	0	0	0	0	0	0	0	0	0	0	0	0.1875	0	0	0	0	0	0.5625	0
	(1,3)	0	0	0	0	0	0	0	0	0	0	0	0	0	0.1875	0	0	0	0	0	0.5625
	(1,4)	0	0	0	0	0	0	0	0	0	0	0	0	0	0.1875	0	0	0	0	0	0.5625

TABLE 5.4: Estimated steady-state vector $\pi_{p,q}$ for Fig. 5.16

	q=1	q=2	q=3	q=4
p=5	0.0188	0.0289	0	0
p=4	0.0208	0.0565	0.0565	0.0868
p=3	0.0148	0.0624	0.0624	0.1694
p=2	0.0032	0.0445	0.0445	0.1872
p=1	0	0	0.0096	0.1336

The intermediate values for the outage results in Fig. 5.16 when $\overline{\gamma}_{SR_1} < \overline{\gamma}_{SR_2}$ and $\overline{\gamma}_{R_1D} = \overline{\gamma}_{R_2D}$,

TABLE 5.5: Estimated state transition matrix for Fig. 5.16

		F	i	n	a	l	S	t	a	t	e	(p,q)									
		(5,1)	(5,2)	(5,3)	(5,4)	(4,1)	(4,2)	(4,3)	(4,4)	(3,1)	(3,2)	(3,3)	(3,4)	(2,1)	(2,2)	(2,3)	(2,4)	(1,1)	(1,2)	(1,3)	(1,4)
I	(5,1)	0.5625	0	0	0	0	0	0.1875	0	0	0	0	0	0	0	0	0	0	0	0	0
n	(5,2)	0.5625	0	0	0	0	0	0.1875	0	0	0	0	0	0	0	0	0	0	0	0	0
i	(5,3)	0	0.5625	0	0	0	0	0	0.1875	0	0	0	0	0	0	0	0	0	0	0	0
t	(5,4)	0	0.5625	0	0	0	0	0	0.1875	0	0	0	0	0	0	0	0	0	0	0	0
i	(4,1)	0.1875	0	0	0	0.5625	0	0.0625	0	0	0	0.1875	0	0	0	0	0	0	0	0	0
a	(4,2)	0.1875	0	0	0	0.5625	0	0.0625	0	0	0	0.1875	0	0	0	0	0	0	0	0	0
l	(4,3)	0	0.1875	0	0	0	0.5625	0	0.0625	0	0	0	0.1875	0	0	0	0	0	0	0	0
S	(4,4)	0	0.1875	0	0	0	0.5625	0	0.0625	0	0	0	0.1875	0	0	0	0	0	0	0	0
t	(3,1)	0	0	0	0	0.1875	0	0	0	0.5625	0	0.0625	0	0	0	0.1875	0	0	0	0	0
a	(3,2)	0	0	0	0	0.1875	0	0	0	0.5625	0	0.0625	0	0	0	0.1875	0	0	0	0	0
t	(3,3)	0	0	0	0	0	0.1875	0	0	0	0.5625	0	0.0625	0	0	0	0.1875	0	0	0	0
t	(3,4)	0	0	0	0	0	0.1875	0	0	0	0.5625	0	0.0625	0	0	0	0.1875	0	0	0	0
e	(2,1)	0	0	0	0	0	0	0	0	0.1875	0	0	0	0.5625	0	0.0625	0	0	0	0.1875	0
(p,q)	(2,2)	0	0	0	0	0	0	0	0	0.1875	0	0	0	0.5625	0	0.0625	0	0	0	0.1875	0
	(2,3)	0	0	0	0	0	0	0	0	0	0.1875	0	0	0	0.5625	0	0.0625	0	0	0	0.1875
	(2,4)	0	0	0	0	0	0	0	0	0	0.1875	0	0	0	0.5625	0	0.0625	0	0	0	0.1875
	(1,1)	0	0	0	0	0	0	0	0	0	0	0	0	0.1875	0	0	0	0	0	0.5625	0
	(1,2)	0	0	0	0	0	0	0	0	0	0	0	0	0.1875	0	0	0	0	0	0.0625	0
	(1,3)	0	0	0	0	0	0	0	0	0	0	0	0	0	0.1875	0	0	0	0	0	0.0625
	(1,4)	0	0	0	0	0	0	0	0	0	0	0	0	0	0.1875	0	0	0	0	0	0.0625

TABLE 5.6: Estimated steady-state vector $\pi_{p,q}$ for Fig. 5.16

	q=1	q=2	q=3	q=4
p=5	0.1336	0.0096	0	0
p=4	0.1872	0.0445	0.0445	0.0032
p=3	0.1694	0.0624	0.0624	0.0148
p=2	0.0868	0.0565	0.0565	0.0208
p=1	0	0	0.0289	0.0188

The intermediate values for the outage results in Fig. 5.16 when $\overline{\gamma}_{SR_1} = \overline{\gamma}_{SR_2}$ and $\overline{\gamma}_{R_1D} > \overline{\gamma}_{R_2D}$,

Table 5.7: Estimated state transition matrix for Fig. 5.16

		F	i	n	a	l	S	t	a	t	e	(p,q)									
		(5,1)	(5,2)	(5,3)	(5,4)	(4,1)	(4,2)	(4,3)	(4,4)	(3,1)	(3,2)	(3,3)	(3,4)	(2,1)	(2,2)	(2,3)	(2,4)	(1,1)	(1,2)	(1,3)	(1,4)
I	(5,1)	0.1250	0	0	0	0	0	0.3750	0	0	0	0	0	0	0	0	0	0	0	0	0
n	(5,2)	0.1250	0	0	0	0	0	0.3750	0	0	0	0	0	0	0	0	0	0	0	0	0
i	(5,3)	0	0.1250	0	0	0	0	0	0.3750	0	0	0	0	0	0	0	0	0	0	0	0
t	(5,4)	0	0.1250	0	0	0	0	0	0.3750	0	0	0	0	0	0	0	0	0	0	0	0
i	(4,1)	0.1250	0	0	0	0.1250	0	0.3750	0	0	0	0.3750	0	0	0	0	0	0	0	0	0
a	(4,2)	0.1250	0	0	0	0.1250	0	0.3750	0	0	0	0.3750	0	0	0	0	0	0	0	0	0
l	(4,3)	0	0.1250	0	0	0	0.1250	0	0.3750	0	0	0	0.3750	0	0	0	0	0	0	0	0
S	(4,4)	0	0.1250	0	0	0	0.1250	0	0.3750	0	0	0	0.3750	0	0	0	0	0	0	0	0
t	(3,1)	0	0	0	0	0.1250	0	0	0	0.1250	0	0.3750	0	0	0	0.3750	0	0	0	0	0
a	(3,2)	0	0	0	0	0.1250	0	0	0	0.1250	0	0.3750	0	0	0	0.3750	0	0	0	0	0
t	(3,3)	0	0	0	0	0	0.1250	0	0	0	0.1250	0	0.3750	0	0	0	0.3750	0	0	0	0
e	(3,4)	0	0	0	0	0	0.1250	0	0	0	0.1250	0	0.3750	0	0	0	0.3750	0	0	0	0
(p,q)	(2,1)	0	0	0	0	0	0	0	0	0.1250	0	0	0	0.1250	0	0.3750	0	0	0	0.3750	0
	(2,2)	0	0	0	0	0	0	0	0	0.1250	0	0	0	0.1250	0	0.3750	0	0	0	0.3750	0
	(2,3)	0	0	0	0	0	0	0	0	0	0.1250	0	0	0	0.1250	0	0.3750	0	0	0	0.3750
	(2,4)	0	0	0	0	0	0	0	0	0	0.1250	0	0	0	0.1250	0	0.3750	0	0	0	0.3750
	(1,1)	0	0	0	0	0	0	0	0	0	0	0	0	0.1250	0	0	0	0	0	0.3750	0
	(1,2)	0	0	0	0	0	0	0	0	0	0	0	0	0.1250	0	0	0	0	0	0.3750	0
	(1,3)	0	0	0	0	0	0	0	0	0	0	0	0	0	0.1250	0	0	0	0	0	0.3750
	(1,4)	0	0	0	0	0	0	0	0	0	0	0	0	0	0.1250	0	0	0	0	0	0.3750

Table 5.8: Estimated steady-state vector $\pi_{p,q}$ for Fig. 5.16

	q=1	q=2	q=3	q=4
p=5	0.0101	0.0080	0	0
p=4	0.0203	0.0303	0.0303	0.0239
p=3	0.0267	0.0609	0.0609	0.0908
p=2	0.0138	0.0800	0.0800	0.1828
p=1	0	0	0.0414	0.2400

The intermediate values for the outage results in Fig. 5.16 when $\overline{\gamma}_{SR_1} = \overline{\gamma}_{SR_2}$ and $\overline{\gamma}_{R_1D} < \overline{\gamma}_{R_2D}$,

TABLE 5.9: Estimated state transition matrix for Fig. 5.16

		F	i	n	a	l	S	t	a	t	e	(p,q)									
		(5,1)	(5,2)	(5,3)	(5,4)	(4,1)	(4,2)	(4,3)	(4,4)	(3,1)	(3,2)	(3,3)	(3,4)	(2,1)	(2,2)	(2,3)	(2,4)	(1,1)	(1,2)	(1,3)	(1,4)
I	(5,1)	0.3750	0	0	0	0	0	0.1250	0	0	0	0	0	0	0	0	0	0	0	0	0
n	(5,2)	0.3750	0	0	0	0	0	0.1250	0	0	0	0	0	0	0	0	0	0	0	0	0
i	(5,3)	0	0.3750	0	0	0	0	0	0.1250	0	0	0	0	0	0	0	0	0	0	0	0
t	(5,4)	0	0.3750	0	0	0	0	0	0.1250	0	0	0	0	0	0	0	0	0	0	0	0
i	(4,1)	0.3750	0	0	0	0.3750	0	0.1250	0	0	0	0.1250	0	0	0	0	0	0	0	0	0
a	(4,2)	0.3750	0	0	0	0.3750	0	0.1250	0	0	0	0.1250	0	0	0	0	0	0	0	0	0
l	(4,3)	0	0.3750	0	0	0	0.3750	0	0.1250	0	0	0	0.1250	0	0	0	0	0	0	0	0
S	(4,4)	0	0.3750	0	0	0	0.3750	0	0.1250	0	0	0	0.1250	0	0	0	0	0	0	0	0
t	(3,1)	0	0	0	0	0.3750	0	0	0	0.3750	0	0.1250	0	0	0	0.1250	0	0	0	0	0
a	(3,2)	0	0	0	0	0.3750	0	0	0	0.3750	0	0.1250	0	0	0	0.1250	0	0	0	0	0
t	(3,3)	0	0	0	0	0	0.3750	0	0	0	0.3750	0	0.1250	0	0	0	0.1250	0	0	0	0
e	(3,4)	0	0	0	0	0	0.3750	0	0	0	0.3750	0	0.1250	0	0	0	0.1250	0	0	0	0
(p,q)	(2,1)	0	0	0	0	0	0	0	0	0.3750	0	0	0	0.3750	0	0.1250	0	0	0	0.1250	0
	(2,2)	0	0	0	0	0	0	0	0	0.3750	0	0	0	0.3750	0	0.1250	0	0	0	0.1250	0
	(2,3)	0	0	0	0	0	0	0	0	0	0.3750	0	0	0	0.3750	0	0.1250	0	0	0	0.1250
	(2,4)	0	0	0	0	0	0	0	0	0	0.3750	0	0	0	0.3750	0	0.1250	0	0	0	0.1250
	(1,1)	0	0	0	0	0	0	0	0	0	0	0	0	0.3750	0	0	0	0	0	0.1250	0
	(1,2)	0	0	0	0	0	0	0	0	0	0	0	0	0.3750	0	0	0	0	0	0.1250	0
	(1,3)	0	0	0	0	0	0	0	0	0	0	0	0	0	0.3750	0	0	0	0	0	0.1250
	(1,4)	0	0	0	0	0	0	0	0	0	0	0	0	0	0.3750	0	0	0	0	0	0.1250

TABLE 5.10: Estimated steady-state vector $\pi_{p,q}$ for Fig. 5.16

	q=1	q=2	q=3	q=4
p=5	0.2400	0.0414	0	0
p=4	0.1828	0.0800	0.0800	0.0138
p=3	0.0908	0.0609	0.0609	0.0267
p=2	0.0239	0.0303	0.0303	0.0203
p=1	0	0	0.0080	0.0101

The below figures in Fig. 5.17 and Fig. 5.18 observed the results under the same conditions as in the above results on Fig. 5.16 but for different harvesting times. The same conclusions drawn from Fig. 5.16 are also applicable to both Fig. 5.17 and Fig. 5.18 but with better performances achieved as harvesting time increases from 0.2 to 0.6 seconds.

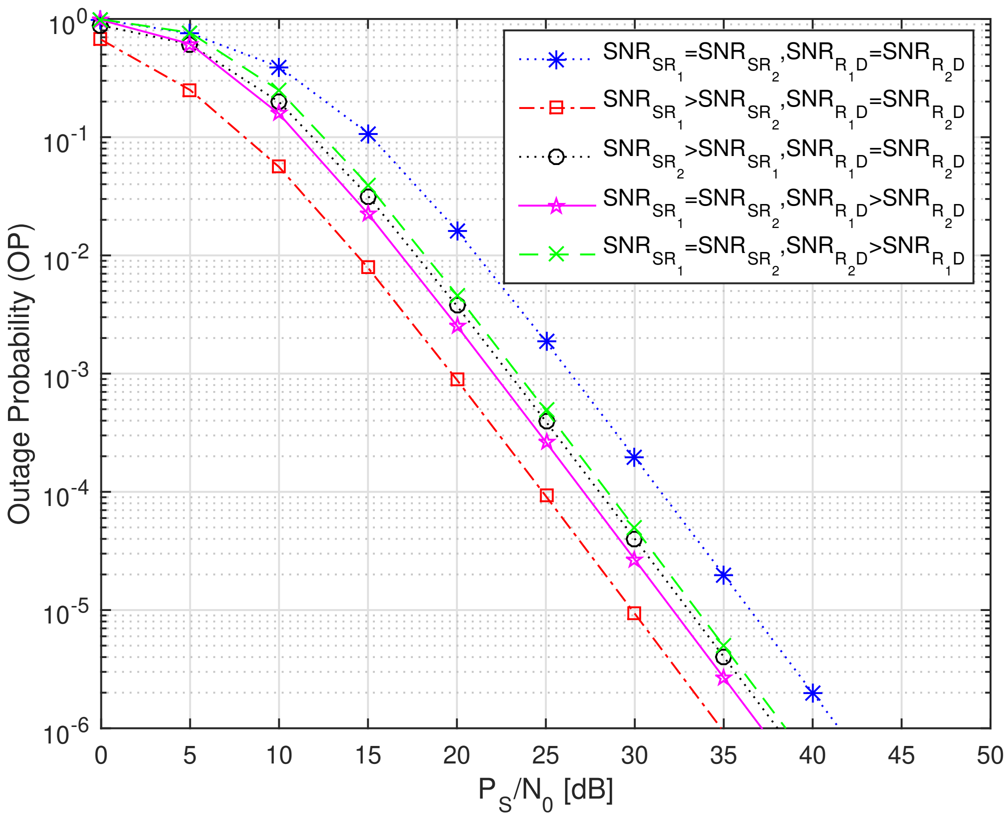

FIGURE 5.17: Results of 5 buffer states by 2 energy states quantization with harvesting time 0.4 seconds, where SNR on the legend is the average $\overline{\gamma}$ of the link.

The intermediate results including state probabilities and transition matrices were exactly the same as for the Fig. 5.16 but with a different harvesting time of 0.4 seconds.

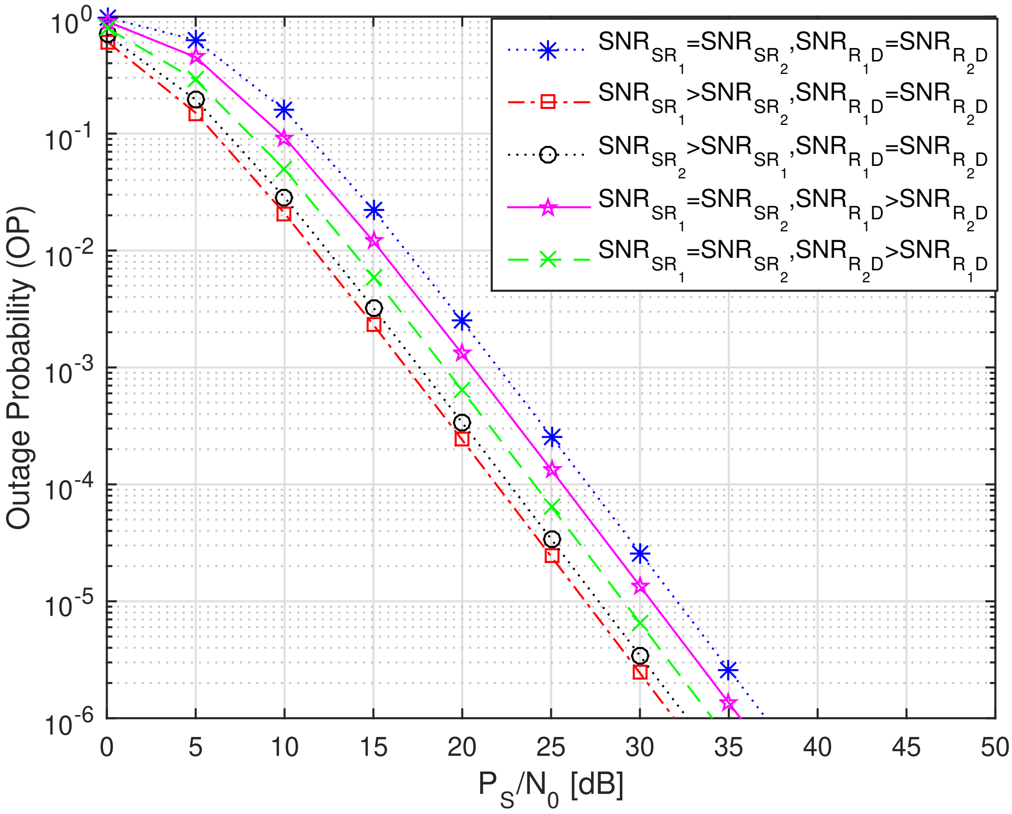

FIGURE 5.18: Results of 5 buffer states with 2 energy states quantization with harvesting time 0.6 seconds, where SNR on the legend is the average $\overline{\gamma}$ of the link.

The intermediate results were also precisely the same with both Fig. 5.16 and Fig. 5.17 with a different harvesting time of 0.6 seconds.

As seen in Fig. 5.16, 5.17 and 5.18 channel links with higher SNRs were subjected to better performances and an increase in harvesting time added improvements in performance. As harvesting time increases the results are slightly different to Chapter 4 because unlike in Chapter 4 with a reactive selection scheme, the selection scheme in Chapter 5 considers both SR_k and R_kD links.

To support the discussion made in Fig. 5.16, 5.17 and 5.18 with variably unequal channel links as harvesting increases, a set of results was generated with fixed and equal average SNRs. As shown in Fig. 5.19, better performances are achieved at higher harvesting times because of increased transmit relay powers.

Assuming the same conditions for transmit rate, variance and equal average SNRs for $\overline{\gamma}_{SR_k}, \overline{\gamma}_{R_kD}$ under different harvesting times $\{0.2, 0.4, 0.6\}$ led to the results in Fig. 5.19.

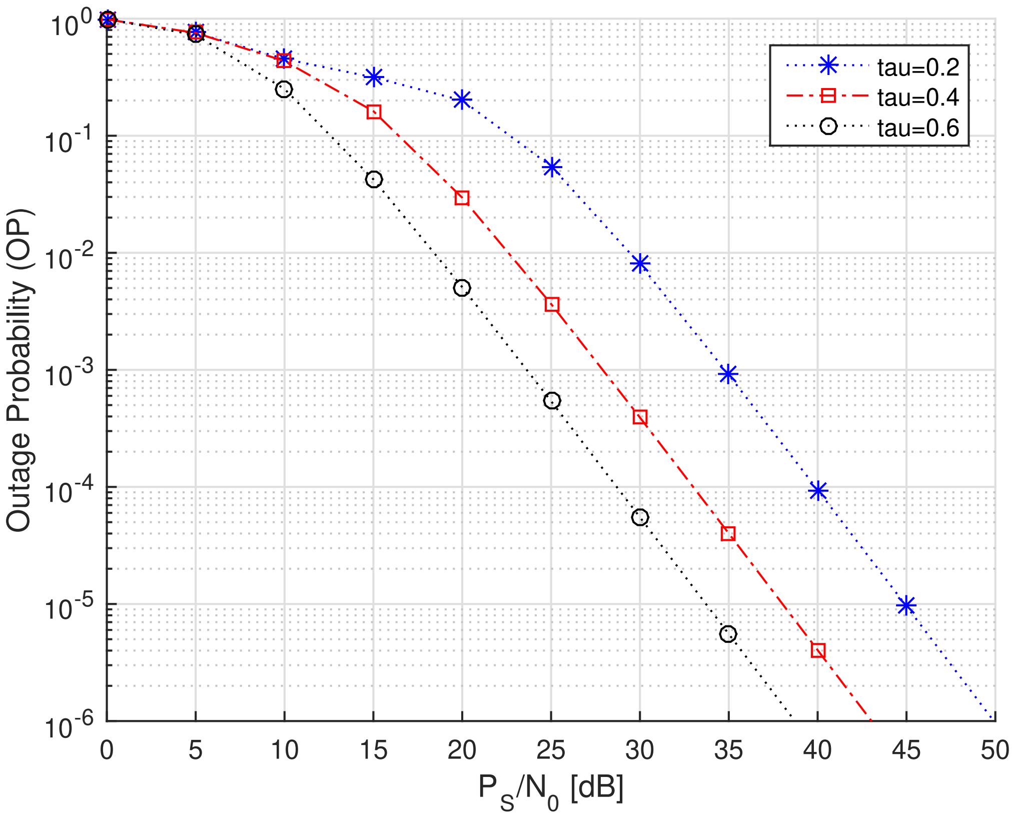

Figure 5.19: Results for 5 buffer states with 2 energy states quantization with different harvesting times $\{0.2, 0.4, 0.6\}$ seconds

The same conditional values for average SNRs in Fig. 5.16 were employed over the system with only one energy harvesting state per relay. The results attained are also found to be in line with those in Fig. 5.16 of two states per relay. The intermediate values for transitional and steady-state distribution probabilities under mentioned channel comparisons are tabled below.

The results of 5 buffer states by 1 discretized energy state are shown below in Fig. 5.20.

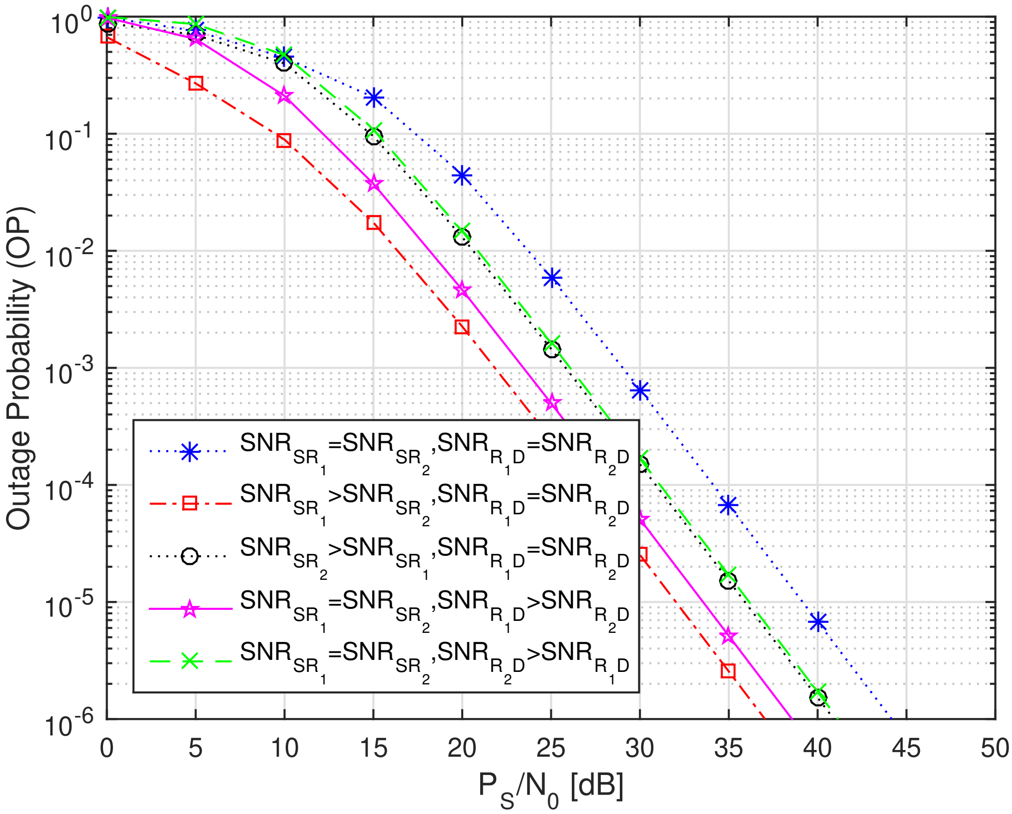

Figure 5.20: Results for 5 buffer states by 1 energy state quantization with harvesting time of 0.2 seconds, where SNR on the legend is the average $\overline{\gamma}$ of the link.

The intermediate values for the above outage results in Fig. 5.17 for 5 buffer states by 1 discretized energy state when $\overline{\gamma}_{SR_1} = \overline{\gamma}_{SR_2}, \overline{\gamma}_{R_1D} = \overline{\gamma}_{R_2D}$:

TABLE 5.11: Estimated state transition matrix for Fig. 5.17

		F	i	n	a	l	(p,q)				
		(5,1)	(5,2)	(4,1)	(4,2)	(3,1)	(3,2)	(2,1)	(2,2)	(1,1)	(1,2)
I	(5,1)	0.2500	0	0	0.2500	0	0	0	0	0	0
n	(5,2)	0.2500	0	0	0.2500	0	0	0	0	0	0
i	(4,1)	0.2500	0	0.2500	0.2500	0	0.2500	0	0	0	0
t	(4,2)	0.2500	0	0.2500	0.2500	0	0.2500	0	0	0	0
i	(3,1)	0	0	0.2500	0	0.2500	0.2500	0	0.2500	0	0
a	(3,2)	0	0	0.2500	0	0.2500	0.2500	0	0.2500	0	0
l	(2,1)	0	0	0	0	0.2500	0	0.2500	0.2500	0	0.2500
(p,q)	(2,2)	0	0	0	0	0.2500	0	0.2500	0.2500	0	0.2500
	(1,1)	0	0	0	0	0	0	0.2500	0	0	0.2500
	(1,2)	0	0	0	0	0	0	0.2500	0	0	0.2500

TABLE 5.12: Estimated steady-state vector for Fig. 5.17

	q=1	q=2
p=5	0.0955	0
p=4	0.1545	0.0955
p=3	0.1545	0.1545
p=2	0.0955	0.1545
p=1	0	0.0955

The intermediate values for the above outage results in Fig. 5.17 for 5 buffer states by 1 discretized energy state when $\overline{\gamma}_{SR_1} > \overline{\gamma}_{SR_2}, \overline{\gamma}_{R_1D} = \overline{\gamma}_{R_2D}$:

Table 5.13: Estimated state transition matrix for Fig. 5.17

		F	i	n	a	l	(p,q)				
		(5,1)	(5,2)	(4,1)	(4,2)	(3,1)	(3,2)	(2,1)	(2,2)	(1,1)	(1,2)
I	(5,1)	0.0625	0	0	0.1875	0	0	0	0	0	0
n	(5,2)	0.0625	0	0	0.1875	0	0	0	0	0	0
i	(4,1)	0.1875	0	0.0625	0.5625	0	0.1875	0	0	0	0
t	(4,2)	0.1875	0	0.0625	0.5625	0	0.1875	0	0	0	0
i	(3,1)	0	0	0.1875	0	0.0625	0.5625	0	0.1875	0	0
a	(3,2)	0	0	0.1875	0	0.0625	0.5625	0	0.1875	0	0
l	(2,1)	0	0	0	0	0.1875	0	0.0625	0.5625	0	0.1875
(p,q)	(2,2)	0	0	0	0	0.1875	0	0.0625	0.5625	0	0.1875
	(1,1)	0	0	0	0	0	0	0.1875	0	0	0.5625
	(1,2)	0	0	0	0	0	0	0.1875	0	0	0.5625

Table 5.14: Estimated steady-state vector for Fig. 5.17

	q=1	q=2
p=5	0.0477	0
p=4	0.0773	0.1432
p=3	0.0773	0.2318
p=2	0.0477	0.2318
p=1	0	0.1432

The intermediate values for the above outage results in Fig. 5.17 for 5 buffer states by 1 discretized energy state when $\overline{\gamma}_{SR_1} < \overline{\gamma}_{SR_2}, \overline{\gamma}_{R_1D} = \overline{\gamma}_{R_2D}$:

TABLE 5.15: Estimated state transition matrix for Fig. 5.17

		F	i	n	a	l	(p,q)				
		(5,1)	(5,2)	(4,1)	(4,2)	(3,1)	(3,2)	(2,1)	(2,2)	(1,1)	(1,2)
I	(5,1)	0.1250	0	0	0.3750	0	0	0	0	0	0
n	(5,2)	0.1250	0	0	0.3750	0	0	0	0	0	0
i	(4,1)	0.1250	0	0.1250	0.3750	0	0.3750	0	0	0	0
t	(4,2)	0.1250	0	0.1250	0.3750	0	0.3750	0	0	0	0
i	(3,1)	0	0	0.1250	0	0.1250	0.3750	0	0.3750	0	0
a	(3,2)	0	0	0.1250	0	0.1250	0.3750	0	0.3750	0	0
l	(2,1)	0	0	0	0	0.1250	0	0.1250	0.3750	0	0.3750
(p,q)	(2,2)	0	0	0	0	0.1250	0	0.1250	0.3750	0	0.3750
	(1,1)	0	0	0	0	0	0	0.1250	0	0	0.3750
	(1,2)	0	0	0	0	0	0	0.1250	0	0	0.3750

TABLE 5.16: Estimated steady-state vector for Fig. 5.17

	q=1	q=2
p=5	0.1432	0
p=4	0.2318	0.0477
p=3	0.2318	0.0773
p=2	0.1432	0.0773
p=1	0	0.0477

The intermediate values for the above outage results in Fig. 5.17 for 5 buffer states by 1 discretized energy state when $\overline{\gamma}_{SR_1} = \overline{\gamma}_{SR_2}, \overline{\gamma}_{R_1D} > \overline{\gamma}_{R_2D}$:

TABLE 5.17: Estimated state transition matrix for Fig. 5.17

		F	i	n	a	l	(p,q)				
		(5,1)	(5,2)	(4,1)	(4,2)	(3,1)	(3,2)	(2,1)	(2,2)	(1,1)	(1,2)
I	(5,1)	0.1250	0	0	0.3750	0	0	0	0	0	0
n	(5,2)	0.1250	0	0	0.3750	0	0	0	0	0	0
i	(4,1)	0.1250	0	0.1250	0.3750	0	0.3750	0	0	0	0
t	(4,2)	0.1250	0	0.1250	0.3750	0	0.3750	0	0	0	0
i	(3,1)	0	0	0.1250	0	0.1250	0.3750	0	0.3750	0	0
a	(3,2)	0	0	0.1250	0	0.1250	0.3750	0	0.3750	0	0
l	(2,1)	0	0	0	0	0.1250	0	0.1250	0.3750	0	0.3750
(p,q)	(2,2)	0	0	0	0	0.1250	0	0.1250	0.3750	0	0.3750
	(1,1)	0	0	0	0	0	0	0.1250	0	0	0.3750
	(1,2)	0	0	0	0	0	0	0.1250	0	0	0.3750

TABLE 5.18: Estimated steady-state vector for Fig. 5.17

	q=1	q=2
p=5	0.0180	0
p=4	0.0506	0.0541
p=3	0.0876	0.1517
p=2	0.0938	0.2628
p=1	0	0.2813

The intermediate values for the above outage results in Fig. 5.17 for 5 buffer states by 1 discretized energy state when $\overline{\gamma}_{SR_1} = \overline{\gamma}_{SR_2}, \overline{\gamma}_{R_1D} < \overline{\gamma}_{R_2D}$:

TABLE 5.19: Estimated state transition matrix for Fig. 5.17

		F	i	n	a	l	(p,q)				
		(5,1)	(5,2)	(4,1)	(4,2)	(3,1)	(3,2)	(2,1)	(2,2)	(1,1)	(1,2)
I	(5,1)	0.3750	0	0	0.1250	0	0	0	0	0	0
n	(5,2)	0.3750	0	0	0.1250	0	0	0	0	0	0
i	(4,1)	0.3750	0	0.3750	0.1250	0	0.1250	0	0	0	0
t	(4,2)	0.3750	0	0.3750	0.1250	0	0.1250	0	0	0	0
i	(3,1)	0	0	0.3750	0	0.3750	0.1250	0	0.1250	0	0
a	(3,2)	0	0	0.3750	0	0.3750	0.1250	0	0.1250	0	0
l	(2,1)	0	0	0	0	0.3750	0	0.3750	0.1250	0	0.1250
(p,q)	(2,2)	0	0	0	0	0.3750	0	0.3750	0.1250	0	0.1250
	(1,1)	0	0	0	0	0	0	0.3750	0	0	0.1250
	(1,2)	0	0	0	0	0	0	0.3750	0	0	0.1250

TABLE 5.20: Estimated steady-state vector for Fig. 5.17

	q=1	q=2
p=5	0.2813	0
p=4	0.2628	0.0938
p=3	0.1517	0.0876
p=2	0.0541	0.0506
p=1	0	0.0180

The comparisons of average SNRs $\overline{\gamma}_{SR_k}$ and $\overline{\gamma}_{R_kD}$ on a 5 buffer states by 1 discretized energy state before drawing final conclusions through a number of rates $\beta = \{0.6, 0.8, 1.2, 1.4, 1.6\}$ were assumed just like in Chapter 4 such that:

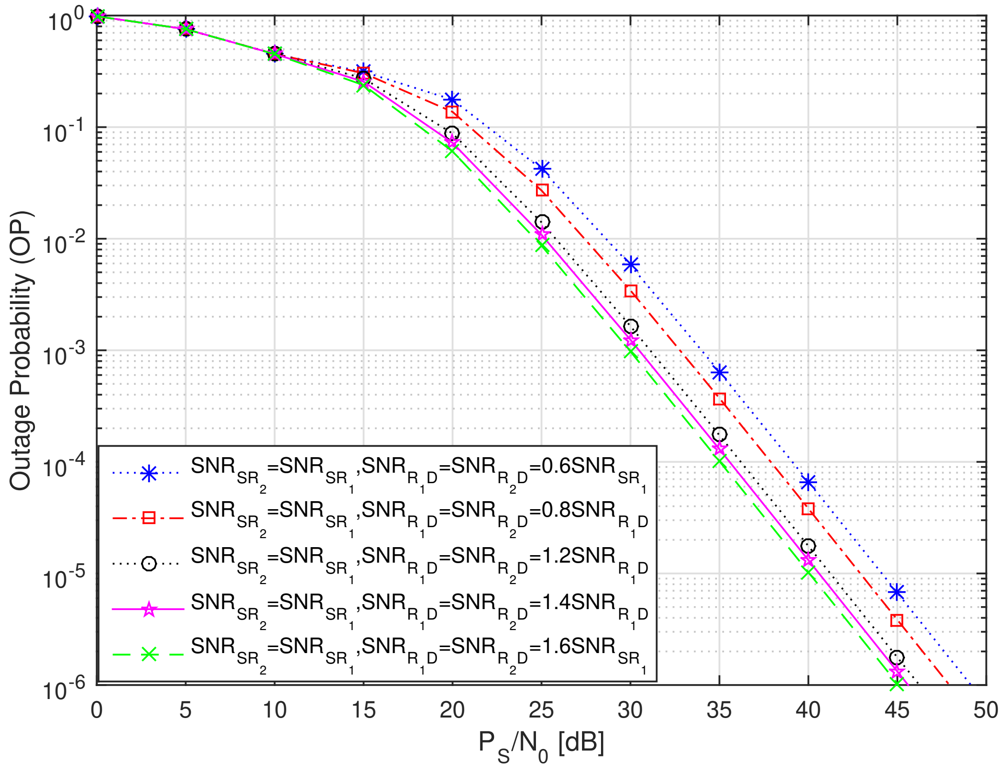

FIGURE 5.21: $\overline{\gamma}_{SR_1} = \overline{\gamma}_{SR_2}$, $\overline{\gamma}_{R_1D} = \overline{\gamma}_{R_2D} = \beta\overline{\gamma}_{SR_1}$, $\tau = 0.2$ seconds, where SNR on the legend is the average $\overline{\gamma}$ of the link.

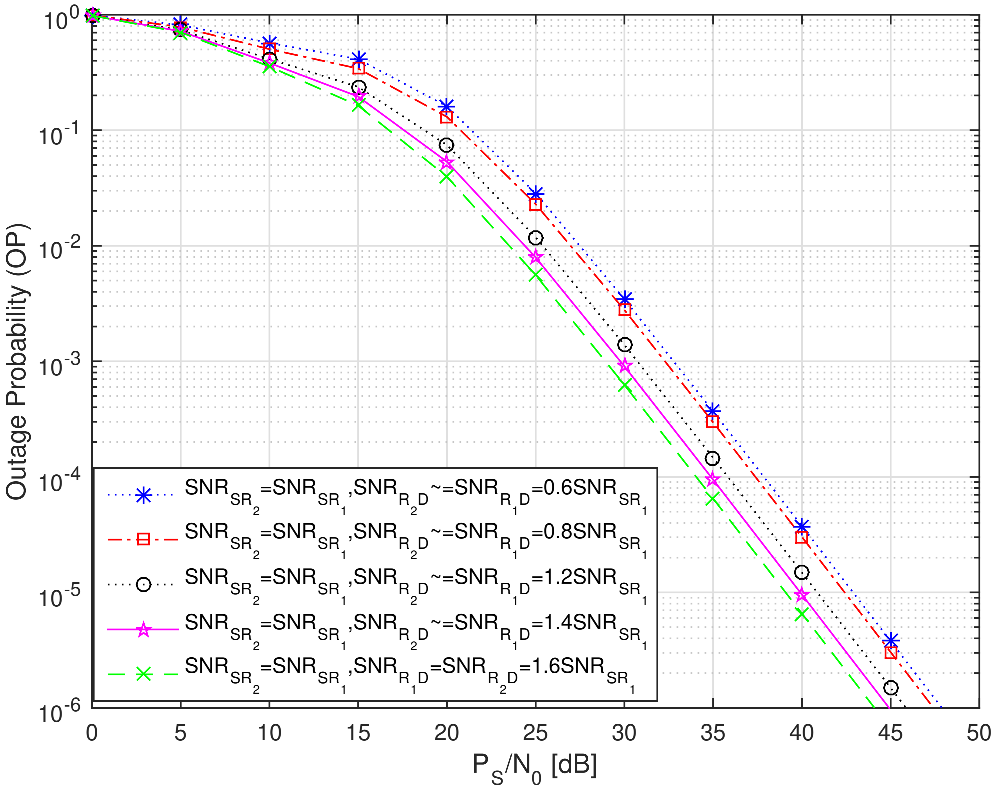

FIGURE 5.22: $\overline{\gamma}_{SR_1} = \overline{\gamma}_{SR_2}$, $\overline{\gamma}_{R_2D} \neq \overline{\gamma}_{R_1D} = \beta\overline{\gamma}_{SR_1}$, $\tau = 0.2$ seconds, where SNR on the legend is the average $\overline{\gamma}$ of the link.

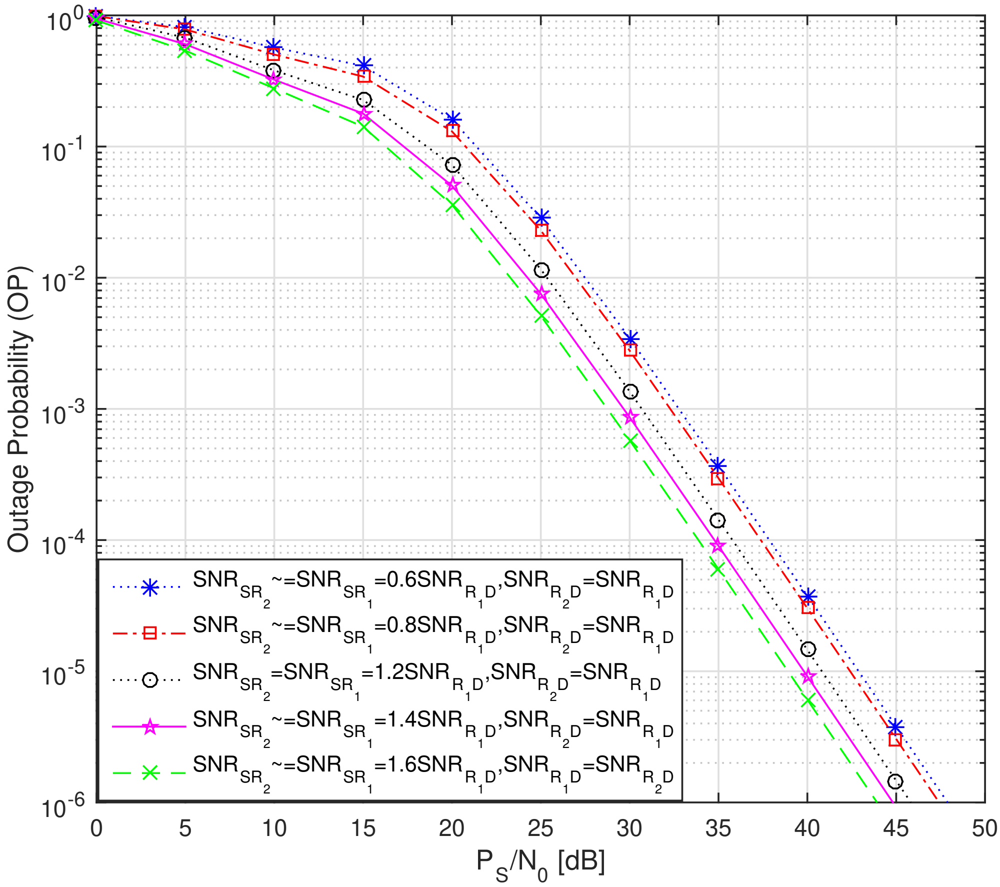

FIGURE 5.23: $\overline{\gamma}_{SR_2} \neq \overline{\gamma}_{SR_1} = \beta\overline{\gamma}_{R_1D}$, $\overline{\gamma}_{R_1D} = \overline{\gamma}_{R_2D}$, $\tau = 0.2$ seconds, where SNR on the legend is the average $\overline{\gamma}$ of the link.

The selection scheme in this Chapter uses a hybrid of ORS and MMRS such that ORS is used whenever the buffers are full or empty and MMRS is used all the time. From the results in Fig. 5.21, 5.22 and 5.23, maximum value channel links, those with the higher β in $\overline{\gamma}_{SR_k}$ and $\overline{\gamma}_{R_kD}$ are favoured for selection and they experienced relatively lower outages.

To show forth the impact of including buffers on the relays besides the delaying factor they add in to the network the performance of a buffer of size one is compared to buffer of size four in Fig. 5.24.

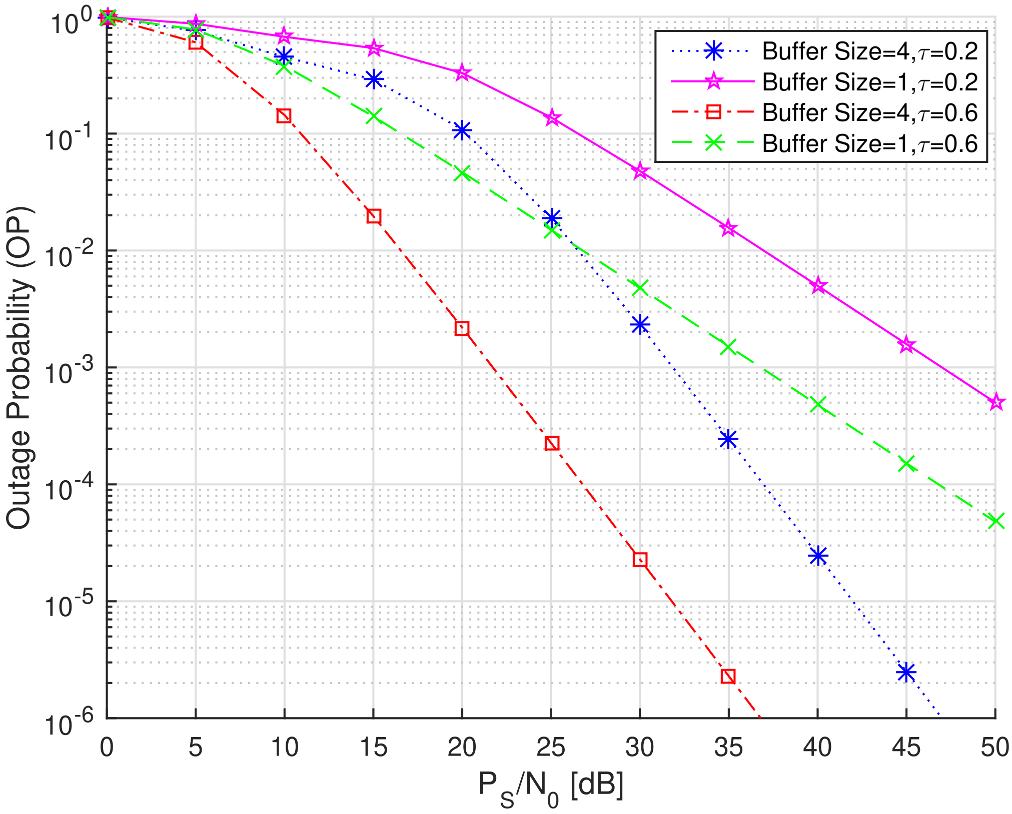

FIGURE 5.24: The effect of increasing buffer size from one to four at harvesting time of $\tau = 0.6$ seconds

From Fig. 5.24, it is clearly evident that a combination of both buffers and energy harvesting improve system performance. This can be seen that with four buffers at a harvesting period of 0.6 seconds, the performance is much better than its counterpart at a harvesting time of 0.2 seconds with an achieved gain of about 10 dB. Again, at the same harvesting period, the performance of four buffers is far superior than of one buffer at the relay. This impact is due to the fact that as more buffers are added the degrees of freedom (or diversity) at the relay are also increasing, hence better performance.

5.5 Conclusion

The probability outage of the proposed hybrid buffer-aided relay selection scheme with energy harvesting mechanism as illustrated in Fig. 5.16 and 5.17 performs better than just an MMRS and a hybrid of MMRS and ORS without energy harvesting as proposed in [67]. This proposed hybrid scheme has better gains compared to the mentioned counterparts such that obtaining an outage of 10^{-2} requires an SNR of $\leq$ 20dB(goes down with higher harvesting periods) with a harvesting period of 0.4 seconds as compared to the SNR($\geq$ 25dB) as required by the counterparts, mainly MMRS [67], ORS [38] and a hybrid scheme without energy harvesting [12]. The main conclusion drawn from this chapter is introducing both buffers and RF energy harvesters in cooperative communication improves performance much better than just having either of them alone. This has also been proven by several simulations of different combinations of buffer sizes and energy states.

This chapter proposed and evaluated a novel multi-relay selection scheme for cooperative communication using a DF strategy for harvesting relays. The relaying nodes in this cooperative network are equipped with buffers of finite size and the performance is found to improve much further because of ease in the exploitation of best source-relay and relay-destination channel pairs for the relaying devices can decide when to receive and/or transmit. This proposed strategy can also be considered as worthy in incorporating cooperation in future wireless network communications, especially in high dense environments experiencing coverage problems and LOS communication constraints.

Chapter 6

Conclusion

In this concluding chapter, a summary of contributions is discussed with potential research directions for the future. The future avenues and directions made here are based on the outcomes and results of this research.

6.1 Summary

The research in this dissertation has primarily looked at a development of a cooperative model based on relay selection with practical energy harvesting model used in time switching. And later on, the same model was proposed with relays coupled with buffers and using a hybrid relay selection scheme.

Initially in Chapter 1, the basic motivation for this research was introduced, followed by a comprehensive literature survey (Chapter 2) thoroughly investigating relay selection and cooperative communication protocols. In Chapter 3, an intensive literature review over RF energy, energy harvesting protocols and their practical challenges over wireless networks were discussed. A robust relay selection scheme was analysed with a detailed cooperative model for an efficient relay selection with evolving harvested energy in Chapter 4. In chapter 5, an extended version of a proposed relay selection scheme in Chapter 4 mainly including buffers at the relay for a packetized storage of the source's data is proposed and analysed. The performance analysis with respect to outage probability is then carefully analysed at steady state and simulated in MATLAB to confirm the theoretical framework matches with the simulation model which represents the practical implementation.

Chapter 5 is a continuance of the discoveries made in Chapter 4 under the application of a combined selection scheme of ORS and MMRS in energy harvesting networks. The buffer-aided relays are assumed to have finite buffers. Therefore, an investigative performances of buffer-aided relaying networks incorporated with the energy model derived in Chapter 4 were analysed in terms of outage probability. It has been found that there is significant drop in outage as average SNR is improving as compared to reactive ORS without buffers. An interesting future work to consider will be to consider the same model with more than five buffer state and a relay cluster ($K > 2$) which is still an open issue.

The Chapter 4 conclusions:

- The analytical framework with both four and three energy states was found to be aligned with the simulation model. This is a verification that the proposed analytical model is indeed correct and practically realizable. This is shown by results in Fig. 4.6 and Fig. 4.11.
- The effect of manipulating and comparing unequal average SNR for all S-R_1, S-R_2, R_1-D and R_2-D has also proven how appropriate the mathematical model of the reactive scheme used is. As expected, the higher relay-destination SNR links were found to outperform all other links. This has been proved by results in Fig. 4.7, Fig. 4.12, Fig. 4.15, Fig. 4.16 and Fig. 4.17.
- As expected according to both the theoretical concept and the mathematical model, an increase in energy harvesting time has an impact on performance. The higher harvesting time leads to increased magnitudes of transmit powers because of relatively large amounts of energy acquired in harvesting. This effect has been shown in Fig. 4.10, Fig. 4.8, Fig. 4.9, Fig. 4.13 and Fig. 4.14.

The Chapter 5 conclusions:

- The analytical framework including both data buffers and energy harvesting was analysed and benchmarked with the simulation model. Both the analytical and simulation results were found to be accurately aligned as shown in Fig. 5.15 and this verified appropriateness of the proposed analytical model.
- The effect of relatively comparing S-R_1, S-R_2, R_1-D and R_2-D was also examined with results in Fig. 5.16, Fig. 5.20, Fig. 5.21, Fig. 5.22 and Fig. 5.23 to show forth how the system performance varies respectively with different sets of unequal SNRs. The results obtained indeed establish that links with higher S-$R-k$ and R_k-D perform better.
- The impact of increased energy harvesting as analysed in Fig. 5.19, Fig. 5.17 and Fig. 5.18 has shown that the higher the harvesting time the higher the performance. This is an expectation due to increased relay transmit powers.
- The consequence of adding data buffers was also studied in Fig. 5.24 where it was established that the higher the buffer size the better the performance. This resultant increase is due to an increase in the system diversity of relays to receive and transmit, and therefore adding more degrees of freedom for the source data.

6.2 Contributions

This dissertation discoursed the performance improvement achieved by using cooperation in wireless communications. The following original contributions were drawn from this work:

- The analysis of outage probability of information exchange is performed between the source, relay and destination nodes as the relaying nodes are harvesting energy from the source's signal before forwarding it. This lead us to establish a closed-form expression for a reactive relay selection scheme only considering the relay-destination link SNR for a successful forwarding. The performance enhancement that the proposed selection scheme offers is quantified as compared to a conventional ORS scheme in [38].

- Again, the outage probability of the same cooperative model is analysed on the relaying nodes that are not only harvesting energy from the source but also have the capability of storing packets into buffers for flexibility. A closed-form expression for a hybrid relay selection scheme that conceives the best source-relay and the best relay-destination links for a successful reception and forwarding at the relay was established. The proposed relay selection scheme has been perceived to outperform the buffered-ORS scheme using an end-to-end SNR.

- The results obtained from the reactive selection scheme in energy harvesting networks as analysed in Chapter 4 has indeed shown RF energy can not only influence relay selection but also improve system performance. A discrete-time Markov chain was used to model the analytical framework for energy stored and exhausted.

- According to Chapter 5, the inclusion of buffers on relays has proved its worthiness by improving system performance further. This was found to be due to the degrees of freedom the buffers add to the cooperative network coupled with a flexible selection scheme (MMRS) adding extra degrees of freedom. Besides resultant delays attached with inclusion of buffers, desirable performances were accomplished when increasing the buffer size from one packet per buffer to four packets per relay buffer. The buffers just like harvested energy also influence the selection of relays to forward to the destination node depending on whether there is free space or not.

6.3 Future Work and Open Challenges

In this work, typically it has been shown how to perform cooperative relaying in RF energy harvesting networks only with two relays. It has also been shown that sufficient amounts of energy can be attained through a $2D$ Markov chains for all energy evolutions. There are more open issues in this interesting concept like having more than 2 relays which by comprehension is only believed the system will be as complex as having a K dimensional Markov chain for energy evolutions.

Future recommendations are provided for further exploring research contributions in this dissertation.

- Chapter 4 and 5 mainly focused on designing an efficient reactive selection scheme using a DF strategy. A half-duplex configuration is used for a feedback channel on selecting the best relay between the destination and the source (reactive relay selection). A further investigation can also be performed by taking into account a full-duplex design on the same system model.
- Chapter 4 and 5 provided a detailed analysis on the outage performance of a dual-hop setup only which can be extended by analysing the bit error performance of both dual and multi-hop configurations. Moreover, analysis of asymptotic optimum power allocation and optimal relay positioning based on symbol error rate (SER) approximation can also be considered in multi-hop scenarios because of their scarcity in the cooperative relay selection literature.
- Better improvements can even be attained if implications of channel estimation towards designing a practical cooperative model using pilot symbols is considered. Assuming a complete CSI at the destination with channel estimation for the proposed scheme might improve performances in terms of SER. Also considering a two-way relaying where both the source and destination nodes have data to send and relays cooperating could be worthwhile in obtaining further improved performances besides being close to a more practical approach of cooperation unlike in a one-way relaying used in this dissertation.

- Multiple relay selection with a fixed number of relays have been looked upon i.e., two. In future, this can be further extended for a more generalized number of relays per transmission and also using higher order STBCs.

In this era of Big Data, there is high demand for networks and applications that manage bandwidth utilization and are spectrally efficient. Cooperative communications in energy harvesting networks have been proposed as the best way not only to improve performance gains that can be achieved due to pathloss gains as well as diversity and multiplexing gains but also by their implementation feasibility. These all translate into decreased transmission powers, higher capacity or better cell coverage.

Cooperative relaying allows better balanced quality of service (QoS) to all users suffering from capacity and/or coverage problems. If cellular systems can be coupled with relaying communication protocols, then deployment and maintenance costs can be lowered.

List of References

[1] C. V. N. Index, "Global mobile data traffic forecast update," Cisco, techreport, Feb. 2017. [Online]. Available: http://www.cisco.com/c/en/us/solutions/collateral/service-provider/visual-networkingindex-vni/mobile-white-paper-c11-520862.html

[2] X. Minghua and S. Aissa, "On the efficiency of far-field wireless power transfer," *IEEE Transactions on Signal Processing*, vol. 63, no. 11, pp. 2835–2847, Jun. 2015.

[3] O. Edenhofer, R. Pichs-Madruga, Y. Sokona, K. Seyboth, P. Matschoss, S. Kadner, T. Zwickel, P. Eickemeier, G. Hansen, S. Schlmer, and C. S. (eds), "Ipcc special report on renewable energy sources and climate change mitigation," IPCC, Cambridge University Press, Cambridge, United Kingdom and New York, NY, USA, 1075 pp., techreport, 2011. [Online]. Available: http://srren.ipcc-wg3.de/ipcc-srren-genericpresentation-1

[4] A. Nosratinia, T. Hunter, and A. Hedayat, "Cooperative communication in wireless networks," *IEEE Communications Magazines*, vol. 42, no. 10, pp. 74–80, Oct. 2004.

[5] E. Meulen, "Three-terminal communication channels," *Advances in Applied Probability*, vol. 3, pp. 120–154, 1971.

[6] K. Azarian, H. E. Gamal, and P. Schniter, "On the achievable diversity-multiplexing tradeoff in half-duplex cooperative channels," *IEEE Transactions on Information Theory*, vol. 51, no. 12, pp. 4152–4172, Dec. 2005.

[7] S. Yang and J. Belfiore, "Towards the optimal amplify-and-forward cooperative diversity scheme," *IEEE Transactions on Information Theory*, vol. 53, no. 9, pp. 3114–3126, Sep. 2007.

[8] Y. Fan, C. Wang, J. S. Thompson, and H. V. Poor, "Recovering multiplexing loss through successive relaying using repetition coding," *IEEE Transactions on Wireless Communications*, vol. 6, no. 12, pp. 4484–4493, Dec. 2007.

[9] A. H. Madsen and J. Zhang, "Capacity bounds and power allocation for wireless relay channels," *IEEE Transactions on Information Theory*, vol. 51, no. 6, pp. 2020–2040, Jun. 2005.

[10] J. Laneman, D. Tse, and G. Wornell, "Cooperative diversity in wireless networks: Efficient protocols and outage behavior," *IEEE Transactions on Information Theory*, vol. 50, no. 12, pp. 3062–3080, Nov. 2004.

[11] M. Wdczak, *In: Autonomic Cooperative Networking SpringerBriefs in Computer Science.* Springer, Boston, MA, Feb. 2012, ch. Conventional and Cooperative Relaying, pp. 19–36.

[12] A. Ikhlef, D. Michalopoulos, and R. Schober, "Max-max relay selection for relays with buffers," *IEEE Transactions on Wireless Communications*, vol. 11, no. 3, pp. 1124–1135, Mar. 2012.

[13] R. Nabar, H. Bolcskei, and F. K. uhler, "Fading relay channels: Performance limits and space-time signal design," *IEEE Journal on Selected Areas in Communications*, vol. 22, no. 6, pp. 1099–1109, Aug. 2004.

[14] N. Zlatanov, R. Schober, and P. Popovski, "Throughput and diversity gain of buffer-aided relaying," *in Proceedings of IEEE Global Communications Conference (GLOBECOM)*, 2011.

[15] H. Sato, "Information transmission through a channel with relay," *The Aloha System University of Hawaii Honolulu Tech. Rep. B76-7*, 1976.

[16] T. M. Cover and A. E. Gamal, “Capacity theorems for the relay channel,” *IEEE Transactions on Information Theory*, vol. IT-25, no. 5, pp. 572–584, 1979.

[17] A. Sendonaris, E. Erkip, and B. Aazhang, “Increasing uplink capacity via user cooperation diversity,” *in Proceedings of IEEE International Symposium on Information Theory Proceedings (ISIT)*, p. 196, Aug. 1998.

[18] S. Efazati and P. Azmi, “Effective capacity maximization in multirelay networks with a novel cross-layer transmission framework and power-allocation scheme,” *IEEE Transactions on Vehicular Technology*, vol. 63, no. 4, pp. 1691–1702, May 2014.

[19] L. Varshney, “Transporting information and energy simultaneously,” *in Proceedings of IEEE International Symposium on Information Theory (ISIT)*, pp. 1612–1616, Aug. 2008.

[20] I. Krikidis, “Simultaneous information and energy transfer in large-scale networks with/without relaying,” *IEEE Transactions on Communications*, vol. 62, no. 3, pp. 900–912, Feb. 2014.

[21] A. Fouladgar and O. Simeone, “On the transfer of information and energy in multi-user systems,” *IEEE Communication Letters*, vol. 16, pp. 1733–1736, Nov. 2012.

[22] Z. Ding, S. M. Perlaza, I. Esnaola, and H. V. Poor, “Power allocation strategies in energy harvesting wireless cooperative networks,” *IEEE Transactions on Wireless Communications*, vol. 13, no. 2, pp. 846–860, Jan. 2014.

[23] B. Medepally and N. B. Mehta, “Voluntary energy harvesting relays and selection in cooperative wireless networks,” *IEEE Transactions on Wireless Communications*, vol. 9, no. 11, pp. 3543–3553, Nov. 2010.

[24] A. A. Nasir, X. Zhou, S. Durrani, and R. A. Kennedy, “Throughput and ergodic capacity of wireless energy harvesting based df relaying network,” *in Proceedings of IEEE International Conference on Communications (ICC)*, pp. 4066–4071, Jun. 2014.

[25] X. Jiang, J. Polastre, and D. Culler, "Perpetual environmentally powered sensor networks," *in Proceedings of Fourth International Symposium on Information Processing in Sensor Networks,IPSN*, pp. 463–468, Apr. 2005.

[26] T. Li, P. Fan, and K. B. Letaief, "Outage probability of energy harvesting relay-aided cooperative networks over rayleigh fading channel," *IEEE Transactions on Vehicular Technology*, vol. 65, no. 2, pp. 972–978, Feb. 2015.

[27] H. Chen, Y. Li, J. Rebelatto, B. F. Ucha-Filho, and B. Vucetic, "Harvest-then-cooperate: Wireless-powered cooperative communications," *IEEE Transactions on Signal Processing*, vol. 63, no. 7, pp. 1700–1711, Apr. 2015.

[28] A. A. Nasir, X. Zhou, S. Durrani, and R. A. Kennedy, "Relaying protocols for wireless energy harvesting and information processing," *IEEE Transactions on Wireless Communications*, vol. 12, no. 7, pp. 3622–3636, Jul. 2013.

[29] B. Gurakan, O. Ozel, J. Yang, and S. Ulukus, "Energy cooperation in energy harvesting wireless communications," *in Proceedings of IEEE International Symposium on Information Theory, ISIT*, pp. 965–969, Jul. 2012.

[30] Y. Chia, S. Sun, and R. Zhang, "Energy cooperation in cellular networks with renewable powered base stations," *IEEE Transactions on Wireless Communications*, vol. 13, no. 12, pp. 6996–7010, Dec. 2014.

[31] D. Niyato, E. Hossain, M. M. Rashid, and V. K. Bhargava, "Wireless sensor networks with energy harvesting technologies: A game-theoretic approach to optimal energy management," *IEEE Wireless Communications*, vol. 14, no. 4, pp. 90–96, Aug. 2007.

[32] V. Nguyen, S. Dinh-Van, and O. Shin, "Opportunistic relaying with wireless energy harvesting in a cognitive radio system," *IEEE Wireless Communications and Networking Conference(WCNC)*, Mar. 2015.

[33] J. Lei, R. Yates, and L. Greenstein, "A generic model for optimizing single-hop transmission policy of replenishable sensors," *IEEE Transactions on Wireless Communications*, vol. 8, no. 2, pp. 547–551, 2009.

[34] D. Poulimeneas, T. Charalambous, N. Nomikos, I. Krikidis, D. Vouyioukas, and M. Johansson, "Delay- and diversity-aware buffer-aided relay selection policies in cooperative networks," in *Proceedings of IEEE Wireless Communications and Networking Conference (WCNC)*, Apr. 2016, pp. 1–6.

[35] N. Zlatanov and R. Schober, "Buffer-aided half-duplex relaying can outperform ideal full-duplex relaying," *IEEE Communication Letters*, vol. 17, no. 3, pp. 479–482, Mar. 2013.

[36] N. Nomikos, T. Charalambous, I. Krikidis, D. Skoutas, D. Vouyioukas, M. Johansson, and C. Skianis, "A survey on buffer-aided relay selection," *IEEE Communications Surveys & Tutorials*, vol. 18, no. 2, pp. 1073 – 1097, 2nd Quarter 2016.

[37] Z. Tian, Y. Gong, G. Chen, and J. Chambers, "Buffer-aided relay selection with reduced packet delay in cooperative networks," *IEEE Transactions on Vehicular Technology*, vol. 66, no. 3, pp. 2567–2575, Mar. 2016.

[38] A. Bletsas, H. Shin, and M. Win, "Cooperative communications with outage-optimal opportunistic relaying," *IEEE Transactions on Wireless Communications*, vol. 6, no. 9, pp. 3450 – 3460, Sep. 2007.

[39] M. Dohler and Y. Li, *Cooperative Communications Hardware, Channel & PHY*. A John Wiley and Sons, Ltd., Publication, 2010.

[40] S. Ikki, "Performance analysis of cooperative-diversity networks with different relaying and combining techniques," Ph.D. dissertation, Memorial University of NewFoundland, 2008.

[41] B. Timus, "Studies on the viability of cellular multihop networks with fixed relays," phdthesis, KTH Information and Communication Technology, Stockholm, Sweden, Jun. 2009.

[42] M. Dong, M. Hajiaghayi, and B. Liang, "Optimal fixed gain linear processing for amplify-and-forward multichannel relaying," *IEEE Transactions on Signal Processing*, vol. 60, pp. 6108–6114, Nov. 2012.

[43] I. A. Faycal and M. Medard, "Optimal uncoded regeneration for binary antipodal signaling," *IEEE International Conference on Communications*, vol. 2, Jul. 2004.

[44] J. Guerreiro, R. Dinis, and P. Montezuma, "Analytical evaluation of nonlinear amplifyand-forward relay systems for ofdm signals," in *Proceedings of IEEE 80th Vehicular Technology Conference*, Sep. 2014, pp. 1–5.

[45] G. Kramer, M. Gastpar, and P. Gupta, "Cooperative strategies and capacity theorems for relay networks," *IEEE Transactions on Information Theory*, vol. 51, pp. 3037–3063, Sep. 2005.

[46] A. Raja and P. Viswanath, "Compress-and-forward ccheme for relay networks: backword decoding and connection to bisubmodular flows," *IEEE Transactions on Information Theory*, vol. 60, pp. 5627–5638, Sep. 2014.

[47] J. Laneman and G. Wornell, "Energy-efficient antenna sharing and relaying for wireless networks," *in Proceedings of Wireless Communications and Networking Conference*, vol. 1, pp. 7–12, 2000.

[48] M. Simon and M. Alouini, *Digital Communication over Fading Channels*, second edition ed. John Wiley & Sons, Inc., 2005.

[49] A. Conti, M. Z. Win, and M. Chiani, "On the inverse symbol-error probability for diversity reception," *IEEE Transactions on Communications*, vol. 51, pp. 753–756, May 2003.

[50] A. Prince, A. Abdalla, H. Dahshan, and A. E. Rohiem, "Performance evaluation of multihop decode and forward cooperative relaying," in *Proceedings of International Conference on Advanced Control Circuits Systems (ACCS) Systems & 2017 International Conference on New Paradigms in Electronics & Information Technology (PEIT)*, Nov. 2017.

[51] U. Khair, Suwadi, and Wirawan, "Performance of hybrid relay selection in cooperative communications system," in *Proceedings of 2nd International conferences on Information Technology, Information Systems and Electrical Engineering (ICITISEE)*, Nov. 2017.

[52] T. Blazek and C. Mecklenbruker, "Measurement-based burst-error performance modeling for cooperative intelligent transport systems," *IEEE Transactions on Intelligent Transportation Systems*, vol. PP, no. 99, pp. 1–10, Mar. 2018.

[53] P. Paul and A. Babu, "Performance evaluation of cooperative communication in wbans with maximal ratio combining," in *Proceedings of International Conference on Computing and Network Communications (CoCoNet)*, Dec. 2015.

[54] T. Li, P. Fan, and K. Letaief, "Outage probability of energy harvesting relay-aided cooperative networks over rayleigh fading channel," *IEEE Transactions on Vehicular Technology*, vol. 65, no. 2, pp. 972 – 978, Feb. 2016.

[55] A. Gaber, J. Halim, and H. E. Hennawy, "Outage probability of af cdma hybrid satellite-terrestrial cooperative networks using multiple relays over shadowed-rician fading channels," in *Proceedings of National Radio Science Conference (NRSC)*, Mar. 2018.

[56] F. Ojo and M.F.M.Salleh, "Throughput analysis of a hybridized power-time splitting based relaying protocol for wireless information and power transfer in cooperative networks," *IEEE Access*, vol. 6, no. 17772124, pp. 24 137 – 24 147, Apr. 2018.

[57] Z. Zhou, M. Peng, Z. Zhao, C. Wang, and R. Blum, "Throughput optimizing for power-splitting based relaying in wireless-powered cooperative networks," in *Proceedings of IEEE Global Communications Conference (GLOBECOM)*, Dec. 2015.

[58] S. Hsu, C. Lin, C. Wang, and W. Chen, "Minimizing upload latency for critical tasks in cellular-based iot networks using multiple relays," in *Proceedings of IEEE International Conference on Communications (ICC)*, Jul. 2017.

[59] G. Bradford and J. N. Laneman, "Low latency relaying schemes for next-generation cellular networks," in *IEEE International Conference on Communications (ICC)*, Jun. 2012, pp. 4294 – 4299.

[60] A. Bletsas, A. Khisti, D. F. Reed, and A. Lippman, "A simple cooperative diversity method based on network path selection," *IEEE Journal on Selected Areas in Communications*, vol. 24, no. 3, pp. 659–672, Mar. 2006.

[61] T. Ratnarajah, M. Sellathurai, Z., and Ding, "Spectrally efficient cooperative diversity protocols for wireless networks," in *Proceedings of Fortieth Asilomar Conference on Signals, Systems and Computers*, Oct. 2006.

[62] Z. Ding, Y. Gong, T. Ratnarajah, and C. N. Cowan, "On the performance of opportunistic cooperative wireless networks," *IEEE Transactions on Communications*, vol. 56, no. 8, pp. 1236–1240, Aug. 2008.

[63] A. Bletsas, "Intelligent antenna sharing in cooperative diversity wireless networks," Ph.D. dissertation, Massachusetts Institute of Technology, 2005.

[64] R. Tannious and A. Nosratinia, "Spectrally-efficient relay selection with limited feedback," *IEEE Journal on Selected Areas in Communications*, vol. 26, no. 8, pp. 1419–1428, Oct. 2008.

[65] A. Bletsas, A. G. Dimitriou, and J. N. Sahalos, "Interference-limited opportunistic relaying with reactive sensing," *IEEE Transactions in Wireless Communications*, vol. 9, no. 1, pp. 14–20, Jan. 2010.

[66] N. Nomikos and D. Vouyioukas, "A successive opportunistic relaying protocol with inter-relay interference mitigation," in *Proceedings of IEEE Wireless Communications on Mobile Computing Conference (IWCMC)*, Aug. 2012, pp. 228–333.

[67] N. Zlatanov, A. Ikhlef, T. I., and R. Schober, "Buffer-aided cooperative communications: opportunities and challenges," *IEEE Journals & Magazines*, vol. 52, no. 4, pp. 146–153, Apr. 2014.

[68] R. Wang, V. Lau, and H. Huang, "Opportunistic buffered decode-wait-and-forward (obdwf) protocol for mobile wireless relay networks," *IEEE Transactions on Wireless Communications*, vol. 10, no. 4, pp. 1224–1231, Apr. 2011.

[69] N. Zlatanov, D. Hranilovic, and J. Evans, "Buffer-aided relaying improves throughput of full-duplex relay networks with fixed-rate transmissions," *IEEE Communications Letters*, vol. 20, no. 12, pp. 2446–2449, Dec. 2016.

[70] J. Zhan, Y. Liu, X. Tang, and Q. Chen, "Relaying protocols for buffer-aided energy harvesting wireless cooperative networks," *IET Networks*, vol. 7, no. 3, pp. 109–118, May 2018.

[71] I. Krikidis, T. Charalambous, and J. S. Thompson, "Buffer-aided relay selection for cooperative diversity systems without delay constraints," *IEEE Transactions on Wireless Communications*, vol. 11, no. 5, pp. 1957–1967, May 2012.

[72] T. Charalambous, N. Nomikos, I. Krikidis, D. Vouyioukas, and M. Johansson, "Modeling buffer-aided relay selection in networks with direct transmission capability," *IEEE Communications Letters*, vol. 19, no. 4, pp. 649–652, Apr. 2015.

[73] N. Zlatanov, R. Schober, and P. Popovski, "Buffer-aided relaying with adaptive link selection," *IEEE Journal on Selected Areas in Communications*, vol. 31, no. 8, pp. 1530–1542, Aug. 2013.

[74] N. Zlatanov and R. Schober, "Buffer-aided relaying with adaptive link selection - fixed and mixed rate transmission," *IEEE Transactions on Information Theory*, vol. 59, no. 5, pp. 2816–40, May 2013.

[75] B. Rankov and A. Wittneben, "Spectral efficient protocols for half-duplex fading relay channels," *IEEE Journal on Selected Areas in Communications*, vol. 8, no. 2, pp. 379–389, Feb. 2007.

[76] H. Wicaksana, S. H. Ting, Y. L. Guan, and X. G. Xia, "Decode-and-forward two-path half-duplex relaying: Diversity-multiplexing tradeoff analysis," *IEEE Transactions on Communications*, vol. 59, no. 7, pp. 1985–1994, Jul. 2011.

[77] T. Riihonen, S. Werner, and R. Wichman, "Hybrid full-duplex/halfduplex relaying with transmit power adaptation," *IEEE Transactions on Wireless Communications*, vol. 10, no. 9, pp. 3074–3085, Sep. 2011.

[78] ——, "Mitigation of loopback selfinterference in full-duplex mimo relays," *IEEE Transactions on Signal Processing*, vol. 59, no. 12, pp. 5983–5993, Dec. 2011.

[79] Z. Ding, I. Krikidis, B. Rong, J. S. Thompson, C. Wang, and S. Yang, "On combating the half-duplex constraint in modern cooperative networks: Protocols and techniques," *IEEE Wireless Communications Magazine*, vol. 19, no. 6, pp. 20–27, Dec. 2012.

[80] I. Krikidis, H. A. Suraweera, P. J. Smith, and C. Yuen, "Full-duplex relay selection for amplify-and-forward cooperative networks," *IEEE Transactions on Wireless Communications*, vol. 11, no. 12, pp. 4381–4393, Dec. 2012.

[81] I. Psaras and L. Mamatas, "On demand connectivity sharing: queuing management and load balancing for user-provided networks," *Computer Networks*, 2010.

[82] K. Fall, "A delay-tolerant network architecture for challenged internets," *SIGCOMM03, ACM*, pp. 27–34, 2003.

[83] L. Hou and S. Tan, "A preliminary study of thermal energy harvesting for industrial wireless sensor networks," in *Proceedings of the10th IEEE International Conference on Software Testing, Verification and Validation (ICST)*, 2016, pp. 1–5.

[84] I. K. et al., "Simultaneous wireless information and power transfer in modern communication systems," *IEEE Communications Magazines*, vol. 52, no. 11, pp. 104–110, Nov. 2014.

[85] S. Priya and D. Inman, *Energy harvesting technologies.* Springer Science+Business Media, LLC 2009, 2008.

[86] C. Huang, R. Zhang, and S. Cui, "Throughput maximization for the gaussian relay channel with energy harvesting constraints," *IEEE Journal on Selected Areas in Communications*, vol. 31, no. 8, pp. 1469–1479, Aug. 2013.

[87] K. Tutuncuoglu, B. Varan, and A. Yener, "Energy harvesting two-way half-duplex relay channel with decode-and-forward relaying: Optimum power policies," in *Proceedings of International Conference on Digital Signal Processing (DSP)*, 2013.

[88] J. Huang, Q. Li, Q. Zhang, G. Zhang, and J. Qin, "Relay beamforming for amplify-and-forward multi-antenna relay networks with energy harvesting constraint," *IEEE Signal Processing Letters*, vol. 21, no. 4, pp. 454–458, Apr. 2014.

[89] B. Chalise, W. Ma, Y. Zhang, H. Suraweera, and M. Amin, "Optimum performance boundaries of ostbc based af-mimo relay system with energy harvesting receiver," *IEEE Transactions on Signal Processing*, vol. 61, no. 17, pp. 4199–4213, Sep. 2013.

[90] D. Mishra, S. De, S. Jana, S. Basagni, K. Chowdhury, and W. Heinzelman, "Smart rf energy harvesting communications: challenges and opportunities," *IEEE Communications Magazine*, 2015.

[91] S. Atapattu, H. Jiang, J. Evans, and C. Tellambura, "Time-switching energy harvesting in relay networks," in *Proceedings of IEEE International Conference on Communications (ICC)*, 2015, pp. 5416 – 5421.

[92] R. Zhang and C. K. Ho, "Mimo broadcasting for simultaneous wireless information and power transfer," *IEEE Transactions on Wireless Communications*, vol. 12, no. 5, pp. 1989–2001, May 2013.

[93] R. Madan, N. Mehta, A. Molisch, and J. Zhang, "Energy-efficient cooperative relaying over fading channels with simple relay selection," *IEEE Transactions on Wireless Communications*, vol. 7, no. 8, pp. 3013–3025, Aug. 2008.

[94] L. R. Varshney, "Transporting information and energy simultaneously," in *Proceedings of IEEE International Symposium on Information Theory (ISIT)*, Jul. 2008, pp. 1612–1616.

[95] P. Grover and A. Sahai, "Shannon meets tesla: wireless information and power transfer," in *Proceedings of IEEE International Symposium on Information Theory (ISIT)*, Jun. 2010, pp. 2363–2367.

[96] L. Liu, R. Zhang, and K.C.Chua, "Wireless information and power transfer: A dynamic power splitting approach," *IEEE Transactions on Communications*, vol. 61, no. 9, pp. 3990 – 4001, Sep. 2013.

[97] I. Yoon, "Wireless power transfer in the radiating near-field region," in *Proceedings of USNC URSI Radio Sci. Meeting (Joint AP S Symp.)*, 2015, p. 344.

[98] K. Huang and X. Zhou, "Cutting the last wires for mobile communications by microwave power transfer," *IEEE Communications Magazine*, vol. 53, no. 6, pp. 86–93, Jun. 2015.

[99] X. Lu, P. Wang, D. Niyato, D. I. Kim, and Z. Han, "Wireless networks with rf energy harvesting: A contemporary survey," *IEEE Communications & Surveys Tutorials*, vol. 17, no. 2, pp. 757–789, 2nd Quarter 2015.

[100] H. Y. et al., "A cooperative modulation recognition: New paradigm for power line networks in smart grid," *Physical Communications*, vol. 25, pp. 268–276, Dec. 2017.

[101] Z. D. et al., "Application of smart antenna technologies in simultaneous wireless information and power transfer," *IEEE Communications Magazine*, vol. 53, no. 4, pp. 86–93, Apr. 2015.

[102] M. Agiwal, A. Roy, and N. Saxena, "Next generation 5g wireless networks: A comprehensive survey," *IEEE Communication Surveys and Tutorials*, no. 3, pp. 1617–1655, 3rd Quarter 2016.

[103] S. U. et al., "Energy harvesting wireless communications: A review of recent advances," *IEEE Journal on Selected Areas in Communications*, vol. 33, no. 3, pp. 360–381, Mar. 2015.

[104] Y. Che, S. Zhang, S. Xu, and G. Y. Li, "Fundamental trade-offs on green wireless networks," *IEEE Communications Magazine*, vol. 49, no. 6, pp. 30–37, Jun. 2011.

[105] Z. Hasan, H. Boostanimehr, and V. K. Bhargava, "Green cellular networks: A survey, some research issues and challenges," *IEEE Communications Surveys & Tutorials*, vol. 13, no. 4, pp. 524–540, Apr. 2011.

[106] C. Yin, T. X. Doan, N. Nguyen, T. Mai, and L. Nguyen, "Outage probability of full-duplex cognitive relay networks with partial relay selection," in *Proceedings of International Conference on Recent Advances in Signal Processing, Telecommunications & Computing (SigTelCom)*, 2017, pp. 115 – 118.

[107] S. Lee, D. B. da Costa, Q.Vien, T. Q. Duong, and R. T. de Sousa, "Non-orthogonal multiple access schemes with partial relay selection," *IET Communications*, vol. 11, no. 6, pp. 846 – 854, Apr. 2017.

[108] O. Omur and S. Ulukus, "Achieving awgn capacity under stochastic energy harvesting," *IEEE Transactions on Information Theory*, vol. 58, no. 10, pp. 6471–6483, Oct. 2012.

[109] K. Tutuncuoglu, O. Ozel, A. Yene, and S. Ulukus, "The binary energy harvesting channel with a unit-sized battery," *IEEE Transactions on Information Theory*, vol. 63, no. 7, pp. 4240 – 4256, Jul. 2017.

[110] S. S. Ikki and M. H. Ahmed, "Exact error probability and channel capacity of the best-relay cooperative-diversity networks," *IEEE Signal Processing Letters*, vol. 16, no. 12, pp. 1051–1054, Dec. 2009.

[111] N. C. Beaulieu and J. Hu, "A closed-form expression for the outage probability of decode-and-forward relaying in dissimilar rayleigh fading channels," *IEEE Communications Letters*, vol. 10, no. 12, pp. 813–815, Dec. 2006.

[112] A. Sendonaris, E. Erkip, and B. Aazhang, "User cooperation diversity - part ii. implementation aspects and performance analysis," *IEEE Transactions on Commununications*, vol. 51, no. 11, pp. 1939–1948, 2003.

[113] ——, "User cooperation diversity - part i. system description," *IEEE Transactions on Commununications*, vol. 51, no. 11, pp. 1927–1938, 2003.

[114] X. Zhou, R. Zhang, and C. K. Ho, "Wireless information and power transfer: Architecture design and rate-energy tradeoff," *IEEE Transactions on Communications*, vol. 61, no. 11, pp. 4754–4767, Oct. 2013.

[115] B. Gurakan, O. Ozel, J. Yang, and S. Ulukus, "Two-way and multiple-access energy harvesting systems with energy cooperation," *in Proceedings of 46th Asilomar Conference on Signals, Systems and Computers, Pacific Grove,*, Nov. 2012.

[116] P. Popovski, A. Fouladgar, and O. Simeone, "Interactive joint transfer of energy and information," *IEEE Transactions on Communications*, vol. 61, no. 5, pp. 2086–2097, May 2012.

[117] K. S. Gomadam and S. A. Jafar, "Optimal relay functionality for snr maximization in memoryless relay networks," *IEEE Journal on Selected Areas in Communications*, vol. 25, no. 2, pp. 390–401, Feb. 2007.

[118] S. Anees and M. Bhatnagar, "Exact performance analysis of df based mixed triple-hop rf/fso/rf communication system," in *Proceedings of IEEE 28th Annual International Symposium on Personal, Indoor, and Mobile Radio Communications (PIMRC)*, Oct. 2017.

[119] Y. Li, K. Sun, and L. Cai, "Cooperative device-to-device communication with network coding for machine type communication devices," *IEEE Transactions on Wireless Communications*, vol. 17, no. 1, pp. 296–309, Jan. 2018.

[120] N. B. Mehta, V. Sharma, and G. Bansal, "Performance analysis of a cooperative system with rateless codes and buffered relays," *IEEE Transactions on Wireless Communications*, vol. 10, no. 4, pp. 1069–1081, Apr. 2011.

[121] v I. Ahmed, A. Ikhlef, R. Schober, and R. Mallik, "Joint power allocation and relay selection in energy harvesting af relay systems," *IEEE Transactions on Wireless Communication Letters*, vol. 2, no. 2, pp. 239–242, Apr. 2013.

[122] I. Ahmed, A. Ikhlef, R. Schober, and R. K. Mallik, "Power allocation for conventional and buffer-aided link adaptive relaying systems with energy harvesting nodes," *IEEE Transactions on Wireless Communications*, vol. 13, no. 3, pp. 1182–1195, Mar. 2014.

[123] W. Wicke, N. Zlatanov, V. Jamali, and R. Schober, "Buffer-aided relaying with discrete transmission rates for the two-hop half-duplex relay network," *IEEE Transactions on Wireless Communications*, vol. 16, no. 2, pp. 967–981, Feb. 2017.

[124] M. Dohler, A. H. Aghvami, Z. Zhou, Y. Li, and B. Vucetic, Eds., *Capacity and outage of TAS schemes over Nakagami channels*, in COST273, Duisburg, Germany, 2004.

[125] R. Blum and J. Winters, "On optimum mimo with antenna selection," *IEEE Communications Letters*, vol. 6, pp. 322–324, Aug. 2002.

[126] S. S. Ikki and M. H. Ahmed, "On the performance of cooperative-diversity networks with the nth best-relay selection scheme," *IEEE Transactions on Communications*, vol. 58, no. 11, pp. 3062–3069, Nov. 2010.

[127] E. Beres and R. Adve, "Outage probability of selection cooperation in the low to medium snr regime," *IEEE Communications Letters*, vol. 11, no. 7, pp. 589–597, Jul. 2007.

[128] Y. Zhao, R. Adve, and T. Lim, "Outage probability at arbitrary snr with cooperative diversity," *IEEE Communications Letters*, vol. 9, no. 8, pp. 700–702, Aug. 2005.

[129] A. Adinoyi, Y. Fan, H. Yanikomeroglu, and H. V. Poor, "On the performance of selection relaying," in *2008 IEEE 68th Vehicular Technology Conference*, Sep. 2008.